

# **Electrical properties of human skin: From linear recordings of exogenous electrodermal activity to non-linear memristor measurements**

**Author:** Oliver Pabst

**Supervisors:** Ørjan Grøttem Martinsen

Christian Tronstad

Steven Ray Haakon Wilson

**Date:** 22 January 2018

© **Oliver Pabst, 2018**

*Series of dissertations submitted to the  
Faculty of Mathematics and Natural Sciences, University of Oslo  
No. 1971*

ISSN 1501-7710

All rights reserved. No part of this publication may be  
reproduced or transmitted, in any form or by any means, without permission.

Cover: Hanne Baadsgaard Utigard.  
Print production: Reprosentralen, University of Oslo.

# Papers included in this thesis

## Paper I:

- Title:** “*Comparison between the AC and DC measurement of electrodermal activity*”
- Authors:** O. Pabst, C. Tronstad, S. Grimnes, D. Fowles, and Ø. G. Martinsen
- Journal:** *Psychophysiology*
- Reference:** [1]

## Paper II:

- Title:** “*Human Skin is a generic, non-volatile memristor*”
- Authors:** O. Pabst, Ø. G. Martinsen, and L. Chua
- Journal:** *To be submitted.*
- Reference:** [2]

## Paper III:

- Title:** “*Instrumentation, electrode choice and challenges in human skin memristor measurement*”
- Authors:** O. Pabst, C. Tronstad, and Ø. G. Martinsen
- Journal:** *Engineering in Medicine and Biology Society (EMBC), 2017 39th Annual International Conference of the IEEE*
- Reference:** [3]

## Paper IV:

- Title:** “*Interpretation of the pinched point position in human skin memristor measurements*”
- Authors:** O. Pabst, and Ø. G. Martinsen
- Journal:** *EMBE & NBC 2017: Springer, 2017*
- Reference:** [4]



# Acknowledgments

First of all, I want to thank my main supervisor Prof. Ørjan Grøttem Martinsen. He was always open for ideas and gave great inspiration and support during the three years.

Thanks also to my second supervisor Christian Tronstad, PhD. He was also always open for discussions, in which he contributed with great ideas and impact.

Further thanks to my third supervisor Prof. Steven Ray Haakon Wilson who also always contributed with great ideas during discussions. This work has been performed as part of Diotech, a strategic initiative of the University of Oslo and I want to thank Prof. Elsa Lundanes, who is the leader of this initiative. Further, I want to thank both for inviting me to contribute as co-author to the paper “Exploring bioimpedance instrumentation for the characterization of open tubular liquid chromatography columns”.

Thanks also to all the external co-authors of the papers within this thesis:

- Prof. emeritus Sverre Grimnes for the inspiration he gave and his great impact during discussions in the first year of my thesis in general and regarding Paper I.
- Prof. emeritus Don Fowles for his great contribution as co-author in the study design and discussions within Paper I.
- Prof. emeritus Leon Chua for his great impact on memristor theory and study design within Paper II. Special thanks to him also for his interest in our research on the human skin memristor.

I want to thank all the employees of the electronics workshop of the department of Physics, especially Stein Stabelfelt Nielsen and Erlend Bårdsen who supported the realization of the developed instrumentations and who shared their experience in Electronics design.

Thanks also to the employees from the mechanical workshop at the department of Physics who built the chassis of the developed instrumentations.

I want to thank Prof. Carsten Andrew Lutken, Associate Professor Arnt Inge Vistnes and Prof. emeritus Iouri Galperine for the discussions we had on memristor theory and related topics.

Finally, I want to thank all the students and other volunteers who participated as test subjects in the experiments. The presented findings would not have been made without all the positivism for participation.



# Contents

1	Introduction.....	5
1.1	Aim, objectives, and research questions.....	6
2	Basics .....	8
2.1	Human skin.....	8
2.2	Note on (linear) impedance and admittance.....	10
2.3	Linear and non-linear measurements.....	13
2.4	The memristor.....	14
3	Linear skin measurements.....	18
3.1	Linear skin admittance .....	18
3.2	Recording of exogenous EDA.....	19
3.3	Direct comparison between the AC and the DC method of recording EDA .....	22
4	Non-linear skin memristor measurements .....	24
4.1	Motivation and Background .....	24
4.2	The sweat duct memristor .....	25
4.3	Stratum corneum NTC thermistor .....	31
4.4	Non-linear (state dependent) skin admittance .....	34
4.5	Parameterization .....	35
4.6	Border between linear and non-linear recordings .....	38
4.7	Different skin sites.....	39
4.8	Application and further research .....	40
5	Instrumentation .....	41
5.1	Analogue part .....	42
5.2	Electrode system.....	44
5.3	Electrode choice .....	45
5.4	Digital part.....	46
6	Memristor simulations .....	49
6.1	Model selection and results .....	49
6.2	NTC thermistor in parallel with HP memristor.....	51
7	Conclusions and findings.....	53



# 1 Introduction

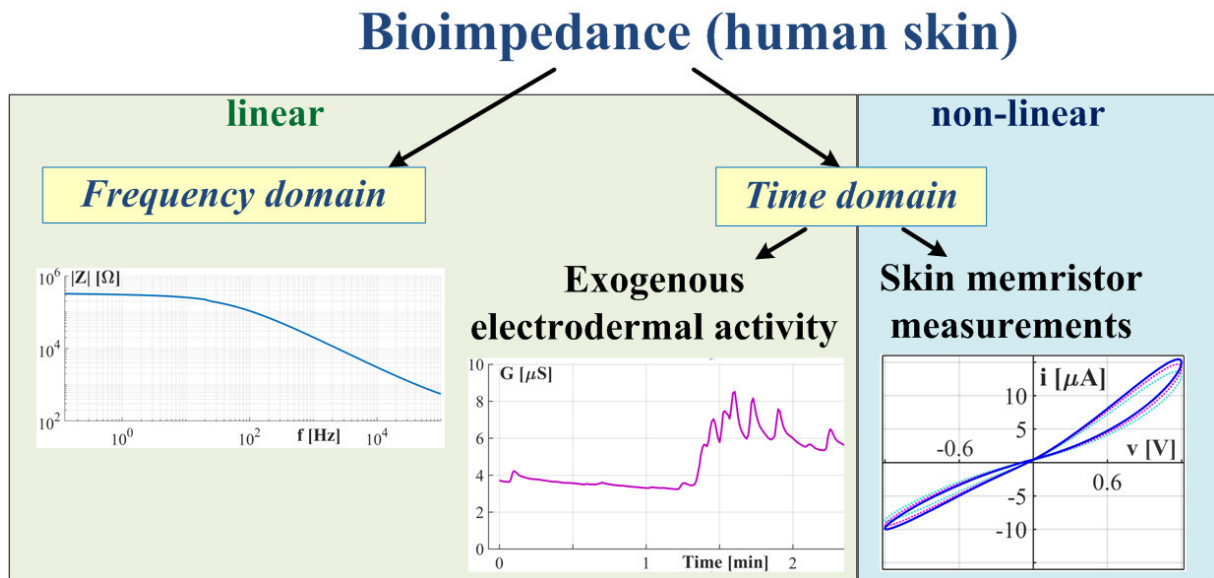


**Figure 1 | Overview of measurement methods on human skin within the field of Bioimpedance.** Recordings are done by the application of an electrical signal via electrodes to the tissue. The focus of this thesis are both, linear exogenous electrodermal activity (EDA) (related paper is [1]) and non-linear skin memristor (related papers are [2-4]) measurements. All linear recordings have in common, that the applied electrical signal itself does not affect the tissue, which is different within the non-linear recordings (see section 2.3).

The presented work can be placed within the field of Bioimpedance. This field encompasses the passive electrical properties of organic tissues and corresponding measurement techniques. The focus here is human skin and possible recording methods are sketched in Figure 1. One technique is the frequency response analysis (not subject of this thesis) that gives information about structure and composition of the skin (and biological tissues in general). Results are usually presented as Bode plots (see left plot in Figure 1). Measurements on human skin within the time domain are part of this thesis. Those can be divided into linear exogenous electrodermal activity (EDA) measurements and non-linear skin memristor measurements.

Recording of exogenous electrodermal activity (EDA) (see chapter 3) is a well-established technique. An external electrical signal (with constant frequency) is applied to the skin and the passive properties are measured over time (see Figure 1). It is consequently part of Bioimpedance. Endogenous EDA recordings on the other hand pick up innate electrical potentials of human skin and may be allocated to the field of Bioelectricity instead.

Recording of the non-linear properties of human skin (human skin acts like a memristor, see chapter 4) is a very new and undeveloped field. Since the memristor is declared as the fourth passive electrical circuit element [5] (see also section 2.4), this

new kind of measurements takes consequently place within the field of Bioimpedance. However, since the term “Bioimpedance” was only associated to linear measurements yet, the non-linear part of it might be also labelled as e.g. “non-linear Bioimpedance”, “state-dependent Bioimpedance” or “Biomempedance”.

## 1.1 Aim, objectives, and research questions

### Aim

The overall aim of this thesis was to *initiate non-linear electrical measurements on human skin as a new field of research*. The non-linear electrical properties of human skin are subject of this class of measurements. Only very little work related to this topic has been done before. If understood, non-linear measurements on human skin may provide new information that cannot be obtained by linear recordings. Potential applications in diagnostics of any disease that affects the non-linear properties of the skin might be found later.

### Objectives

This thesis contains pretty much pioneer work and in order to reach the overall aim, several objectives can be identified:

- *Signal conditions (frequency, amplitude) for linear and non-linear electrical measurements*. It was known that a measurement becomes non-linear if the amplitude of the applied electrical signal is high and the frequency is low. The exact conditions for the transition from linear to non-linear measurement were never studied before.
- *Direct comparison between the alternating current (AC) and the direct current (DC) method of recording electrodermal activity (EDA)*. For an EDA (small signal conductance) recording, the linear properties of human skin are subject of interest. This recording technique does not affect the skin itself and it can be used in combination with non-linear measurements for further insights into the skin physiology. However, the standard DC method may cause already a non-linear measurement and the AC method should be used instead. The comparability between both methods has to be studied.
- *Design, build and test of a measurement instrumentation suitable for non-linear measurements*. A measurement system (including electrode choice) has to be developed.
- *Development of non-linear recording methods*. There is no standard method for conducting non-linear skin (memristor) measurements. Recording techniques has to be developed.
- *Development of Parameterization for quantitative analysis of non-linear measurements on human skin*. There was no method available.

## Research questions

The non-linear electrical properties of human skin are only little understood and several research questions can be formulated:

- *Is it possible to characterize human skin as memristor?* This theory was given before, but it was never confirmed by a systematic study.
- *If yes, which type of memristor is human skin?*
- *Are there variations in the non-linear properties of human skin among subjects?*
- *Are there variations in the non-linear properties of human skin among different skin sites?*
- *Is it possible to store information in human skin?*
- *What causes the shifts in pinched point positions from the coordinate origin in the voltage-current plots?* A pinched hysteresis loop in the voltage-current plot (with pinched point in coordinate origin) is the fingerprint of a memristor.

## 2 Basics

### 2.1 Human skin

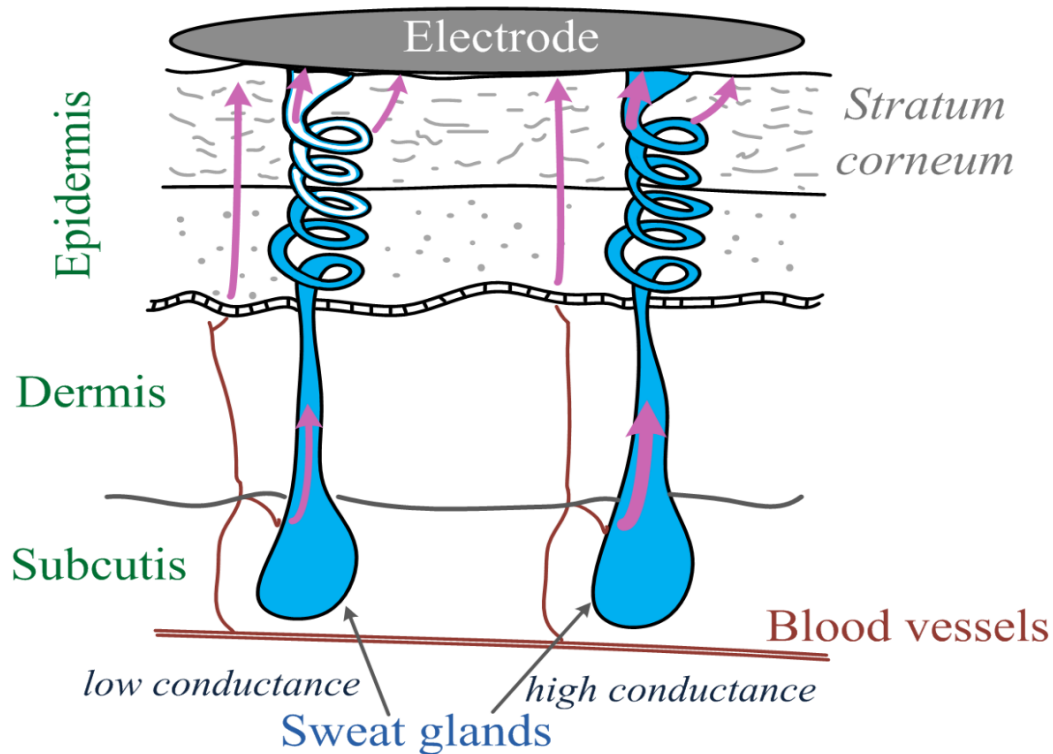


**Figure 2 | Schematic of human skin** showing different layers, sweat glands, blood vessels and possible current pathways through the glands and the epidermis (indicated by the purple arrows). The illustration is not to scale, e.g. the epidermis is actual much thinner than the dermis.

#### **Skin physiology and sweat gland density**

Human skin consists of different layers (see Figure 2). The thickness of the epidermis is usually 50 to 200  $\mu\text{m}$  except for the palmar and plantar sites where it is about 1 mm [6]. The epidermis consists of epithelial tissue. The stratum corneum is the outer part of the epidermis and consists of fully keratinized cells. The dermis is composed of tough, fibrous connective tissue and the subcutis consists of loose connective tissue. The secretory parts of the glands are located within the subcutis and the upper part of a sweat gland which is extending from the dermis to the epidermis up to the skin surface is called “sweat duct”. Sweat can reach the skin surface via a pore that forms the upper part of the sweat duct.

The secretion contains noticeable amount of cytoplasm from glandular cells in “apocrine” glands (the cytoplasm in the cells has to be replaced after the secretion) while it does not in “eccrine” glands [6]. Apocrine glands are mainly found on specific skin sites (like the areola region of the breast, axillaries and within the genital region)

**Table 1: Number of (eccrine) sweat glands per  $cm^2$  (mean values) at different sites of adult skin.**

Skin site:	palms	soles	forehead	tights	forearm	back
given in [7] <sup>1</sup>	233	620	360	120	-	-
given in [8]	600-700	600-700	181	-	108	64

and their contribution to the total amount of sweating is negligible [6]. Changes in sweating at skin sites apart from those regions (e.g. at the palms, the forehead and the forearm), are mainly determined by secretion and absorption of sweat from the eccrine glands. An estimation of the total number of sweat glands on the human body (skin area of an adult is about  $1.7 m^2$ ) is given as 1.6 million – 4 million [8]. The density of (eccrine) sweat glands differs among skin sites as it is shown Table 1.

### **Electrical measurements and current pathways through the skin**

Electrical recordings (of the passive properties of skin) are done by applying an external electrical signal via electrodes. In order to do so, it needs at least two electrodes to obtain a closed electrical circuit (with the skin as the load). The applied electrical signal can be either a constant current source or a constant voltage source<sup>2</sup>.

The whole skin tissue under an electrode (including e.g. many sweat glands) will contribute to an electrical measurement and possible current pathways are illustrated in Figure 2. Blood contains many free movable ions and pathways through the blood vessels are therefore highly conductive. The blood vessels do not extend to the skin surface (see illustration in Figure 2). Human sweat contains free ions and is therefore also well conductive. When the sweat ducts are highly filled, the sweat may reach the skin surface resulting in high conductive pathways (through the ducts) from the blood vessels and wet/viable tissue to the electrode (at the skin surface). As soon as the sweat duct is not filled up to the skin surface, its conductance decreases. However, a small film of sweat may remain on the sweat duct wall [9], allowing small currents to pass. Changes in sweating can consequently be recorded by electrical measurements.

Another current pathway goes from the blood vessels through the epidermis to the electrode. The stratum corneum mainly contains bound ions (causing capacitive properties) that do not allow direct current (DC) to pass but alternating current (AC). However, direct current pathways consisting of free movable ions are also existing within the stratum corneum [10]. Results from e.g. [1] indicate that there may be a current pathway from the sweat duct through the epidermis to the electrode. The sweat duct wall that has to be passed within this pathway is mainly capacitive (no free movable, but bound ions) and blocks direct currents but allows alternating current to pass (see chapter 3 for more explanations). Human hair is very high-ohmic [11] and

<sup>1</sup> According to [6].

<sup>2</sup> The measured electrical signal will be a voltage in the former case or a current in the latter case.

potential current pathways through the hair follicles<sup>3</sup> (at hairy skin sites like the dorsal forearm) are negligible.

### **Different types of sweating**

The secretory parts of the sweat glands are innervated by efferent vegetative nerve fibres that stimulate sweat secretion. The term “sweating” describes the secretion of sweat and implies that sweat reaches the skin surface. Sweating originates from activity in the sympathetic nervous system (that is part of the autonomic nervous system) and which may be triggered and controlled by the central autonomic network (CAN). The latter includes “*the insular cortex, amygdala, hypothalamus, periaqueductal gray matter, parabrachial complex, nucleus of the tractus solitarius, and ventrolateral medulla*” [12], regions of the brain. Sweat activity may be triggered by several of those regions and has several functions [6]. Thermal sweating (that is controlled by structures within the hypothalamus) regulates the body to an ambient temperature. Thermal sweating may change the sweat level over a quite long period (e.g. several minutes). “Emotional sweating” on the other hand may appear as response to external stimuli and emotional states like increased stress level. This type of sweating is mainly related to palmar and plantar skin sites but may occur also at other skin sites like e.g. the forehead [13]. Emotional sweating arises from different structures in the brain like e.g. hypothalamic structures (like thermal sweating, as well) but also from the amygdala. Single stimuli may elicit short lasting (several seconds) skin conductance responses (SCRs, see example of such a response in Figure 7 c)).

## **2.2 Note on (linear) impedance and admittance**

The term “Bioimpedance” is the short for “Biological impedance”. Impedance means “complex resistance” and its real part is called “resistance” and its imaginary part “reactance”. The inverse of the impedance  $Z$  is the admittance  $Y$  with  $Y=1/Z$ . Real and imaginary part of the admittance are called “conductance” and “susceptance”, respectively. The choice of admittance parameters instead of impedance parameter, in order to describe the human skin, is useful. The admittance (see also presentation in complex plane in Figure 3 a)) is defined by

$$Y = G + jB \quad (1)$$

and the impedance in analogy is defined by

$$Z = R + jX, \quad (2)$$

with  $j$  as the imaginary unit. In complex number theory it is defined that  $j^2$  is equal  $-1$ .

---

<sup>3</sup> Not illustrated in Figure 2.

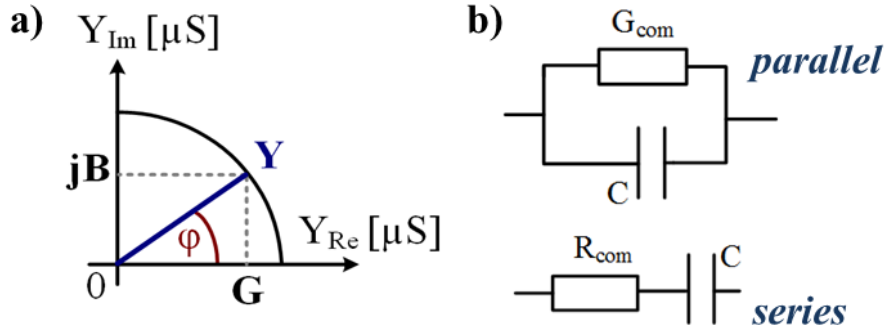


**Figure 3 | Complex load.** a) Admittance illustrated in a complex plane. b) Examples of complex loads: parallel and serial connections between a resistor and a capacitor (RC circuits).

The absolute values of impedance and admittance can be calculated by

$$|Z| = \sqrt{R^2 + X^2} \quad (3)$$

$$|Y| = \sqrt{G^2 + B^2} \quad (4)$$

and the phase angle is in general defined as

$$\tan \varphi = \frac{\text{imaginary part}}{\text{real part}} \quad (5)$$

For the impedance it is

$$\tan \varphi_{\text{imp}} = \frac{X}{R} \quad (6)$$

and for the admittance it is

$$\tan \varphi_{\text{adm}} = \frac{B}{G}. \quad (7)$$

### Simple RC parallel and simple RC series circuit

The admittance of the shown parallel circuit (see Figure 3 b)) is described by

$$Y = G_{\text{com}} + j2\pi fC = G + jB \quad (8)$$

with  $G_{\text{com}}$  as the conductance value of the electrical component itself and  $G$  as the overall conductance of the circuit. In this specific case,  $G_{\text{com}}$  and  $G$  are the same.

If impedance parameters are chosen the parallel circuit, it is described by

$$Z = \frac{1}{Y} = \frac{1}{G_{\text{com}} + j2\pi fC} \cdot \frac{G_{\text{com}} - j2\pi fC}{G_{\text{com}} - j2\pi fC} = \frac{G_{\text{com}}}{G_{\text{com}}^2 + (2\pi fC)^2} - j \frac{2\pi fC}{G_{\text{com}}^2 + (2\pi fC)^2} \quad (9)$$

$$= \frac{R_{\text{com}}}{1 + (2\pi fC \cdot R_{\text{com}})^2} - j \frac{2\pi fC \cdot R_{\text{com}}^2}{1 + (2\pi fC \cdot R_{\text{com}})^2} = R + jX. \quad (10)$$

It is important for the reader to understand that the overall resistance  $R$  of the parallel circuit is **not** 1 divided by the overall conductance  $G$ .

On the other hand, the component value of the resistor in the circuit  $R_{com}$  is equal to  $1/G_{com}$ . The overall resistance  $R$  of the parallel circuit is frequency dependent while the overall conductance  $G$  is not. Equation (10) simplifies to  $Z = R_{com} = R$ , if frequency is equal 0 Hz which is the case when a direct current (DC) signal is applied.

The serial connection of a resistor and a capacitor (see Figure 3 b)) can easily be described by the use of impedance parameters with

$$Z = R_{com} + j \frac{1}{2\pi fC} = R + jX . \quad (11)$$

The admittance of the series connection is described by

$$Y = \frac{1}{Z} = \frac{2\pi fC}{2\pi fC \cdot R_{com} + j} \cdot \frac{2\pi fC \cdot R_{com} - j}{2\pi fC \cdot R_{com} - j} = \frac{(2\pi fC)^2 \cdot R_{com}}{1 + (2\pi fC \cdot R_{com})^2} - j \frac{2\pi fC}{1 + (2\pi fC \cdot R_{com})^2} \quad (12)$$

$$= \frac{(2\pi fC)^2 \cdot G_{com}}{G_{com}^2 + (2\pi fC)^2} - j \frac{2\pi fC \cdot G_{com}^2}{G_{com}^2 + (2\pi fC)^2} = G + jB . \quad (13)$$

The overall conductance  $G$  in this connection is frequency dependent and if the frequency is zero, it becomes zero, since no DC current can pass the capacitor. The obtained impedance and admittance parameters are summarized in Table 2. The phase angle of the admittance and impedance parameters can be calculated by the use of equations (6) and (7). The relation

$$\varphi_{adm} = -\varphi_{imp} \quad (14)$$

applies for both, the RC parallel, as well as, the series circuit.

**Table 2: Admittance and impedance parameters of simple RC series and simple RC parallel circuits.**

	<b>RC parallel</b>	<b>RC series</b>
$R =$	$\frac{R_{com}}{1 + (2\pi fC \cdot R_{com})^2}$	$R_{com}$
$X =$	$-\frac{2\pi fC \cdot R_{com}^2}{1 + (2\pi fC \cdot R_{com})^2}$	$\frac{1}{2\pi fC}$
$G =$	$G_{com}$	$\frac{(2\pi fC)^2 \cdot G_{com}}{G_{com}^2 + (2\pi fC)^2}$
$B =$	$2\pi fC$	$-\frac{2\pi fC \cdot G_{com}^2}{G_{com}^2 + (2\pi fC)^2}$

## 2.3 Linear and non-linear measurements

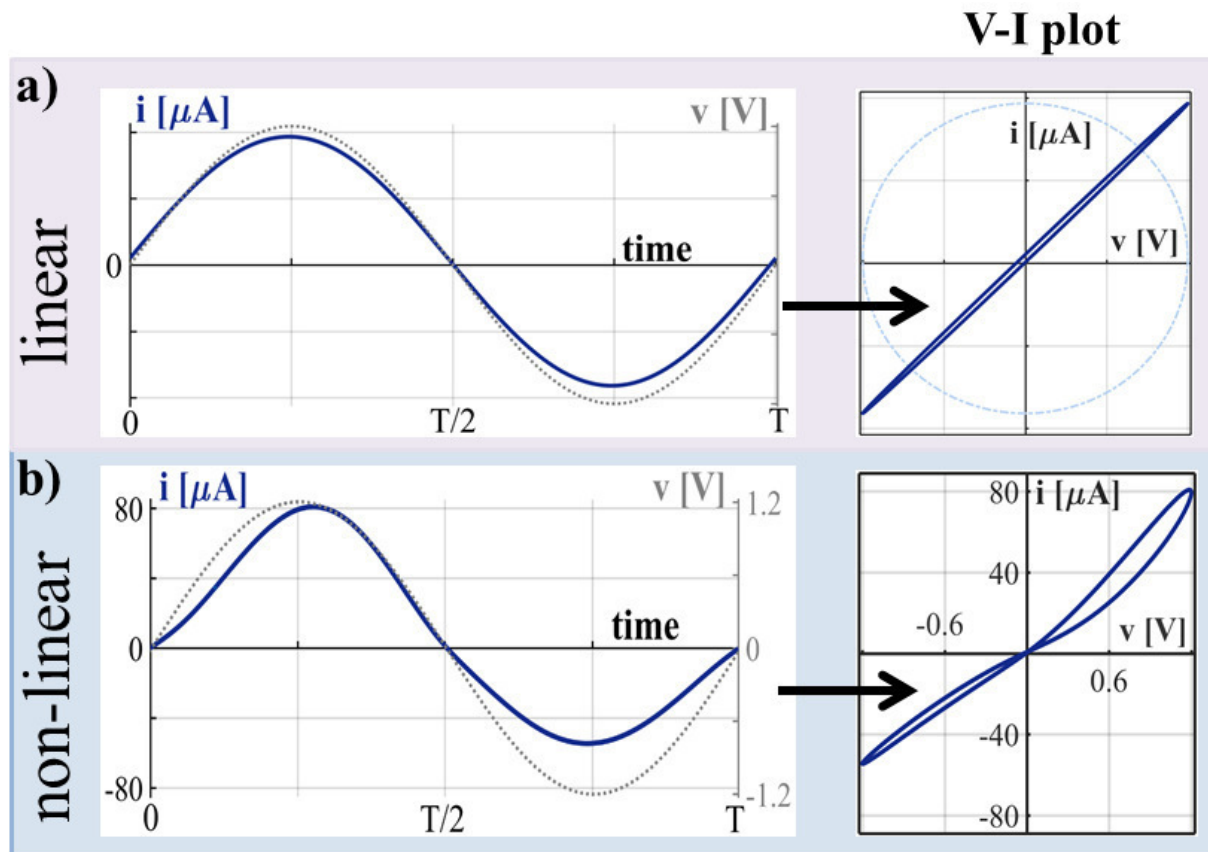


**Figure 4 | Examples of linear and non-linear signals.** Applied sinusoidal voltage  $v$  and measured current  $i$  over time (left) and corresponding voltage-current (V-I) plots (right). **a)** Illustration of applied and measured signal that is linear. The current  $i$  has a small phase shift (1.44 degree) with respect to the voltage  $v$  and a small DC offset. The shape of the current is sinusoidal as it is for the voltage. The resulting V-I plot shows an elliptic shape. It would result in a straight line if the phase angle is zero or in a circle (as it is shown additionally, see light blue plot) if the phase angle is 90 degrees. **b)** Real measurement on human skin within the non-linear range. The recording is done at the forehead with applied sinusoidal voltage with  $f=0.05$  Hz and amplitude of 1.2 V. The shape of the measured current  $i$  is deformed and deviates from sinusoidal shape. The measured current  $i$  might have a small phase shift and DC offset in addition. The resulting V-I plot shows a pinched hysteresis loop with pinched point position in the coordinate origin.

An illustration of a linear recording with sinusoidal signal is given in Figure 4 a). If e.g. a sinusoidal voltage  $v$  is applied, the measured current  $i$  might have a phase shift and a DC offset but its shape will be sinusoidal, as well. The corresponding voltage-current (V-I) plot (also called Lissajous figure) of a linear measurement will show an elliptic shape like illustrated in Figure 4 a), if there is a small phase shift between current and voltage. If the phase shift is 90 degree (measurement on a single capacitor) the V-I plot turns into a circle like illustrated in Figure 4 a), and a straight line can be seen, if the phase shift is zero (measurement on a single resistor).

If the measured signal is deformed (see Figure 4 b)), i.e. its shape is different from the shape of the applied signal, the measurement is non-linear. The applied signal itself affects the tissue, which is the reason for the deformations. The resulting voltage current plot in Figure 4 b) shows a hysteresis loop with pinched point in coordinate origin, which is the “fingerprint” of a memristor (see below).

Measurements on human skin can be either linear (see chapter 3) or non-linear (see chapter 4) dependent on the applied signal. It is stated in [14] that the “*the non-linearity (of human skin) is more apparent with a larger current (and) a lower frequency*”. Estimation of a boundary in the frequency-amplitude plane between linear and non-linear measurements at the forehead (based on the data from Paper II) is presented in chapter 4. Recording techniques can be found within both (see Figure 1). However, if a linear recording technique is conducted, a quite high frequency and/or low amplitude should be chosen in order to assure that the measurement does not become non-linear.

## 2.4 The memristor

In 1971, Leon Chua postulated the existence of a fourth passive electrical circuit element, which he called a “memristor” [5]. His argumentation was based on the missing definition of the relationship (see also illustration in [15]) between two out of the four fundamental circuit variables (current  $i$ , voltage  $v$ , flux  $\phi$ , charge  $q$ ). Charge is the time integral of the current and flux is the time integral of the voltage, given as

$$dq = \int i \cdot dt \quad (15)$$

$$d\phi = \int v \cdot dt . \quad (16)$$

Further linkages are known as

$$dv = R \cdot di \quad (17)$$

$$d\phi = L \cdot di \quad (18)$$

$$dq = C \cdot dv , \quad (19)$$

with  $R$  as the resistance,  $L$  the inductance and  $C$  the capacitance. Leon Chua pointed out that there is a missing definition of the relationship between the charge  $q$  and the flux  $\phi$ . A definition can be given by

$$d\phi = M \cdot dq , \quad (20)$$

with  $M=M(q)$  as the memristance and multiplication on both sides with  $1/dt$  leads to

$$v = M \cdot i = M(q) \cdot i . \quad (21)$$

Equation (21) describes the state-dependent version of Ohm's law and the memristance  $M(q)$  (in analogy to resistance) depends on the internal state that is determined by the charge  $q$  and hence on the previous history. The term "memristor" is a composition of the terms "**memory**" and "**resistor**" and the unit of the memristance is  $\Omega$ , as well. Further, equation (21) describes the current controlled version of the state dependent Ohm's law and the voltage controlled variant can be described by

$$i = G(\varphi) \cdot v, \quad (22)$$

with  $G(\varphi)$  as the state dependent conductance (memductance) in analogy to (linear) conductance  $G$ .

### **Memristor fingerprints**

The term "memristor" is now used as a more generalized concept and different classes are defined (see section below). Chua stated that "*every 2-terminal device that is pinched for any periodic signal in the V-I plane and that passes the origin is called a memristor*" [16] (see pinched hysteresis loop example in e.g. Figure 4 b)). He called this pinched hysteresis loop property as the "fingerprint" of a memristor [17]. The V-I plot can have several pinched points and the branches of the hysteresis loop can even pass the second and the fourth quadrant. The crucial property is the pinched point in the origin. It can be either "transversal", implying that the two branches of the hysteresis loop cross the pinched point with different slopes or "tangential" which implies that those branches are just "touching". The pinched point can be slightly shifted from the origin as an exception made for organic memristors since parasitic elements might influence the measurement [16, 18].

Two additional fingerprints are defined in [19]: The lobe area of the hysteresis loop decreases with increasing signal frequency  $f$  and the V-I plot tends towards a single valued curve for  $\lim f \rightarrow \infty$ . Thus, the appearance of the pinched hysteresis loop depends on the signal frequency as well as the signal amplitude.

Produced components that fulfil the mentioned fingerprints can be classified as memristors. Corresponding models (containing the component specific state dependent Ohm's and state equations) enable calculation and prediction of the voltage-current characteristics (see e.g. the model of the Hewlett Packard memristor in [20]). Any (not man-made) tissue that fulfils the mentioned fingerprints can be classified as a memristor (component), as well, and a corresponding model can be developed. Any tissue that does not fulfil the fingerprints is not a memristor and cannot be modelled as a memristor. The term "memristive properties" implies that the tissue or device fulfils the mentioned fingerprints and describes corresponding voltage-current characteristics.

## Different classes of memristors

**Table 3: Overview of the four memristor classes [21] (voltage controlled versions).**

Memristor type	<i>Ideal</i>	<i>Ideal generic</i>	<i>Generic</i>	<i>Extended</i>
<b>State dependent Ohms law</b>	$i = G(\varphi) \cdot v$	$i = G(x) \cdot v$	$i = G(\mathbf{x}) \cdot v$	$i = G(\mathbf{x}, v) \cdot v$ $G(\mathbf{x}, 0) \neq \infty$
<b>State equation</b>	$\frac{d\varphi}{dt} = v$	$\frac{dx}{dt} = g(x) v$	$\frac{d\mathbf{x}}{dt} = \mathbf{g}(\mathbf{x}, v) v$	$\frac{d\mathbf{x}}{dt} = \mathbf{g}(\mathbf{x}, v) v$
<b>Internal state variable</b>	Flux $\varphi$	General variable $x$	Vector of internal state variables $\mathbf{x}$	
<b>Indication</b>	*1, *2, *3	*1, *3	*3	*4
	*1 Pinched hysteresis loop in the V-I plot is odd-symmetric. *2 $\varphi$ -q plot results in a straight line. *3 V-I plot tends towards a straight line for $\lim f \rightarrow \infty$ . *4 V-I plot tends towards a single valued curve for $\lim f \rightarrow \infty$ .			

Different classes of memristors can be defined [21] based on the internal state variable of the memristance (or memductance) and the state equation that describes its change (see Table 3). Ideal memristors (like originally published in [5]) are most specific and the internal state of the memductance is directly determined by the flux  $\varphi$  (and the memristance is a direct function of the charge  $q$ ). Ideal memristors form a subgroup of ideal generic memristors. A general variable  $x$  describes the internal state of the latter and the substitution from  $\varphi$  to  $x$  is described by the morphing function  $g(x)$ . Ideal generic memristors are a subgroup of generic memristors. The morphing function of the latter depends on the voltage  $v$  in addition and the memductance might be determined by several internal states ( $\mathbf{x}$  is a state vector). The class of extended memristors is most the general (generic memristors form a subgroup of it). The memductance itself may a function of the voltage in addition to the internal state variables.

Indications of either memristor classes are the appearances of the pinched hysteresis loops (see Table 3). Ideal memristors and ideal generic memristors are odd symmetric with respect to the origin (in the V-I plane). The  $\varphi$ -q plot of an ideal memristor will additionally result in a straight line, while it is a single valued curve for ideal generic memristors. Generic and extended memristors can be identified by pinched hysteresis loops that are not odd-symmetric. The V-I plot of a generic memristor will tend towards a straight line for signal frequency  $\lim f \rightarrow \infty$  while it will be a single valued curve (in general) for extended memristors.

### **Volatile and non-volatile property**

Independent of the class (see above), memristors can be divided into volatile and non-volatile memristors. Volatile memristors imply that there is only one steady state and that the current responses to periodic constant voltage steps are periodic. A non-volatile memristor has at least two steady states. Current responses to periodic constant voltage steps are not periodic (see e.g. Figure 11 a)) and pinched hysteresis loops depend on the initial state of the memristor. Since non-volatile memristors have several steady states, they may be used for information storage.

### **Closure theorem of memristors**

Electrical circuits (one port) that only contain memristors can be described by single memristor equivalents [5]. If a single sweat duct can be classified as a memristor, the parallel connection of several sweat ducts (under the same electrode) can be described as a single memristor, as well (see illustration in Figure 1 in [3]). The theorem is valid even when the circuit contains different memristor types.

### **Research on memristors**

The memristor as a subject of research became more popular after a research group from Hewlett Packard presented a first realization (based on titanium dioxide) in 2008 [20, 22]. One part of recent research is the realization of memristors based on different materials (e.g. tantalum oxide [23, 24] and zinc oxide [25]) and the investigation of the underlying resistive switching mechanism [26, 27]. Circuits based on memristors that fulfill different functions represent another field of recent research. Examples are the use of memristors in neuromorphic computing [28-30], or e.g. memristor circuits that fulfill arithmetic operations [31, 32]. A 4-memristor bridge circuit (like a Wheatstone bridge but all resistors are replaced by memristors) can be used for synaptic weight programming [33], for generation of  $n$ th-order harmonics and frequency-doubling [34] or for generation of signals similar to neuronal pulses [35]. The first organic memristors beside human skin have been demonstrated lately, as well. Examples are the Venus flytrap [36] and slime mould memristors [37].

### 3 Linear skin measurements

*Characteristics:* The tissue is not affected by the applied electrical signal.

*Related paper:* The paper[1] which is part of this thesis can be placed within the linear measurement range. Small signal (linear) conductance measurements were also done within experiment 2 in [2].

#### 3.1 Linear skin admittance

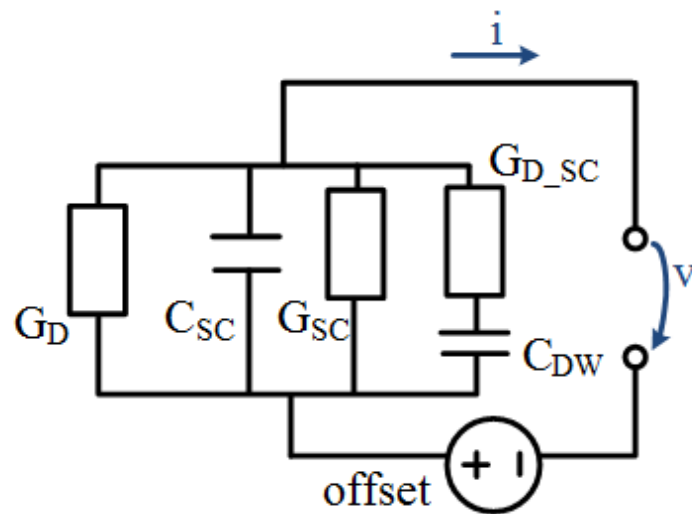


**Figure 5** | *Skin equivalent circuit with the linear measurement range.*

The conductive pathway through the sweat ducts (see Figure 2) is represented by  $G_D$ . Its value is dependent on the sweat duct filling and the number of sweat glands that contribute to the measurement. The capacitance  $C_{SC}$  represents capacitive properties of the epidermis (dominated by bound charges in the stratum corneum). The capacitance value increases with increasing humidity in the stratum corneum [38]. The component  $G_{SC}$  represents the conductive pathway through the stratum corneum (as described in section 2.1). The overall skin conductance increases with increasing frequency (see Figure 2 in [39]), which means that it contains a frequency dependent part that may be modelled by a series connection of a capacitance and resistance (see Table 2). The series connection of  $C_{DW}$  with  $G_{D\_SC}$  reflects a possible current pathway from the sweat duct through the sweat duct wall (represented by  $C_{DW}$ ) through the upper part of the stratum corneum. The current through this pathway would be affected by the sweat duct filling and may explain variations in the difference between AC and DC conductance recordings [1] (this is the frequency dependent part ( $G(f)$ ) of the AC conductance  $G_{AC}$ , see also section 3.3 within this thesis). The overall admittance of the equivalent circuit shown in Figure 5 is determined by the parallel connection of the described pathways and can be expressed by (single components are found in Table 2)

$$Y = G_{DC} + \frac{(2\pi f C_{DW})^2 \cdot G_{D\_SC}}{G_{D\_SC}^2 + (2\pi f C_{DW})^2} + j \left( 2\pi f C_{SC} - \frac{2\pi f C_{DW} \cdot G_{D\_SC}^2}{G_{D\_SC}^2 + (2\pi f C_{DW})^2} \right) \quad (23)$$

$$= G_{DC} + G(f) + j B = G_{AC} + j B = G + j B \quad (24)$$

with  $G_{DC} = G_D + G_{SC}$  as the part of the overall conductance that is not frequency dependent and  $G(f)$  as the frequency dependent part that becomes zero if the frequency is equal 0 Hz (see DC method of recording EDA) and  $G_{AC} = G = G(f) + G_{DC}$  as the conductance that is measured within an AC measurement (see below). The frequency dependent part of the skin conductance and the susceptance are related to each other (e.g. the denominator of both is equal) but both are describing different quantities (see equations (23) and (24)). The offset (see Figure 2) originates from e.g. skin potential differences and may interfere the measurement.

## 3.2 Recording of exogenous EDA

### Background

The term electrodermal activity (EDA) (introduced in [40]) describes all “*electrical phenomena in skin*” [6]. Recording of exogenous (EDA) is an established “*tool in basic, as well as in applied, psychophysiological research*” [6] that has been used among several research groups and decades. Temporal changes in low-frequency skin conductance due to sudomotor activity can be recorded. The sudomotor activity is regulated by the autonomic/sympathetic nervous system and EDA recordings thus reflect its activity [41]. EDA is also labelled as a “measure of arousal”. Recordings are usually done on skin sites that are known for emotional sweating (i.e. palmar and plantar skin sites, see section 2.1). Different psychological disorders may be diagnosed by exogenous EDA e.g. it is shown that schizophrenic patients show little sweat activity to stimuli compared to a control group on the one hand but show higher amount of spontaneous skin conductance responses on the other hand [42]. Recent research groups try to classify emotions by exogenous EDA recordings (mostly as part of multisensory approaches including the recordings of other Bio-signals, as well) [43-45].

### Parameterization (EDA scores)

EDA scores are commonly used in order to evaluate recorded data quantitatively. The distinction between tonic and phasic electrodermal activity is given in the literature [6]. Phasic electrodermal activity describes the short-term changes in skin conductance that are directly related to the sweat gland activity. Phasic responses (an example is presented in Figure 7 c)) may occur directly to external stimuli but also spontaneously (in absence of external stimuli). Examples of phasic EDA scores are

response amplitude (illustrated in Figure 7 c)), rise and recovery times (see Figure 5 in [1] for illustration) and number of responses within a specific time frame.

Tonic activity reflects the (long-term) change in overall skin conductance level that can have many origins like a change in temperature of the skin or an increase of the corneal hydration due to increased sweating.

### **Different methods of recording exogenous EDA**

Recording of exogenous EDA (admittance/conductance in general) can be done by either applying a direct current (DC) or an alternating current (AC) signal. Further, the applied signal might be provided by a constant current source but the choice of a constant voltage source instead is recommended [46].

#### DC method

The most common method is the application of a constant DC voltage (0.5 V) [46]. Only resistive properties of the skin are measured by the DC method (those are mainly determined by the sweat duct filling [10]) and the conductance can be obtained by Ohm's law as it is illustrated in Figure 6 a). Skin potential differences will erroneously add to the measurement. Electrodes are usually placed on skin sites that have similar skin potential levels in order to meet this problem. Furthermore, the influence of the potential differences are reduced by the use of the quite high DC level (0.5 V) of the applied voltage. Electrode polarization is another error source that will add to a DC measurement and the effect can be reduced by the use of non-polarizable electrodes like silver/silver chloride (Ag/AgCl) electrodes. The results in [2] indicate that non-linear properties of human skin may already occur at a DC level of 0.5 V and thus erroneously affect the EDA measurement.

#### AC method

A sinusoidal voltage with a certain frequency is used as source (Figure 6 b)) and capacitive properties of human skin will consequently add to the measurement. The measured current will experience a phase shift with regard to the applied voltage and it is not possible to determine the conductance directly by Ohm's law. The signal can be separated into real part (conductance) and imaginary part (susceptance) by means of phase shift sensitive rectification (lock-in amplification) [47] (see also section 5.3 within this thesis). Each conductance and susceptance value is usually obtained from several signal periods of the measured current as it is indicated in Figure 6 b). The chosen signal frequency of the applied voltage is not standardized but it should be within a limited range. The frequency has to be high enough in order to enable the detection of quick changes [39]. On the other hand, if the signal frequency is too high (e.g. above 500 Hz) [48], the frequency dependent part of the conductance dominates [39] and the sensitivity of the measurement will be reduced. Examples of chosen signal frequencies are 20 Hz in [1], and 8 Hz and 88 Hz in [38]. The AC method has several advantages compared to the DC method. Non-linear effects in skin and

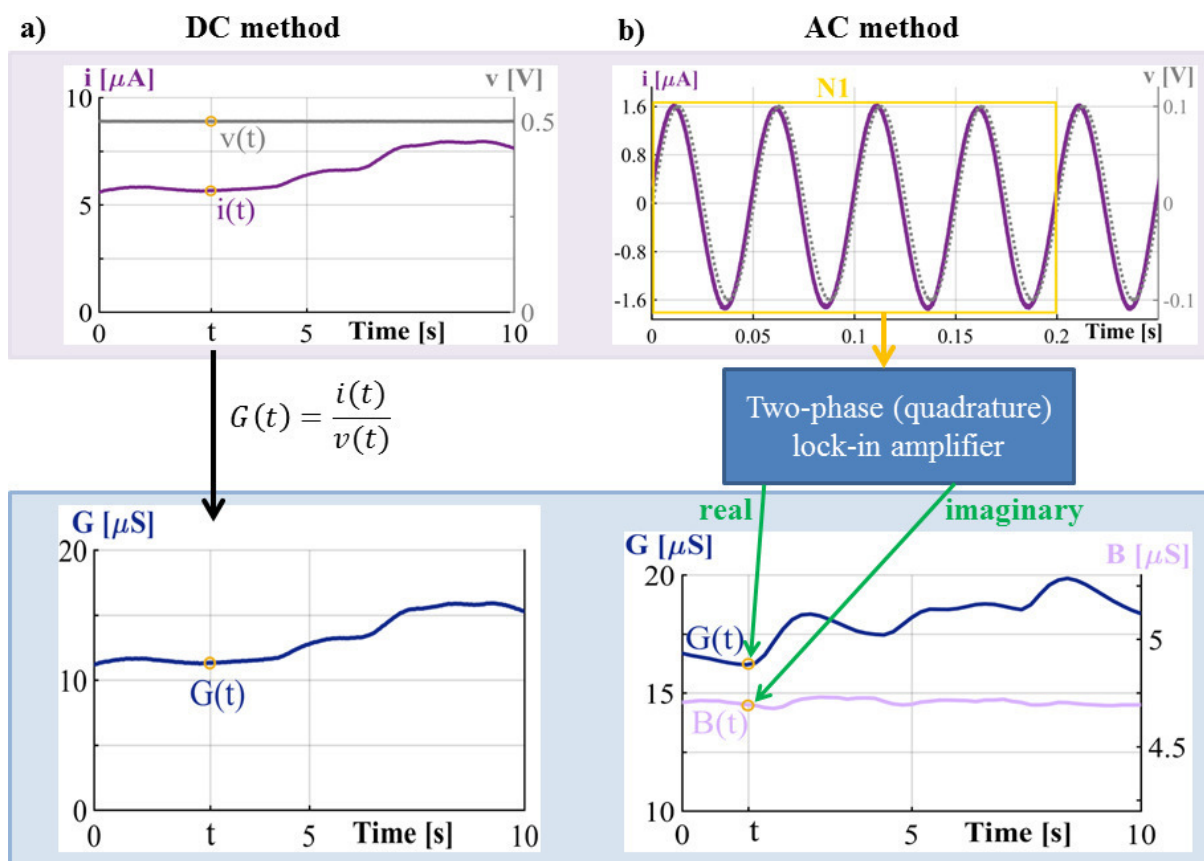


**Figure 6 | Two different methods of recording exogenous electrodermal activity are illustrated. a)** A DC (direct current) voltage is applied and the corresponding current is measured. The conductance at time  $t$  can simply be determined by Ohm's law. The applied voltage level in the standard DC method is 0.5 V. **b)** AC (alternating current) method. A sinusoidal voltage is applied (e.g. with  $f=20$  Hz and amplitude of 0.1 V like in this example). The measured current may be phase shifted and its real and imaginary part (in order to calculate conductance and susceptance, respectively) can be obtained by lock-in amplification. The skin susceptance is a measure that becomes available if the AC rather than the DC method is chosen. Several signal periods of the measured current are used for calculating one conductance and one susceptance value as it is illustrated. In this example, the four signal periods within the yellow frame are used for calculating one sample  $N1$  of the conductance and the susceptance at time  $t$ . The following sample is calculated by the following four periods of the measured current and so on.

electrode polarization will be avoided if the AC method is chosen. The skin potential difference (which is a DC component with changing magnitude) can be easily separated from the actual recording (which is a sinusoidal signal). Endogenous skin potential and exogenous skin conductance can be measured in parallel under the same electrode [49], as one consequence. Furthermore, the chosen amplitude of the applied voltage can be rather small (e.g. 30 mV in [50], 100 mV in [2]). The skin susceptance is an additional measure that becomes available if the AC method is chosen. The skin susceptance is mainly related to the humidity in the stratum corneum [38] and might

provide complementary information to the conductance measurement. The combination of skin conductance, susceptance and endogenous potential might be subject of further studies. First related papers are [51, 52].

### **3.3 Direct comparison between the AC and the DC method of recording EDA**

#### **Motivation**

Measuring electrodermal activity with a DC rather than an AC signal demands less instrumentation effort, which might be the reason for its establishment as a standard. There are some research groups that used the AC method (e.g. [53], [54]) already decades ago, but many more studies have been conducted by using an applied DC signal. Today, it is also quite easy to implement the AC method with current technology, but still there are more recent research groups that use the DC method (e.g. [55, 56]) rather than groups using the AC method (e.g. [50]).

In their publication recommendation report of the Society of Psychophysiological Research [46], the authors acknowledged the superiority of the AC method but did not recommend it as a standard since too little was known about the comparability between the AC method and the DC method. They appealed for research on a comparison between both and this request was met with paper I ([1]). EDA was recorded with both methods at the same time under the same electrodes. This was achieved by superposition (see Figure 1 in [1]) of a DC voltage of 0.5 V (standard level in the DC method) with a sinusoidal voltage with amplitude of 0.5 V and frequency of 20 Hz. It was the first time that a direct comparison between both methods was done.

#### **Results**

The obtained conductance recordings of both methods are quite similar as it can be seen from the example in Figure 7. Based on the statistical evaluation of different EDA scores<sup>4</sup> it was shown that there are in general no statistical significant differences between  $G_{AC}$  and  $G_{DC}$  except for the conductance level ( $G_{DC}$  is always below  $G_{AC}$ ). However, the difference between both varies slightly with time as it can be seen from the plot “ $G_{AC} - G_{DC}$ ” (which reflects the frequency dependent part  $G(f)$ , see equation (24)). This might be explained by the current pathway from the sweat ducts through the sweat duct wall through the epidermis ( $C_{DW}$  in series with  $G_{D\_SC}$ , see Figure 5). As the sweat gland/duct filling increases, both  $G_{AC}$  and  $G_{DC}$  increase and sweat that reaches the skin surface may penetrate the surrounding stratum corneum, which can be noticed by a small susceptance increase (see Figure 7 b)). This may also increase the

---

<sup>4</sup> Evaluation was done over all recorded responses from all 28 test subjects in [1].

amount of free movable ions within the upper part of the stratum corneum (which increases the conductance of this part). An increased sweat duct filling will in any way increase  $G(f)$  (see Figure 7 b)) since the contributing area between sweat duct and epidermis (through which the AC current can pass) will be increased, as well. The (small) time varying differences between AC and DC conductance may be part of future research in order to obtain more insights into the skin and sweat gland/duct physiology.

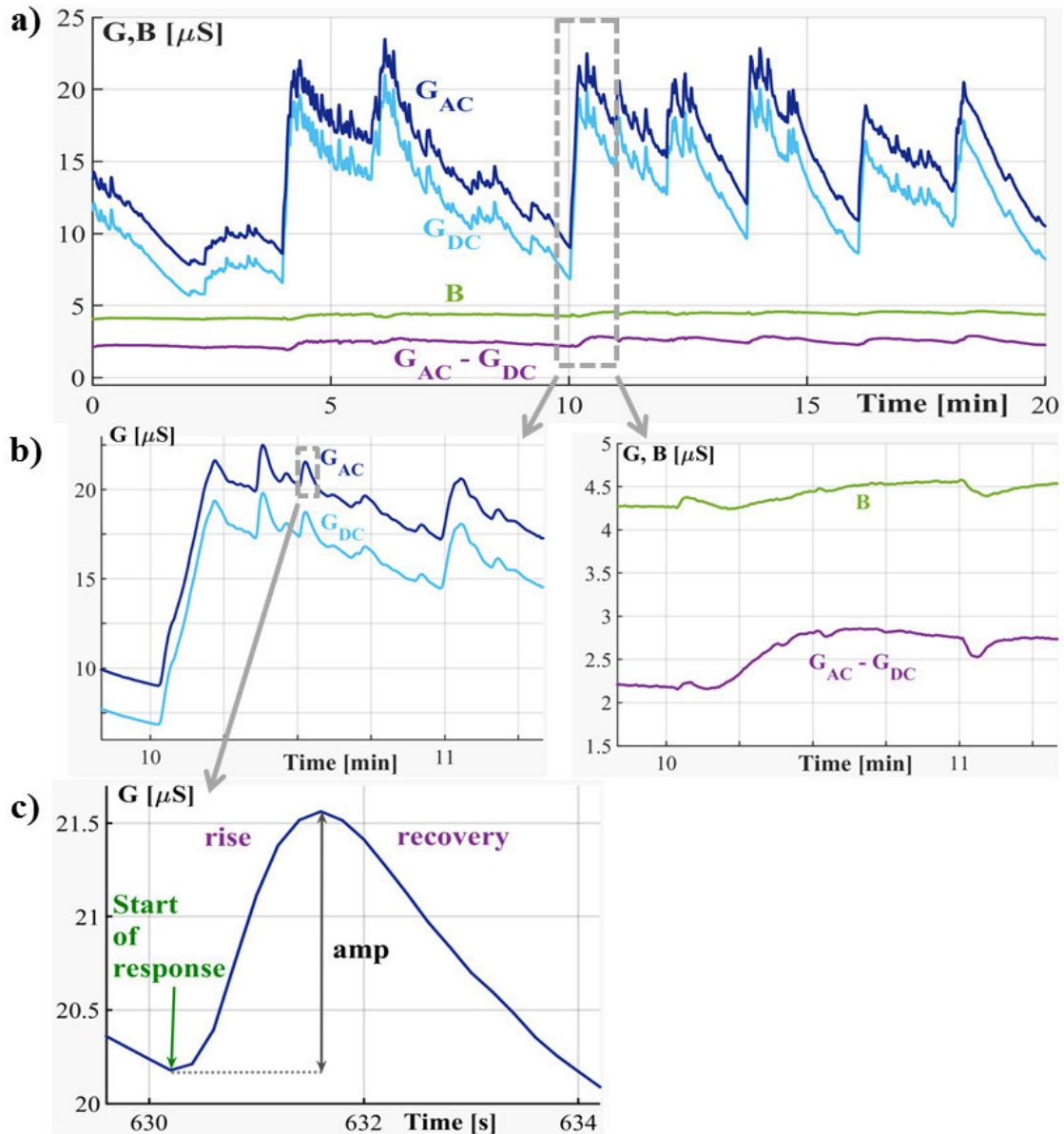


**Figure 7 | Exogenous EDA simultaneously recorded with the AC and the DC method** shown for one test subject **a)** within the whole duration of experiment 1 in [1] and **b)** over a duration of about 1.5 minutes. Conductance plots are labeled with  $G_{AC}$  and  $G_{DC}$  respectively. The pairwise conductance difference  $G_{AC} - G_{DC}$  reflects the frequency dependent part  $G(f)$  of the AC conductance (compare with equation (24)). The susceptance  $B$  is only obtained by the AC measurement. **c)** Single skin conductance (phasic) response that has duration of about 4 seconds (from the  $G_{AC}$  recording).

## 4 Non-linear skin memristor measurements

*Characteristics:* The tissue is affected by the applied electrical signal. The tissue has an internal state that might change by the measurement itself.

*Related papers:* The papers [2-4] which are part of this thesis can be placed within the non-linear measurement range. The results that are presented in this chapter are mainly from paper [2].

### 4.1 Motivation and Background

Grimnes reported non-linear deformations of the measured current through the skin when he applied low frequency sinusoidal voltages with high amplitudes (e.g. 13 V) to the ventral forearm and dorsal hand sites [57]. He explained the observations by electro-osmosis, the directed motion of liquids caused by an electric field. Yamamoto and Yamamoto presented pinched hysteresis loops in the V-I plane (Lissajous figure) already in 1981 from recordings at the forearm using a constant current source [14] (sinusoidal, low frequencies) but did not link the observations to the memristor<sup>5</sup> theory. Johnsen *et. al.* concluded later that human skin behaves like a memristor and presented a first model [58] according to the data presented in [57]. Since then, the non-linear properties of human skin have not been studied further, yet.

The non-linear skin (memristor) properties may provide new information that cannot be obtained by linear measurements, which gives already good reason for further research. The properties of the skin memristor were studied (for the first time) systemically in Paper II ([2]). This was a first step into this new undeveloped field of research. The “skin memristor” as it is first described in [58] has to be labelled more precisely as “sweat duct memristor” (see also section 4.2) since there is strong evidence for a second non-linear mechanism [2]. It is likely that the latter one is located within the stratum corneum and may be regarded as a negative temperature coefficient (NTC) thermistor, which may be modelled as a memristor itself (see section 4.3). The skin memristor as such is a combination of the sweat duct memristor and the stratum corneum NTC thermistor (see section 4.3). Findings of the study in Paper II are presented within this chapter and an outlook for possible applications and research within the field of non-linear skin memristor measurements will be given.

---

<sup>5</sup> The concept of the memristor was hardly known at that time.

## 4.2 The sweat duct memristor

### Effect of electro-osmosis on skin

The polarity of the applied signal determines the direction of the motion of the sweat as illustrated in Figure 8 a) and c). The level of sweat duct filling changes consequently, resulting in a change of the state dependent conductance (memductance). When the direction of the motion is towards deeper skin layers, a small film of sweat may remain at the sweat duct walls [9, 58], allowing a small current to pass. The mechanism of the electro-osmotic effect in human skin, as it is described so far, was already explained in [57, 58]. The results from experiment 2 (applied DC voltage pulses) in Paper II indicate that the states of the sweat ducts do not remain constant after the voltage is released. If the applied voltage is negative (see Figure 9 a)), the memductance decreases (resulting in a decrease of the amount of current). As soon as the voltage is released, the memductance increases immediately (the amount of current is larger at the beginning of a pulse than at the end of the previous pulse). When the applied voltage is positive (see Figure 9 b)), the memductance increases but as soon as the voltage is released, it decreases immediately. The changes between pulses are quite fast and might be explained by pressure driven forces (see illustrations in Figure 8 b) and d)). Those may occur in the corneum [59] and since the memductance increases immediately after a negative applied voltage is released, the forces may occur also in deeper skin layers (see illustrations in Figure 8 a) and b)). It is not certain how much sweat is actual moved during the electro-osmotic process in the sweat duct. If the moved sweat volume in the duct is quite large, it is likely that the sweat duct/gland in the deeper layers expands, as well (as it is illustrated in Figure 8 a) and b)). However, small changes in sweat level in the ducts may already cause a noticeably change in memductance. It might be possible that the volume of moved sweat in the duct (during electro-osmosis) is rather small. If so, only pressure driven forces within the stratum corneum would contribute noticeably to the change in memductance after the voltage is released.

The pressure driven forces might not occur in some subjects and the state of the sweat ducts/glands consequently remains almost constant between pulses (compare the results of different subjects in Figures 4 a) and c) in [2]). Reabsorption processes will affect the state of the sweat duct memristor, as well. Changes in the state dependent conductance by reabsorption processes are slower than the changes caused by pressure driven forces.

The recording from the fingertip (see Figure 9 c)) is an example in which the change in current is not caused by electro-osmosis but by sympathetic activation of the sweat glands. Skin conductance responses interfere the measurement (compare e.g. with the small signal conductance plot in Figure 7 b)) and there is no clear trend in current development.

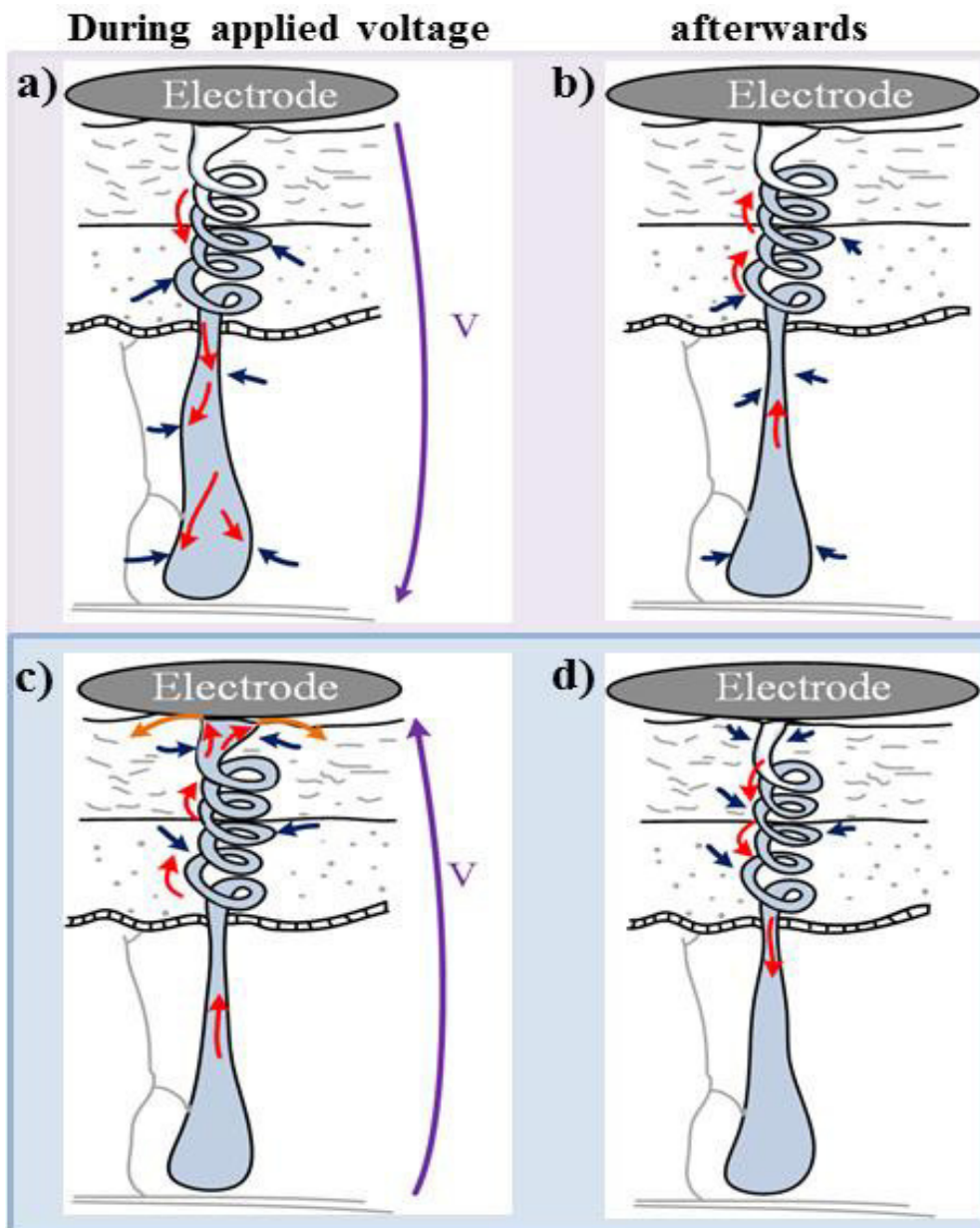


**Figure 8 | Illustration of change in sweat level in a single sweat gland/duct while a voltage  $v$  is applied and afterwards released.** The here shown illustration is based on the findings from applied DC pulse series (Paper II, see also Figure 9). Red arrows indicate direction of ion movements. Red arrows indicate possible ion movements, while blue arrows indicate possible pressure driven counter-forces that build up when the volume of the sweat gland/duct increases. **a)** The direction of the voltage is from skin surface towards deeper skin layers. The sweat is pushed towards deeper layers, resulting in a membrane conductance decrease, as well as an increase of the sweat gland/duct volume within the deeper layers. **b)** Resulting counter-forces will move the sweat back towards the skin surface as soon as the voltage is released. **c)** The direction of the voltage is from deeper skin layers towards the skin surface. The sweat is pulled towards the skin surface resulting in a strong membrane conductance increase. Sweat that reaches the skin surface may diffuse into the surrounding tissue (illustrated by orange arrows). **d)** Pressure driven forces will push the sweat back towards deeper skin layers as soon as the voltage is released.

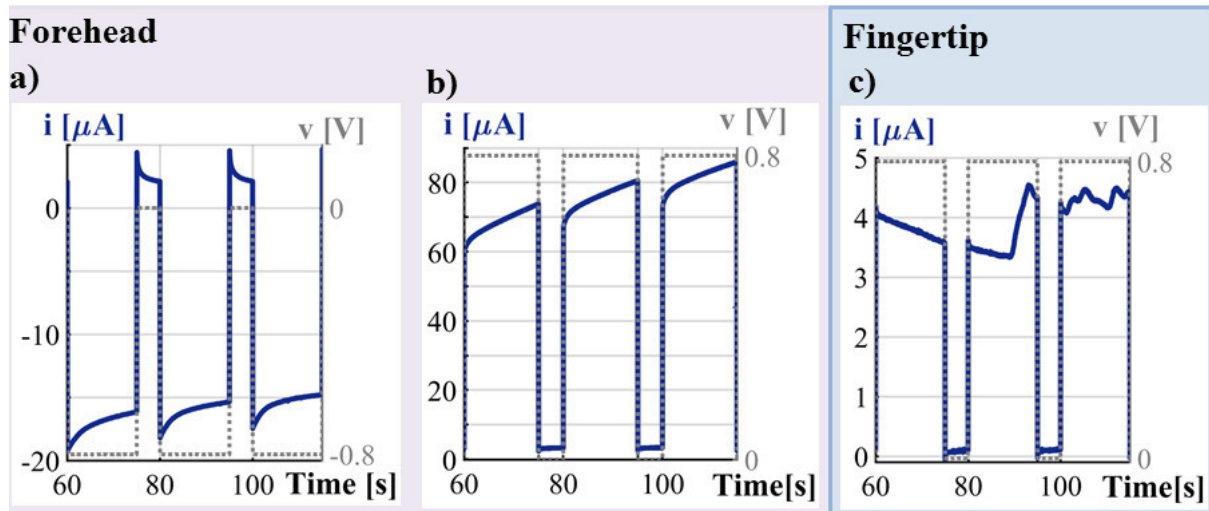


**Figure 9 | Applied DC voltage pulses and measured current over time, shown for one test subject (which is labeled as subject A in [2]). The presented data always show the third to fifth period from a series of DC pulses (see experiment 2 in [2]). The voltage is applied from deeper skin layers towards the skin surface. Duration of applied pulses is 15 seconds followed by five seconds of 0 V level. a) Recording from the forehead, pulse height = -0.8 V (series 1), (compare with illustration in Figure 8 a)) b) Recording from the forehead, pulse height = +0.8 V (series 2), c) Recording from the fingertip, pulse height = +0.8 V (series 2). Change in current can be explained by sympathetic nerve activation rather than by the applied voltage.**

### AC voltage-current characteristics of the sweat duct memristor

Within experiment 1 in [2] it was confirmed that the human skin is a memristor, since hysteresis loops with pinched points close to the origin could be observed for different signal shapes, amplitudes and frequencies<sup>6</sup> (see example recordings with triangular waveform in Figure 10) and skin sites (see section 4.7). Slight shifts of the pinched point from the origin can be explained by the stratum corneum capacitance and the endogenous skin potential [4].

Within the positive half of the applied voltage, the memductance increases, which can be seen from the measured current in Figure 10 a). The current does not increase linearly with the applied voltage and its shape differs from the applied waveform. From  $T/4$  to  $T/2$  of each signal period, the magnitude of the applied signal decreases, but the memductance continues to increase since the applied voltage is still positive. The resulting V-I plot shows a clear pinched hysteresis loop and the orientation of the pinched hysteresis loop in the first quadrant is counter-clockwise (as indicated in Figure 10 a)), consequently. Within the negative half period of the applied voltage, the sweat is pushed towards deeper skin layers and the memductance decreases and the

<sup>6</sup> Voltages with different shapes (sinusoidal with amplitudes 0.4 V, 0.8 V and 1.2 V, triangular with amplitude and a non-periodic waveform) in combination with different signal frequencies each (0.05 Hz, 0.1 Hz, 0.25 Hz, 0.5 Hz, 1 Hz and 2.5 Hz) were applied to the test subjects in randomized order, for three periods each.

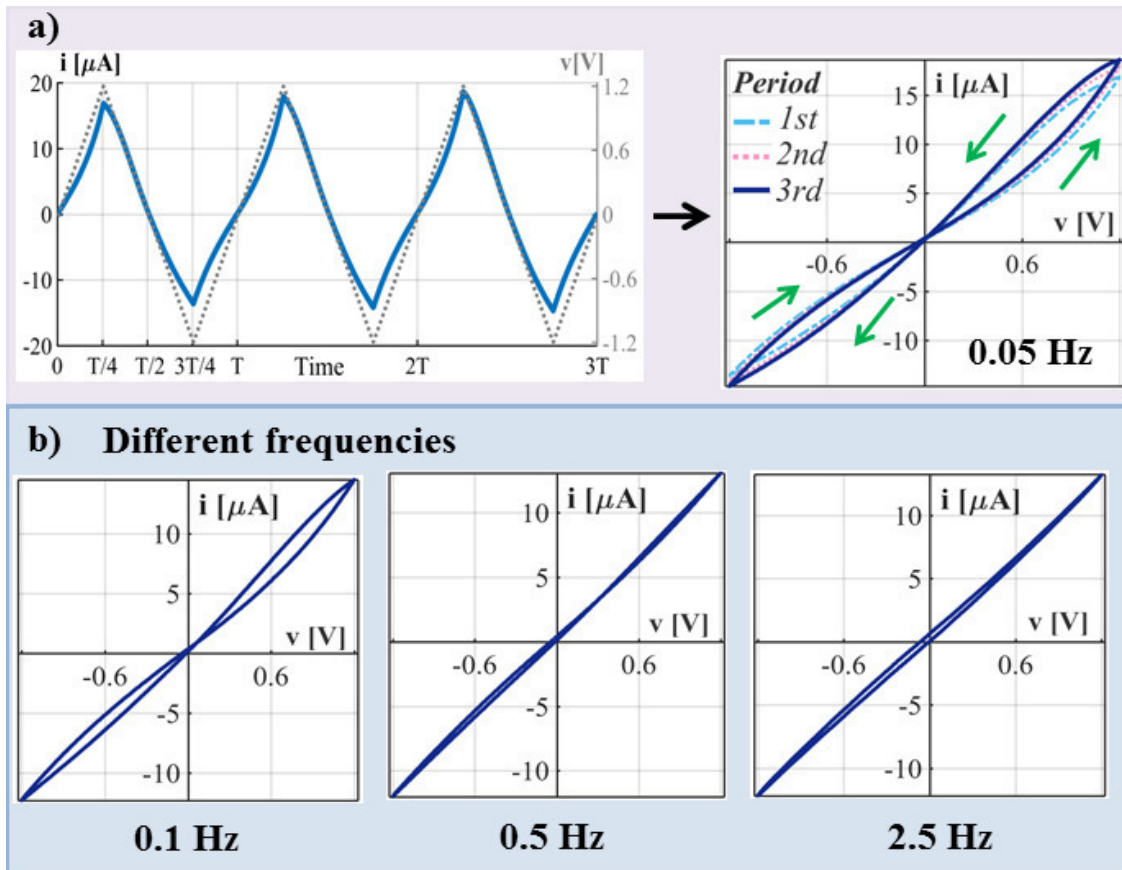


**Figure 10 | Voltage current plots derived from applied triangular voltage** with amplitude of 1.2 V shown for one test subject labeled as “R” in [2], recorded from the forehead. **a)** Applied voltage  $v$  ( $f=0.05$  Hz, three signal periods) and measured current over time (left) and corresponding V-I plot (right). **b)** V-I plots of the same subject and triangular waveform with amplitude of 1.2 V but different signal frequencies.

orientation of the pinched hysteresis loop in the third quadrant is clockwise. The two branches of the loop cross the pinched point with different slopes (transversal hysteresis loop) and the resulting memductance will have one maximum within one signal period. The maximum will be somewhere close to  $T/2$  but not exactly at  $T/2$  (since the pressure driven forces will counter-act the memductance increase during positive voltage (half), see illustration in Figure 8).

The memductance change within the sweat ducts is based on ion movements, which are quite slow. The higher the signal frequency, the less the memductance change since the ions have less time to move. Decreasing of the lobe area with increasing frequency is another fingerprint of memristors [18] and can be seen in Figure 10 a) and b). It was concluded in [2] that the sweat duct memristor (at the forehead) is a generic memristor up to a certain magnitude of applied voltage (e.g. 0.8 V) and an extended memristor above. This conclusion is based on the appearance of the V-I plots. Obtained pinched hysteresis loops from recordings with low frequencies were usually not odd-symmetric and tended towards a straight line (up to a certain magnitude) with increasing frequency. Those findings were supported by quantitative analysis (based

on lobe area and a non-linearity parameter, see [2] but also section 4.5 within this thesis).

### **Non-volatility property of the sweat duct memristor**

It can be shown, that the sweat duct memristor (at the forehead) is non-volatile “*since the current responses to periodic constant voltage steps are not periodic*” [2] (see e.g. Figure 9 a), b) and Figure 11 a)).

The non-volatile property [21] implies that the sweat duct memristor may obtain at least two different equilibrium states. The memductance will change naturally after the voltage is released (see e.g. Figure 9 a), b)) and one aim of experiment 2 in [2] was to study the natural development over some period of time. Three series of DC voltage pulses (with pulse height of -0.8 V in series 1 and 3 and pulse height of + 0.8 V in series 2, see Figure 11 a)) were applied to the skin for three minutes each. According to Figure 8, the sweat was pushed towards deeper skin layers with each pulse during series 1, pulled towards skin surface during series 2 and pushed inwards again during series 3.

Small signal (linear) conductance (EDA) measurements (using the AC method)<sup>7</sup> under the same electrodes were done (for three minutes, as well) after each series (see example recordings in Figure 11 b)). The small signal conductance increased after series 1 and 3 while it decreased after series 2 and slight changes still can be observed within the shown period (two minutes to three minutes after the last DC pulse). However, the small signal conductances at e.g. minute 3 after the last DC pulse are still very different from each other (see example in Figure 11 b)), indicating that the sweat duct memristor tends towards different equilibrium states. Those differences are statistical significant (evaluation of 28 subjects, Friedman test) at the forehead and earlobe<sup>8</sup> but not at the fingertip [2].

The frequency dependent part of the skin conductance (see Figure 5 and equation (23)) will add to the small signal AC conductance measurement. Sweat that reaches the skin surface may moisture the surrounding stratum corneum that will in turn cause an increase in the measured conductance, which may be one origin of the different states in Figure 11 b). However, the frequency dependent part of the conductance does not contribute when DC pulses are applied (see Figure 11 a)). The memductances (measured currents) at the end of series 1 and 3 are quite different from each other and might reflect different equilibrium states since the current does not change much further for both. The different equilibrium states may origin from the amount of wetting at the sweat duct walls, as well as changes in the total amount of sweat within

---

<sup>7</sup> Applied sinusoidal voltage had amplitude of 0.1 V and a frequency of 20 Hz. It is certain that the voltage itself did not affect the measurement (linear recording).

<sup>8</sup> Pairwise comparison (Tukey test) shows that the small signal conductance state at the earlobe at three minutes after series 1 was different from the ones after series 2 and 3 but the states after series 2 and 3 did not differ significantly from each other.

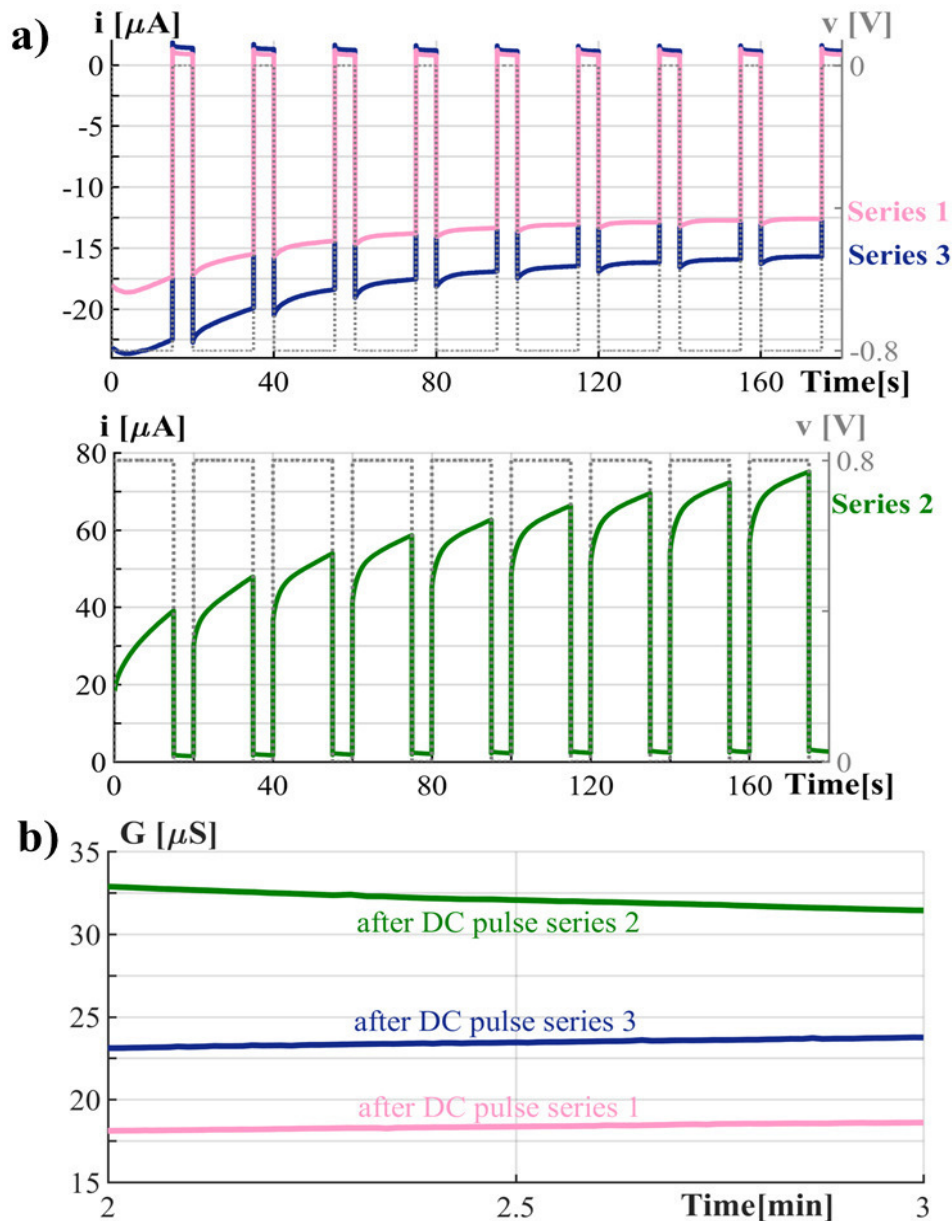


**Figure 11 | Applied voltage DC voltage pulses and small signal conductance measurements afterwards** recorded from the forehead, shown for one subject that is labeled as "D" in [2]. The data was recorded during experiment 2. **a)** Applied DC voltage pulses and corresponding current. Pulse height of the pulses was  $-0.8$  V in series 1 and 3 and  $+0.8$  V in series 2. **b)** Small signal conductance measurements (minute 2 to minute 3) after each DC pulses series. The small signal conductance states are quite different even after three minutes of recovery.

the sweat glands/ducts. The results indicate that it is possible to store information (e.g. pin number of the bank account) electrically (at least for some minutes) within human skin. A state can be set by applying a constant DC voltage (or DC pulse) and the reading can be done by small signal conductance measurements. Since thermal sweating will also interfere the memductance state, stored information might get lost after physical exercise.

## 4.3 Stratum corneum NTC thermistor

There is strong evidence for a second non-linear mechanism in human skin beside the sweat duct memristor [2]. Hysteresis loops recorded from the forehead usually had one pinched point (see Figure 12 a), subject T). However, 3 out of 28 subjects at the forehead and 18 out of 28 subjects at the earlobe (but none at the fingertip) showed hysteresis loops with two pinched points (see Figure 12 a), subject U).

### Observations

Those hysteresis loops with two pinched points were usually quite symmetric and the measured currents were quite low<sup>9</sup>. Corresponding subjects responded with a state dependent conductance increase when negative pulses were applied (amount of current increased for subject U in Figure 12 b)) which is opposite from the behavior of the sweat duct memristor (see subject T in Figure 12 b)). If positive pulses were applied, the state dependent conductance of subject U increased, as well. The non-linear mechanism that is dominating the measurement in subject U seems to cause an increase in the state dependent conductance that is independent of the sign of the applied voltage. This is different from the sweat duct memristor represented by subject T.

### When was this second non-linear mechanism observed?

There is indication that those observations were made as long as the galvanic contact through the sweat ducts was not present (or very poor). The electrodes<sup>10</sup> were taped to the skin during the experiments and the contact at the earlobe might have been difficult to obtain by this method. It was possible to change the appearance of a hysteresis loop with two pinched points to a hysteresis loop with one pinched point (measured current was higher in addition) just by pressing the electrode against the earlobe (only done for testing). Pressing might enable galvanic contact through the sweat ducts that was not given before. Further, it was shown that the appearance of the hysteresis may change significantly before and after physical exercise (compare e.g. recordings with “M3” in Figures 7 and 8 in [3]). Before the exercise, the measured current was very little (up to 0.4  $\mu\text{A}$ ) and the hysteresis loop showed two pinched points. After the physical exercise, the level of sweating was increased, the measured current was much higher (up to 10  $\mu\text{A}$ ) and a hysteresis loop with one pinched point was observed, indicating that the galvanic contact through the sweat ducts was given.

---

<sup>9</sup> Measured currents from subject U (see Figure 12 a)) were highest among subjects that showed hysteresis loops with two pinched points.

<sup>10</sup> Dry Ag/AgCl electrodes were chosen.

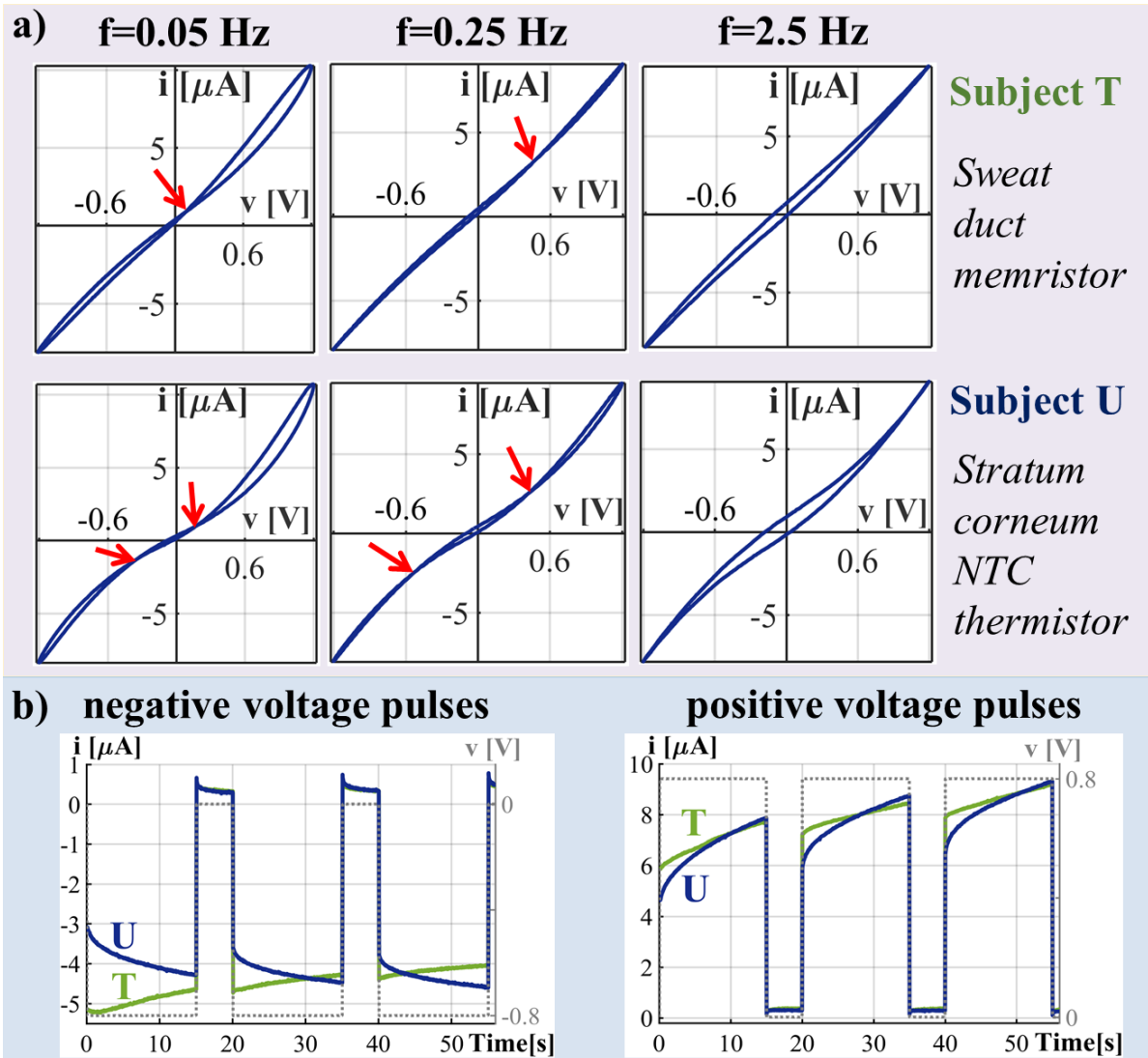


**Figure 12 | Example recordings that demonstrate the difference between the sweat duct memristor and the stratum corneum NTC thermistor.** The results are obtained from recordings at the forehead of two different subjects T and U (additional subjects to the ones presented in [2]). **a)** V-I plots shown for three different signal frequencies of applied sinusoidal voltage with amplitude of 1.2 V. The arrows indicate the pinched point positions. Subject T: hysteresis loops with one pinched point are observed for frequencies of 0.05 Hz and 0.25 Hz. The results imply that the sweat duct memristor dominates that measurement. Subject U. Obtained hysteresis loops at 0.05 Hz and 0.25 Hz show two pinched points. The results imply that the galvanic contact through the sweat duct was not given and the stratum corneum NTC thermistor dominates that measurement. **b)** Current responses to positive and negative DC voltage pulses (data from experiment 2 in [2], first three pulses of DC pulse series 1 and 2 are shown).

### Origin of the observed non-linear mechanism

The observations indicate that the described non-linear effect appears apart from the sweat glands/ducts and it is likely (based on the structure of the skin, see possible current pathways in Figure 2) that it originates in the epidermis / stratum corneum. An explanation, which fits well with all the observations made, is that the stratum

corneum has similar properties (and may be modelled) as a negative temperature coefficient (NTC) thermistor. As an electrical current passes through an NTC thermistor its state dependent conductance increases<sup>11</sup> regardless of the direction of the current (similar to the recording of subject U in Figure 12 b)). The NTC thermistor properties of the stratum corneum were not studied further, yet. However, stratum corneum consists of keratinized tissue [47] and it is shown that the conductance of human hair which consists of keratinized tissue as well, increases with a temperature increase [11]. This might be a confirmation of the stratum corneum (SC) NTC thermistor theory but further research has to be done.

### **Voltage current characteristics of a NTC thermistor**

Like other NTC thermistor types (see e.g. [18]), the stratum corneum NTC thermistor might be modeled as a memristor itself. The appearance of the observed hysteresis loops with two pinched points, that are both shifted from the coordinate origin (see subject U in Figure 12), might be explained by the capacitive properties of the stratum corneum, which are electrical in parallel with the NTC thermistor (see suggested equivalent circuit in Figure 13). It was possible to obtain hysteresis loops with two pinched points by simulating a NTC thermistor model as it was given in [18] with a capacitance in parallel (see [2] and chapter 6 within this thesis for further information).

### **Superposition of both non-linear effects**

The stratum corneum NTC thermistor was usually noticed when the galvanic contact through the sweat ducts was not given. The sweat duct memristor dominated the measurements more or less otherwise. However, if the galvanic contact through the sweat ducts is given, the measurement always reflects a combination of both non-linear effects and the contribution of the stratum corneum may become noticeably in some recordings. The example recordings (from the two different subjects T and U) presented in Figure 12 demonstrate that both state dependent conductances may obtain similar values. The “skin memristor” is actual a combination of two memristors (sweat duct memristor and stratum corneum NTC thermistor) connected in parallel. Some recorded pinched hysteresis loops (with one pinched point, see e.g. subject A in Extended Data Figure 1 and subject D in Figure 2, both in [2]) were quite asymmetric with a large lobe area in the first quadrant but small lobe area in the third quadrant. One possible reason for the asymmetry is that both, the stratum corneum NTC thermistor and the sweat duct memristor, contributed noticeably to the measurement (see also the asymmetric pinched hysteresis obtained by simulation in Figure 21 c)). Furthermore, it was concluded that the skin memristor (e.g. at the forehead) is a

---

<sup>11</sup> The term negative temperature coefficient is with regard to the state dependent resistance that in turn decreases as a current passes through.

generic memristor up to a certain magnitude of applied voltage and becomes an extended one above [2]. It might be possible that this “extended memristor” property above a certain magnitude mainly originates from the NTC stratum corneum thermistor, which is part of the overall skin memristor.

#### 4.4 Non-linear (state dependent) skin admittance

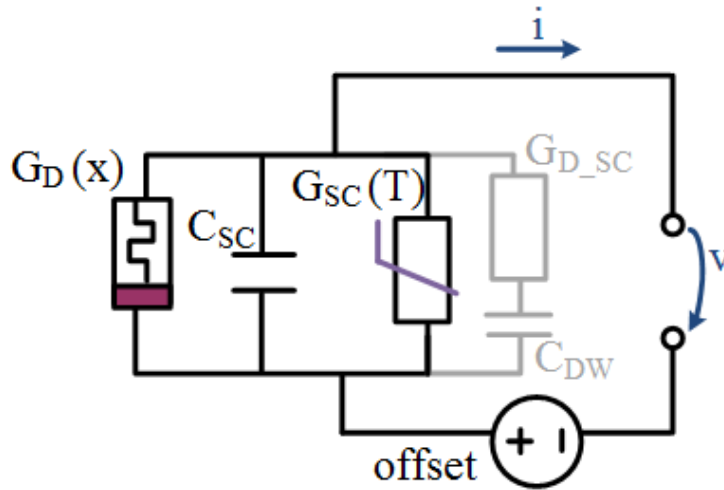


**Figure 13 | Equivalent circuit of human skin within non-linear recording range.** The conductive pathways are state dependent, which is the main difference to the equivalent circuit within the linear range (see Figure 5). Further, the chosen frequency range of the measurements was from 0.05 Hz to 2.5 Hz and the pathway (see section 2.1) from the sweat duct through the duct wall through the stratum corneum might be negligible (shown grayed out). If not, the component  $G_{D\_SC}$  might be state dependent, as well.

The internal state of the sweat duct memristor  $G_D(x)$  (see Figure 13) may be expressed by  $x$ , the extension of the sweat duct filling. The state dependent conductive pathway of the NTC thermistor  $G_{SC}(T)$  may depend on the temperature  $T$ , that increases as current passes through. The overall state dependent admittance of this circuit can be described by

$$Y(x, T) = G_D(x) + G_{SC}(T) + j 2\pi f C_{SC} \quad (25)$$

$$= G(x, T) + j B \quad (26)$$

with  $G(x, T)$  as the overall state dependent conductance (memductance). The overall phase angle  $\alpha(x, T)$  will change as the internal states of  $G(x, T)$  change. It is consequently state dependent and may be described by (adaption of equation (7))

$$\alpha(x, T) = \tan^{-1} \frac{B}{G(x, T)}. \quad (27)$$

## 4.5 Parameterization

A useful parameterization has to be found in order to enable quantitative analysis of obtained data. In linear EDA recordings, the parameterization is e.g. based on the geometrical appearance of the skin conductance responses over time (see Figure 7 c)). Within non-linear skin memristor recordings, parameterization of the obtained V-I plots may be a first approach (see Figure 14).

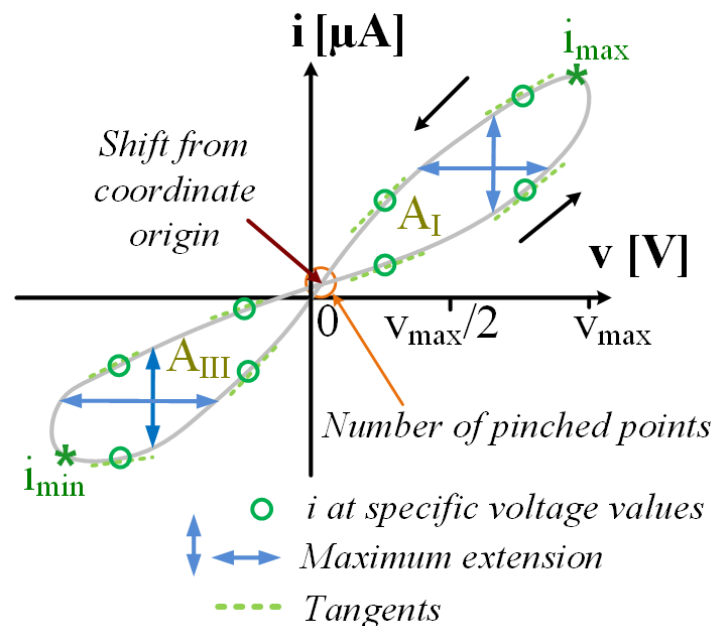


**Figure 14 | Illustration of possible parameters that describe the appearance of the V-I relation.** The parameters might be useful for the quantitative analysis of non-linear skin recordings.

Possible parameters are current values at specified voltage values and corresponding tangents, as well as, maximum and minimum current values ( $i_{\max}$ ,  $i_{\min}$ ). Further possible parameters are the lobe areas ( $A_I$  and  $A_{III}$ ), maximum extensions (vertical and horizontal) of the hysteresis loop within the first and third quadrant, number of pinched points and (if existent) their shifts from coordinate origin. A measure of asymmetry between the appearance of the pinched hysteresis within the first and the third quadrant might be useful, as well. However, the maximum current  $i_{\max}$  and the total lobe area ( $A_I + A_{III}$ ) were chosen for the quantitative analysis in [2]. A third chosen parameter “Non-linearity” is discussed below.

### Non-linearity definition

A first non-linearity (NL) parameter definition (for applied sinusoidal voltage) was introduced in [60] for the characterization of technical memristors (based on tantalum oxide and titanium oxide). It simply is

$$NL = \frac{i(v_{max})}{i(v_{max}/2)\downarrow}, \quad (28)$$

with  $i(v_{max})$  as the corresponding current value when the magnitude of the applied voltage reaches its maximum<sup>12</sup> and  $i(v_{max}/2)\downarrow$  as the corresponding current when the voltage magnitude dropped to  $v_{max}/2$  afterwards. A non-linearity parameter seems to be quite useful for the characterization of the skin memristor (and organic memristors in general), as well, but some adaptations have to be made.

As it is demonstrated in Figure 6 a) in [2], the maximum current does not necessarily occur at  $v_{max}$  as a consequence of the non-linear deformations. A NL parameter based on the maximum current ( $i_{max}$ ) rather than  $i(v_{max})$  might be more meaningful. Further, instead of  $i(v_{max}/2)\downarrow$  (the current value at the falling lobe), the current value  $i(v_{max}/2)\uparrow$  at the rising lobe can be chosen. An adapted definition of the NL parameter can be given by

$$NL = \frac{i_{max}}{i(v_{max}/2)\uparrow}. \quad (29)$$

Any DC offset in the measured current (e.g. caused by the endogenous potential differences under the recording electrodes) will affect the NL value as it is defined in equation (29) (as well as it is defined in equation (28)). The smaller the current the larger is the effect. To correct for DC offsets, the NL definition

$$NL = \frac{i_{max} - i(v_{max}/2)\uparrow}{i(3v_{max}/4)\uparrow - i(v_{max}/2)\uparrow}, \quad (30)$$

was suggested in [2] and chosen for the data representation.

All three NL definitions (see equations (28) to (30)) will lead to a value of 2 if the measurement is purely resistive (straight line in the V-I) plot. NL values above 2 indicate that a measurement is non-linear (for all three definitions). The NL values in Figure 15 are based on the definition given in equation (29) and can be directly compared to the NL values in Figure 3 c) in [2] (that are based on equation (30)). The obtained boxplots are quite similar. The NL values decrease with increasing frequency and decreasing amplitude in both plots. The main difference is the interpretation of the recordings with amplitude of 0.4 V. From Figure 3c) in [2], the interpretation is that the corresponding measurements at the forehead are non-linear up to e.g. a signal frequency of 0.5 Hz. The interpretation from the results in Figure 15 (here) would be that the measurements are linear for amplitude of 0.4 V (mean and median NL values are always close or even below 2) which might not reflect the results correctly as it is demonstrated by the example in Figure 16.

---

<sup>12</sup> At  $t=T/4$  for applied sinusoidal voltage with zero phase shift.

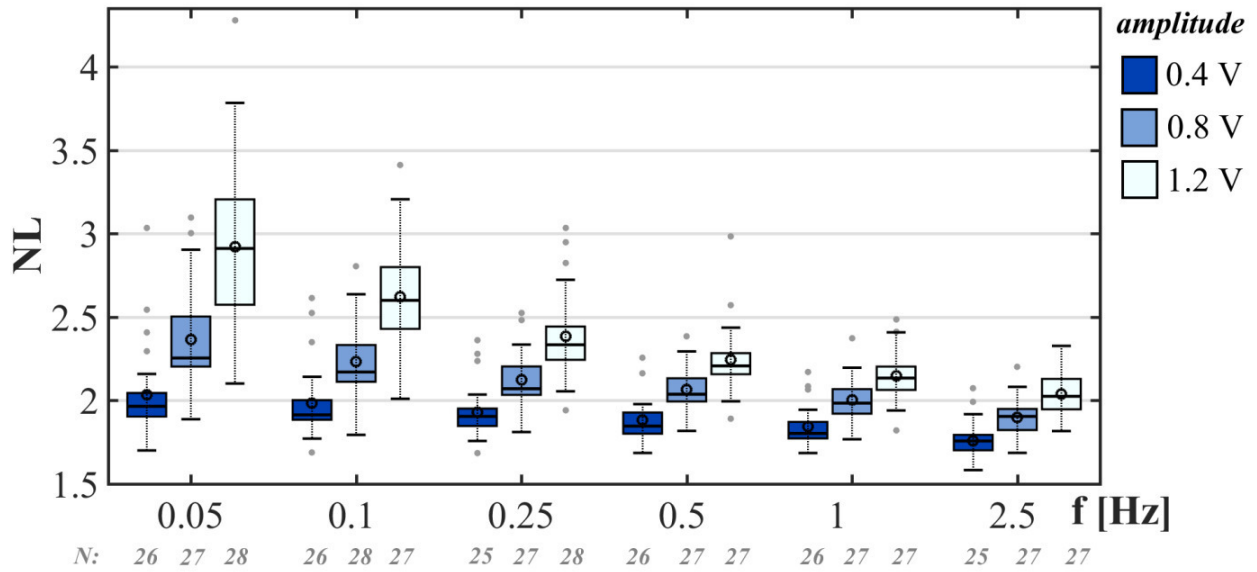


**Figure 15 | Non-linearity boxplot over all subjects recorded from the forehead, for applied sinusoidal voltage of different amplitudes and frequencies. The plot is based on the same data that is presented in Figure 3 c) in [2] but the chosen NL definition here is different. Here it is based on equation (29), in [2] it was based on equation (30). The horizontal line in the middle of each boxplot denotes the median, the circle the mean value, the whiskers the 5% and 95% percentiles. The number N of subjects, included in the evaluations, is written under each boxplot.**

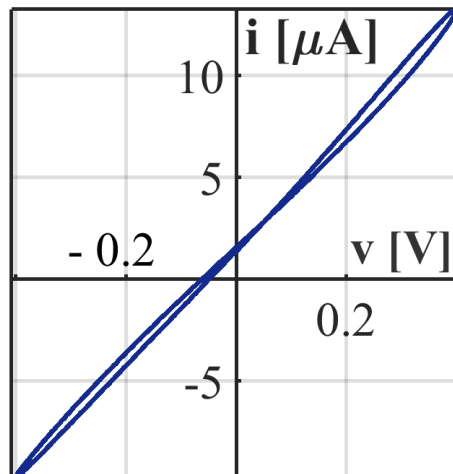


**Figure 16 | Pinched hysteresis loop example recorded from the forehead, applied sinusoidal voltage with amplitude of 0.4 V and frequency of 0.05 Hz. The data is from the subject that is labeled as “A” in [2]. The NL value of this example is 1.946 (suggesting a linear measurement) based on the definition in equation (29) and 2.258 (indicating a non-linear measurement) based on the definition in equation (30).**

## 4.6 Border between linear and non-linear recordings

The non-linearity of the measured signal increases with decreasing frequency and increasing amplitude. An approximation for the border between linear and non-linear range is given here (see Figure 17). The measurements (with the chosen methods in [2]) may become non-linear already for amplitudes less or equal 0.4 V (of the applied voltage if the frequencies are very low). This low amplitude border is quite surprising (e.g. voltages of 13 V and above were used in [57]) and should be considered for the chosen methods in linear recordings. The border between linear and non-linear recordings in the amplitude-frequency plane might be different for different skin sites and methods (i.e. electrode choice).

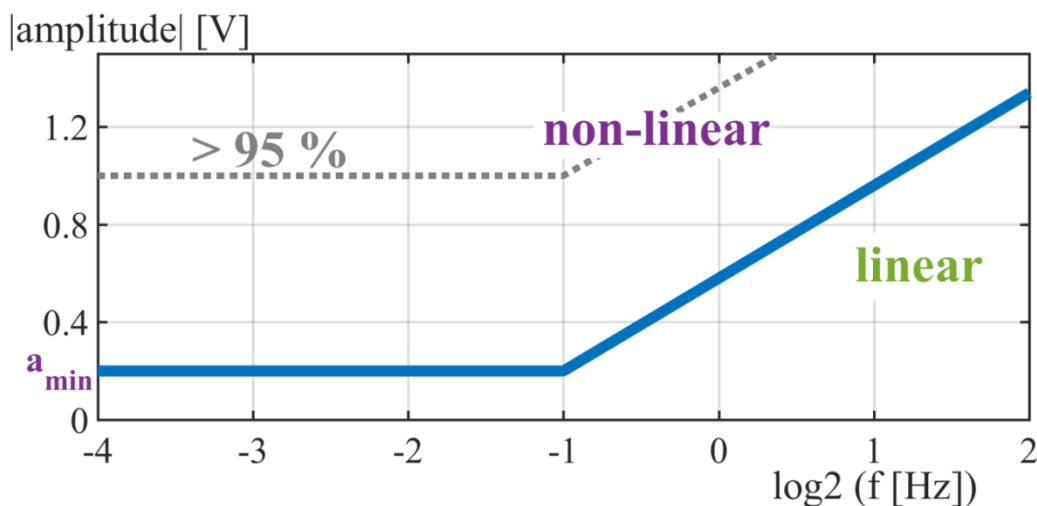


**Figure 17 | Approximation of boundary between non-linear and linear measurement range** (blue line) in the amplitude - frequency plane. Approximation is based on the recorded data at the forehead in [2] and the chosen recording methods (e.g. use of dry Ag/AgCl electrodes, applied sinusoidal voltage). Based on the boxplots (28 subjects) of the non-linearity (NL) parameter (see Figure 3 c) in [2]), a measurement was considered to be non-linear as soon as the NL value (median) was larger than 2.05. The measurements at very low frequencies were mostly non-linear, even when sinusoidal voltage with amplitude of 0.4 V was applied. A state change might not occur if the voltage amplitude is below  $a_{min}$  (somewhat below 0.4 V) and any measurement with lower signal amplitude might be linear. The measurements become more and more linear with increasing frequency. The recordings at very low frequencies of some subjects were linear even with amplitude of 0.8 V. The area above the grey dotted line is an approximation for a range in which more than 95 % of the subjects will show non-linear behavior (at the forehead). The range is based on the lower whiskers (that are above 2.05) in the non-linearity (NL) boxplots in [2].

## 4.7 Different skin sites

Non-linear properties of human skin have been demonstrated at the forearm (see [57], [14], [4], [3]) at the dorsal hand site (see [57]), at the forehead, earlobe and fingertip (all three in [2]<sup>13</sup>). The memristive properties of the latter three can be directly compared since the recordings of those were done simultaneously on the same subjects. The conclusion that human skin is a generic (up to a certain magnitude of applied voltage) and non-volatile memristor is based on the findings at the forehead and the earlobe. A systematic study at e.g. the forearm might result in the same findings. The main difference between the earlobe and the forehead was the galvanic contact through the sweat ducts with the chosen methods. While this contact was easy to obtain at the forehead for most subjects, it was not given for many subjects at the earlobe and much of the recorded data from the earlobe reflected the stratum corneum NTC thermistor. The access at the forearm was also difficult to obtain for several subjects (experience from pilot studies, see also recordings from one subject before and after physical exercise in [3]).

The fingertip memristor is quite different. The fingertip is part of the palmar skin site, and palmar and plantar skin sites are known to be emotionally active. It was stated in [57] that the palmar skin site was much less dependent on current flow than the forearm and the dorsal hand site. The measurements at the fingertip were usually much more linear than at the forehead and earlobe (see [2]). However, pinched hysteresis loops were recorded from the fingertip, as well. Lobe areas were quite small and variations in lobe area and measured currents among subjects were much smaller than e.g. at the forehead. The non-linearity parameter was much higher for amplitude of 0.4 V than for amplitudes of 0.8 V and 1.2 V (see Extended Data Figure in [2]). This finding is unexpected and opposite from the forehead and the earlobe recordings. A good explanation has not been found, yet. No hysteresis loops with two pinched points were observed from the fingertip. The galvanic contact through the sweat ducts was always given at the fingertip and the epidermis at the fingertip (as part of the palmar skin site) is much thicker than at the earlobe and the forehead (see section 2.1), resulting in a much lower (state-dependent) conductance. The contribution of the stratum corneum NTC thermistor to the measurements at to fingertip might be negligible, consequently. Unlike the recordings at the forehead and the earlobe, no clear tendencies in current change were observed during applied DC voltage pulses (see Extended Data Figure 6 in [2]). Emotional sweating overlaps the recordings on the one hand and the electro-osmotic effect was little on the other hand. Based on the recorded data in [2], it is not possible to determine whether the skin memristor at the fingertip is volatile or non-volatile. However, since low frequency measurements at

---

<sup>13</sup> Example plots can be found in Figure 2, Extended Data Figure 1 and Extended Data Figure 4 of paper [2], respectively.

the fingertip with amplitude of 0.4 V are non-linear, standard DC EDA recordings with applied voltage level of 0.5 V might be non-linear, as well, which is another argument for choosing the AC method instead.

## 4.8 Application and further research

The non-linear skin memristor measurements provide new information that is not obtainable by linear recordings. As it is demonstrated in Figure 2 in [2], the appearances of the pinched hysteresis loops vary largely among test subjects. As it is stated in [2], “*physiological properties that may affect the shape of the measured current and the hysteresis loop are the number and diameter of sweat ducts, initial sweat duct filling, skin thickness, ion concentration, composition of the sweat, pH value of the skin, moisture content of the stratum corneum, endogenous skin potential differences and possibly more*”. The non-linearity of a measurement (e.g. expressed by the NL parameter, see equation (30)) gives information of how much the memductance of the skin is influenced by the applied electrical signal itself, which is determined by the mentioned properties and the applied signal. Part of future research is the search for possible factors that affect the non-linearity and the appearance of the hysteresis loops that can be done by e.g. between group comparisons. Potential applications from this kind of research might be found in e.g. diagnostics (of diseases that affect any of the mentioned properties). If the galvanic contact through the skin is present, the skin memristor measurements are mainly determined by the sweat duct memristor. However, the stratum corneum NTC thermistor might be interesting to study further, as well. Its properties depend on the tissue in the stratum corneum and its voltage-current characteristics might provide useful information. A negative DC voltage (to reduce the contribution of the sweat duct memristor within the recordings) in superposition with a low frequency AC voltage could be chosen in order to study the properties of the stratum corneum NTC thermistor. Models for both, the sweat duct memristor and the stratum corneum NTC thermistor may be developed later.

The skin (sweat duct) memristor is capable of storing information and applications related to this property might be found, as well. Increasing the sweat level (by a positive DC voltage) could enable recordings of emotional sweating on skin sites different from the palmar and the plantar sites.

A first application of the skin memristor as part of an electrical circuit was demonstrated in [2] (see experiment 3). The presented circuit (made of two skin memristors) functioned for some subjects as a frequency doubler, for some others like a half wave rectifier and for most subjects, the circuit did not show noticeable differences to single memristor measurements. This selective behaviour might find application in authentication systems.

# 5 Instrumentation

*Related papers:* Different versions of custom-built measurement systems were used for the recordings in all studies related to this thesis [1-4].

*Note:* The chosen instrumentation for linear EDA measurements is quite similar to the one for the non-linear skin memristor measurements. Both are described within this chapter and differences between both in e.g. electrode choice and recording modes are stated.

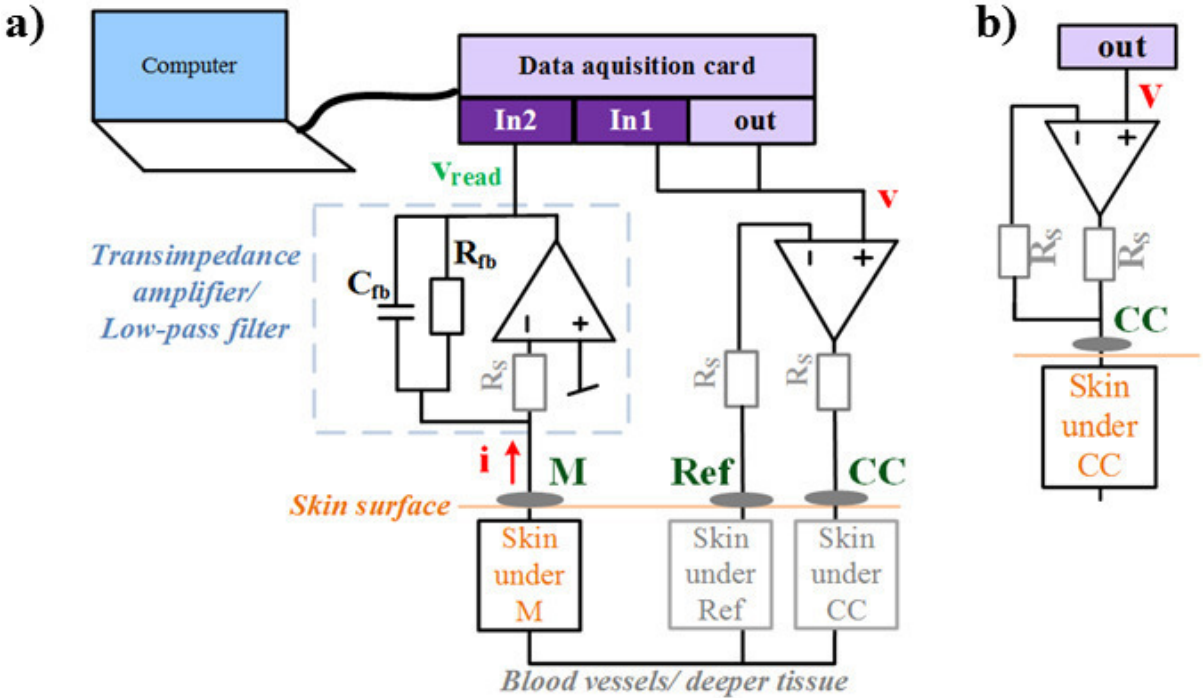


**Figure 18 | Schematic of the developed measurement system, a) Overall instrumentation that is based on a three electrode configuration, chosen in [2-4], b) Modification on the voltage application side as it was chosen in [1] (two-electrode system).**

All studies within this thesis were conducted by the use of custom-build measurement systems. The instrumentation shown in Figure 18 a) is suitable for linear EDA measurements, as well as, non-linear skin memristor measurements. A Data acquisition card (DAQ) enables the application of a constant voltage and simultaneous reading. It is controlled by a personal computer or laptop.

## 5.1 Analogue part

The generated voltage  $v$  is provided at the “out” port of the DAQ. The current  $i$  through the skin (see Figure 18 a) is determined by the skin admittance ( $Y_{\text{skin}}$ ) and can be described by

$$i = v \cdot Y_{\text{skin}} . \quad (31)$$

The transimpedance amplifier converts the current  $i$  into a voltage  $v_{\text{read}}$  that is read by the DAQ card and which can be described by

$$v_{\text{read}} = - \frac{i}{Y_{\text{fb}}} , \quad (32)$$

with  $Y_{\text{fb}} = 1/R_{\text{fb}} + j\omega C_{\text{fb}}$  as the feedback admittance. The chosen resistance of  $R_{\text{fb}}$  is 56 k $\Omega$  which is quite suitable for the expected range of the (state dependent) skin admittance in both, linear EDA and non-linear skin memristor measurements (for the chosen methods, e.g. voltage amplitudes not higher than 1.2 V). The higher the feedback resistance, the higher the amplification of the obtained signal (see equation (32)). The voltage  $v_{\text{read}}$  is limited to about  $\pm 15$  V by the chosen operational amplifier (type TL074 from Texas instruments). This has to be considered for the choice of  $R_{\text{fb}}$ . On the other hand, if  $v_{\text{read}}$  becomes too small (e.g. amplitude smaller than 0.05 V)<sup>14</sup>, the obtained signal after the analogue to digital conversion (that is part of the signal input channels e.g. In2 of the DAQ) may become very noisy. The transimpedance amplifier additionally functions as a low-pass filter (in order to reduce noise) by adding a capacitance  $C_{\text{fb}}$  to the feedback. The chosen capacitance value is 4.7 nF. Simultaneous recordings at three different skin sites (done in [2]) was enabled by the implementation of three separate input channels (each consisting of a measurement electrode, followed by a transimpedance amplifier that is connected to a signal “In”-port of the DAQ, like the one shown in Figure 18 a)).

### Calibration and timing

The chosen feedback admittance enabled linear conductance measurements with errors less than 0.6 % and susceptance measurements with errors less than 0.7 % over the whole calibration range (combination of different resistances from 14.91 k $\Omega$  (68.67  $\mu\text{S}$ ) to 563 k $\Omega$  (1.78  $\mu\text{S}$ ) in parallel with different capacitances from 9.17 nF to 91.29 nF, see [1]). It was possible to correct any parasitic phase shift of  $v_{\text{read}}$  with regard to the applied voltage  $v$  (e.g. caused from the feedback admittance, as well as from parasitic elements from the overall electronic circuit) by adjusting slightly the phase angle of the reference signals (that are used for lock-in amplification, see below, the adjustment was realized digitally).

---

<sup>14</sup> i.e. if the chosen feedback resistance is too low for the expected skin admittance

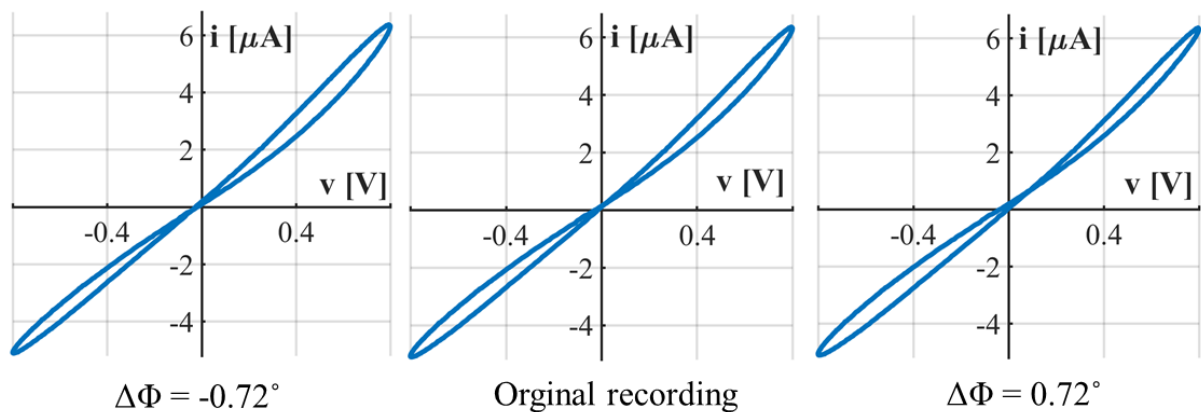


**Figure 19 | V-I plot of an example recording and V-I plots of the same recording but different phase shifts.** The phase shifts ( $\Delta\phi = -0.72^\circ$  and  $\Delta\phi = 0.72^\circ$ ) were added to the measured current (“original recording”) with regard to the applied voltage. The original recording was done at the forehead with applied sinusoidal voltage with amplitude of 0.8 V and frequency of 0.05 Hz.

Correct timing between output and input signal(s) is also essential within the non-linear skin memristor measurements. The measured current is directly plotted (sample-wise) against the corresponding voltage in the V-I plot and any (parasitic) phase shift affects its appearance (see example in Figure 19). The DAQ card type USB-6356 from National instruments was chosen because it enables simultaneous reading (one analogue digital converter per input channel, no multiplexing) and good synchronization between output and input channels. The direct connection from the signal out to a signal in port (“In1” in Figure 18) was realized in order to measure any delay between the signal generation inside the DAQ card and the actual provision at the “out” port. The chosen feedback admittance of the transimpedance amplifier (see above) itself causes a parasitic phase shift which is negligible ( $\Delta\phi = 0.0047^\circ$ ) if the frequency of the applied voltage is 0.05 Hz and may have a small noticeable effect ( $\Delta\phi = 0.237^\circ$ ) if the frequency is 2.5 Hz.

### Safety

An international medical isolation device (IMEDe 1000 from Noratel AG, Germany) always ensured separation between the mains and the test subjects. The personal computer, the monitor and the data acquisition card<sup>15</sup> were connected to it. If a laptop was chosen, it was powered by battery. The safety resistors  $R_S$  (see Figure 18) are included in order to reduce the current through the test subjects in case of a breakdown of the operational amplifiers. Resistances of  $R_S = 47 \text{ k}\Omega$  are chosen in [1] and  $R_S = 56 \text{ k}\Omega$  are chosen for the instrumentation in [2-4].

<sup>15</sup> Not all DAQ cards but the chosen USB-6356 from National instruments requires external power supply.

## 5.2 Electrode system

**Summary:** *The use of a three-electrode instead of a two-electrode system is recommendable for both, linear and non-linear skin measurements.*

The illustrated instrumentation in Figure 18 a) is based on a three-electrode system. Beside the measuring electrode M and the current carrying electrode CC, a third electrode is used as reference (Ref). With this topology monopolar recordings under M are possible [61]. The voltage difference at the input side of an ideal operational amplifier with feedback is zero and the impedance at the input is infinitely high. The voltage in the deeper skin layers (referred to ground) will be regulated to the same level as the applied voltage  $v$ . The skin under the CC and Ref electrodes do not contribute to the measurement and the voltage drop is from deeper skin layers to the skin surface under the M-electrode. This is an important issue as it will be discussed below. The three-electrode system has the additional advantage that any ground referenced noise will be suppressed [62].

If a two-electrode system would be chosen instead (without a reference electrode), the skin under the CC electrode will contribute additionally to the measurement (the skin under the M electrode is electrically connected in series with the skin under the CC electrode). This reduces already the quality of the measurements within the linear range. A common method in (DC) EDA recordings is the application of the CC and M electrodes close to each other, either at the palmar or plantar skin sites [46] (bipolar recording). Since the recorded skin sites are close to each other, they are also similarly active. However, the single contribution of each skin site to the overall conductance is unknown. A higher resistance dominates in a series connection and if the skin under one electrode is low conductive for some reason, it might cover the activity of the skin under the other electrode. A two-electrode modification of the developed instrumentation (see Figure 18 b)) was chosen for the study in [1]. The only reason for this choice was the common use of two-electrode systems for conducting (DC) EDA measurements [46], as it is mentioned before. Since ground referenced noise is not automatically suppressed in a two-electrode system, a 50 Hz notch-filter was implemented within the instrumentation in [1] (see A1 in the corresponding paper) in order to suppress the 50 Hz component from the mains<sup>16</sup>.

The series connection of the skin under the M and CC electrodes (if a two-electrode system would be chosen) is even more critical within the non-linear measurement range since the resulting load would contain two sweat duct memristors that are connected in opposite directions (see Figure 2 in [3] for illustration). While the sweat moves towards deeper skin layers within the ducts under one electrode, it moves towards the skin surface within the ducts under the other and vice versa when the

---

<sup>16</sup> This component interferes the measurement since the human body acts like an antenna.

polarity of the applied voltage changes. The resulting pinched hysteresis loop will have e.g. a small lobe area and does not reflect the actual properties of a (single) sweat duct memristor.

## 5.3 Electrode choice

### *Measurement (M-electrodes)*

The use of pre wired solid hydrogel Ag/AgCl electrodes (Kendall 1050 NPSM, active electrode area of  $5.05 \text{ cm}^2$ ) are recommended for small signal AC EDA measurements [63]. However, those electrodes are not suitable for the non-linear skin memristor measurements which was demonstrated in [3]<sup>17</sup>. Any gel of pre-gelled electrode types consist of ions and electro-osmosis may affect the gel itself if the applied field is strong enough and dry electrodes (e.g. made of Ag/AgCl) are consequently recommended for non-linear skin memristor measurements [3]. It was shown that the orientations of obtained pinched hysteresis loops from the recordings (at the forearm) with the Kendall 1050 NPSM electrodes were clock-wise in the first quadrant and counter clock-wise in the third quadrant (see recordings with “M2” in Figures 6 and 8 in [3])<sup>18</sup>. This implies a decrease in the state dependent conductance when a positive voltage is applied and an increase when the applied voltage is negative. A high ionic strength of the gel is an explanation for this observation. The gel penetrates the skin (including the ducts) and the less conductive sweat takes place as soon as electro-osmosis towards the skin surface occurs (positive voltage).

Two dry Ag/AgCl electrodes<sup>19</sup> with different effective electrode areas ( $0.283 \text{ cm}^2$  and  $0.503 \text{ cm}^2$ ) were tested and the results were quite similar. The smaller electrodes were chosen for the studies in [2, 4] in order to reduce the current through the subjects and also because the chosen company provided those electrodes in a pre-wired version.

However, it is recommended to use only dry (Ag/AgCl) electrodes that are designed for the dry use (like the chosen ones from the company Wuhan Greentek PTY LT). Electrodes that are not designed for the dry use may consist of a plastic core, only covered by a small Ag/AgCl layer and it may appear that some of this layer migrates into the skin as it happened twice during pilot studies (applied sinusoidal voltages with amplitudes of 1.2 V and above).

### *Current carrying (CC) and reference (ref) electrodes*

The choice of the current carrying and reference electrodes is less critical than it is for the M electrode. It is recommendable that all three electrodes are based on the same material (e.g. Ag/AgCl) in order to reduce half-cell potentials that add as DC

---

<sup>17</sup> Four different electrode types were tested.

<sup>18</sup> Opposite from the recordings on human skin with dry Ag/AgCl electrodes.

<sup>19</sup> Both from the company Wuhan Greentek PTY LTD.

offset to the measurement. A solid hydrogel Ag/AgCl electrode (type Kendall 1050 NPSM) is chosen as reference electrode in the human skin memristor studies in [2-4] because they are easy in use (i.e. no tape is needed in order to attach them to the skin). A saline solution is chosen as CC electrode in those studies in order to minimize the voltage that has to be provided by the operational amplifier at the signal output side (three-electrode system in Figure 18 a)) which will in turn increase the possible measurement range of the whole system. The voltage is applied to the solution by several Ag/AgCl electrodes.

## 5.4 Digital part

The software of the measurement system is written in NI LabVIEW (version 2014). Different recording modes were developed for the linear (AC) EDA and the non-linear skin memristor measurements.

### EDA recording mode

A sinusoidal voltage with constant frequency of 20 Hz and amplitude of 0.1 V<sup>20</sup> is provided at the signal out port. In fact, three periods of the signal were generated and the corresponding current was measured in order to calculate one conductance and one susceptance value (see illustration in Figure A2 in [1]). Only the second and third period per run were chosen for the calculation. The sample rate for obtaining one conductance and one susceptance value was about 5 Hz in the instrumentation in [1] and it was about 2 Hz in the instrumentation [2] (dependent on the pause/delay time between voltage runs). The sample rate for reading the voltage  $v_{\text{read}}$  at the input side was 50,000 samples/s.

### Calculation of the skin admittance

Combining equations (31) and (32) and solving for  $Y_{\text{Skin}}$  will lead to the expression

$$Y_{\text{Skin}} = -\frac{v_{\text{read}}}{v} Y_{\text{fb}} \quad (33)$$

The voltage  $-v_{\text{read}} = a_{\text{read}} \sin(\omega t + \phi)$  is phase shifted with regard to the applied voltage  $v = a \cdot \sin(\omega t)$ . The voltages can be expressed by exponential functions and equation (33) turns into

$$Y_{\text{Skin}} = -\left( \frac{a_{\text{read}} \frac{e^{i(2\omega t + \phi)} - e^{-i(2\omega t + \phi)}}{2i}}{a \frac{e^{i(2\omega t)} - e^{-i(2\omega t)}}{2i}} \right) Y_{\text{fb}} \quad (34)$$

$$= -\left( \frac{a_{\text{read}} \cdot e^{i(\phi)}}{a} \right) Y_{\text{fb}} \quad (35)$$

---

<sup>20</sup> In [1], amplitude of 0.5 V was chosen instead.

$$= - \left( \frac{a_{\text{read}} \cdot (\cos \phi + j \sin \phi)}{a} \right) (G_{\text{fb}} + j B_{\text{fb}}) \quad (36)$$

$$G_{\text{Skin}} + j B_{\text{Skin}} = - \frac{v'_{\text{read}} + j v''_{\text{read}}}{a} (G_{\text{fb}} + j B_{\text{fb}}), \quad (37)$$

with

$$v'_{\text{read}} = \cos \phi \cdot a_{\text{read}} \quad (38)$$

as the real part and

$$v''_{\text{read}} = \sin \phi \cdot a_{\text{read}} \quad (39)$$

as the imaginary part of the measured voltage  $v_{\text{read}}$ .

By solving equation (37) and comparing real and imaginary part on the left and the right side, the equations for skin conductance ( $G_{\text{Skin}}$ ) and susceptance ( $B_{\text{Skin}}$ ) are derived with

$$G_{\text{Skin}} = - \frac{v'_{\text{read}} G_{\text{fb}} - v''_{\text{read}} B_{\text{fb}}}{a} \quad (40)$$

$$B_{\text{Skin}} = - \frac{v'_{\text{read}} B_{\text{fb}} + v''_{\text{read}} G_{\text{fb}}}{a}. \quad (41)$$

### Lock-in amplification

Real and imaginary part of the voltage can be derived by lock-in amplification which is done over  $n$  signal periods (see illustration in Figure 6 b)). A reference signal that has the same frequency and is in phase with the applied voltage  $v$  is multiplied to the measured voltage  $v_{\text{read}}$  in order to obtain  $v'_{\text{read}}$ . The real part is the area under the curve of the obtained product normed by the number of signal periods and can be described by

$$v'_{\text{read}} = \frac{1}{nT} \int_0^{nT} (a_{\text{read}} \sin(\omega t + \phi) \cdot a_{\text{ref}} \sin(\omega t)) dt \quad (42)$$

$$= \frac{a_{\text{read}} \cdot a_{\text{ref}}}{2nT} \int_0^{nT} (\cos(\phi) - \cos(2\omega t + \phi)) dt \quad (43)$$

$$= \frac{a_{\text{read}} \cdot a_{\text{ref}}}{2nT} \left[ \cos(\phi) t - \frac{1}{2\omega} \sin(2\omega t + \phi) \right]_0^{nT} \quad (44)$$

$$v'_{\text{read}} = \frac{a_{\text{read}} \cdot a_{\text{ref}}}{2} \cos(\phi), \quad (45)$$

with  $n \in \mathbb{N}$ . Comparing equation (45) with equation (38) makes clear, that the amplitude  $a_{\text{ref}}$  of the reference signal has to be 2.

If the multiplication is done with a reference signal that is shifted by 90 degree (with regard to the applied voltage), the imaginary part  $v''_{\text{read}}$  is obtained with

$$v''_{\text{read}} = \frac{1}{nT} \int_0^{nT} (a_{\text{read}} \sin(\omega t + \phi) \cdot a_{\text{ref}} \cos(\omega t)) dt \quad (46)$$

$$= \frac{a_{\text{read}} \cdot a_{\text{ref}}}{2nT} \int_0^{nT} (\sin(\phi) + \sin(2\omega t + \phi)) dt \quad (47)$$

$$= \frac{a_{\text{read}} \cdot a_{\text{ref}}}{2nT} \left[ \sin(\phi) t - \frac{1}{2\omega} \cos(2\omega t + \phi) \right]_0^{nT} \quad (48)$$

$$v''_{\text{read}} = \frac{a_{\text{read}} \cdot a_{\text{ref}}}{2} \sin(\phi), \quad (49)$$

with  $n \in \mathbb{N}$  and  $a_{\text{ref}} = 2$ . The number  $n$  of signal periods can be increased in order to reduce noise on the cost that it lowers the speed of the instrumentation [47].

### **Skin memristor recording mode**

The program enables variation of the applied voltage in shape, amplitude and frequency. Signal generation and reading is chosen to be done with 500 samples per period for any signal frequency  $f$ . The corresponding sample frequency  $f_{\text{sam}}$  on the signal reading side can be calculated by

$$f_{\text{sam}} = f \cdot N, \quad (50)$$

with  $N$  as the number of samples per period ( $N=500$  in the developed instrumentation). The read voltage  $v_{\text{read}}$  can be plotted sample per sample against the generated voltage. In order to change this presentation into a current vs. generated voltage (V-I) plot, the read voltage was simply multiplied with the conductance value of the feedback resistor ( $1/R_{\text{fb}}$ ). This is a valid approximation since the contribution of the feedback susceptance to the total amount of the feedback admittance (see equation (4)) can be omitted for the chosen feedback ( $R_{\text{fb}} = 56 \text{ k}\Omega$  and  $C_{\text{fb}} = 4.7 \text{ nF}$ ) within the chosen frequency range (0.05 Hz to 2.5 Hz).

# 6 Memristor simulations

*Related papers:* Simulations based on different memristor models were done in [2, 4].

All simulations were done by the use of Maple (Version 2016.2). Obtained differential equations were solved numerically by the Runge-Kutta-Fehlberg 45 method.

## 6.1 Model selection and results

While recording on human skin, small shifts in the pinched point positions from coordinate origin were usually observed. It is known that shifts may originate from parasitic elements in organic memristor recordings in general [16, 18]. Possible effects of a parallel capacitance and a DC offset (see skin equivalent circuit in Figure 13) were studied in [4] by simulations. The HP memristor (model) was chosen for those simulations. It can be classified as an ideal generic memristor [16] and is of course different from the skin memristor, which is a generic one up to a certain magnitude of applied voltage [2]. The change of the inner state happens much faster in the HP memristor and maximum and minimum memductance are higher than in skin. However, there are several similarities between both memristors allowing conclusions based on the simulations. The inner state of both can be described by the extension  $x$  of the high conductive region vs. the low conductive region. The orientations of the pinched hysteresis loops are counter clockwise in the first quadrant and the two branches of the loops are crossing in the pinched point with different slopes (“transversal”). A first skin memristor model based on the data in [57] was presented in [58]. This model has some similarities to the HP memristor model and the shapes of the obtained hysteresis loops are comparable (compare e.g. Figure 20 here with Figure 3 in [58]). The HP memristor model was chosen for the simulations because it is much better known. It was shown in [4] that a DC offset and a parallel capacitance will both cause a shift in pinched position and the results from simulations were similar to example measurements on the forearm.

The second non-linear mechanism in skin (see above and [2]) may be modelled by a NTC thermistor. A model of the supposed NTC stratum corneum thermistor is not available, yet, and a general NTC thermistor model (from [18]) was chosen for the simulations. The chosen model is of course different from the stratum corneum but it may reflect observations from the skin memristor measurements. It is possible to obtain hysteresis loops with two pinched points (that are quite symmetric with regard to the coordinate origin) from the chosen NTC thermistor model with a capacitance in parallel as it was demonstrated by simulation in [2]. Essential is the “tangential” shape

of the pinched hysteresis loop (see Figure 21 a)). The state change in the NTC thermistor model is a function of  $v^2$  (see equation (55)). Thus, the memductance change will be independent of the sign of the applied voltage and two memductance maxima occur (see Figure 21 b)) during one period which is different to the HP memristor model. It was not possible to obtain hysteresis loops with two pinched points by simulating the HP memristor in parallel with a capacitance.

### HP memristor

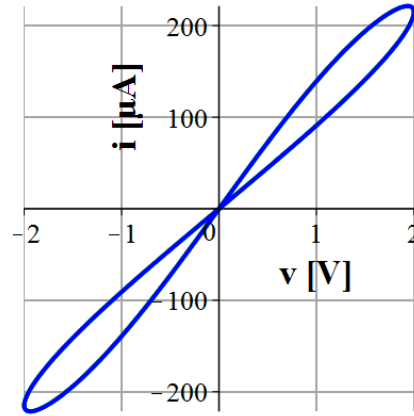


**Figure 20** | *V-I-plot of a single HP memristor obtained by simulation over two periods. A constant sinusoidal voltage with  $f=2.5$  Hz and amplitude=2 V was chosen as signal source. The initial state (internal stat  $x$  at simulation start) was 0.3.*

The HP memristor [20] is described by the equations

$$M(x) = R_{on} \cdot x + R_{off} \cdot (1 - x) \quad (51)$$

$$\frac{dx}{dt} = \frac{\mu_v \cdot R_{on}}{D^2} \cdot I_M(t), \quad (52)$$

with  $x$ <sup>21</sup> as the internal state variable which reflects the extension of the high conductive (doped) region, normalized with the absolute extent  $D$  of the titanium dioxide layer which is equal to 10 nm. The state  $x$  can obtain values between 0 to 1. If  $x$  is equal 1, the overall memristance is lowest and equal to  $R_{on} = 0.1$  k $\Omega$ , while a state  $x = 0$  reflects the highest memristance with  $M(x)$  equal to  $R_{off} = 16$  k $\Omega$ . The constant  $\mu_v = 10^{-14} \frac{m^2}{sV}$  reflects the oxygen vacancy mobility. A window function [64] is multiplied to the state equation in (53) like it was done in [35] in order to take saturation into account. However, this window function only has noticeable effects as soon as  $x$  obtains values close to the boundaries (0 and 1), which was not the case in the simulations that are part of this thesis.

<sup>21</sup> The presentation of the equations was slightly different in [23]. The internal state was given by the total extension  $w$  of the doped region instead of the normalized extension  $x$ .

### HP memristor (adapted)

An adapted version of the HP memristor model with

$$\frac{dx}{dt} = \frac{\mu_v \cdot R_{on}}{D^2} \cdot I_M(t) \cdot 0.005 \quad (53)$$

is chosen for the simulations presented in Figure 21. The only difference of this adapted HP memristor model to the original one is that the state change happens much slower (with a factor of 0.005). This was done in order to avoid that the internal state  $x$  reaches its boundaries almost instantly for sinusoidal voltage source with amplitude 4 V and  $f = 0.05$  Hz (which would happen without the adaption). The low frequency of the voltage itself was chosen with regard to the chosen NTC thermistor model.

### NTC thermistor model

The NTC thermistor model [18] is described by

$$G(T_N) = \left( R_{0N} \cdot e^{\beta_N \left( \frac{1}{T_N} - \frac{1}{T_{0N}} \right)} \right)^{-1} \quad (54)$$

$$\frac{dT_N}{dt} = \frac{\delta_N}{H_{CN}} (T_{0N} - T_N) + \frac{G(T_N)}{H_{CN}} \cdot v^2, \quad (55)$$

with  $G(T_N)$  as the temperature dependent conductance which becomes equal to the inverse of  $R_{0N} = 3.89 \text{ k}\Omega$  at ambient temperature  $T_{0N} = 300 \text{ K}$ . The material specific constant  $\beta_N$  is equal to  $5 \cdot 10^5 \text{ K}$ . The dissipation constant is given with  $\delta_N = 0.1 \text{ W/K}$  and the heat capacitance  $H_{CN}$  is equal to  $0.14 \text{ J/K}$ .

## 6.2 NTC thermistor in parallel with HP memristor

A simulation with the chosen NTC memristor model and the adapted HP memristor (see above) in parallel is done (see Figure 21 c) and d)). The overall current is obtained by

$$i = i_{th} + i_{HPa} = v \cdot (G_{th}(T) + G_{HPa}(x)) \quad (56)$$

$$= v \cdot \left( G_{th}(T) + \frac{1}{M_{HPa}(x)} \right) \quad (57)$$

with  $G_{th}(T)$  and  $G_{HPa}(x)$  as the state dependent conductances of the NTC thermistor and adapted HP memristor models respectively. The obtained V-I plot (see Figure 21 c)) shows a pinched hysteresis loop that is quite asymmetric. It is possible that asymmetric shapes of the pinched hysteresis that were observed in [2] may partly explained by noticeable contributions (to the measurement) of both, the sweat duct memristor and the stratum corneum NTC thermistor (compare e.g. the recording from subject C in Figure 2 c) in [2] with the simulation result in Figure 21 c) here).

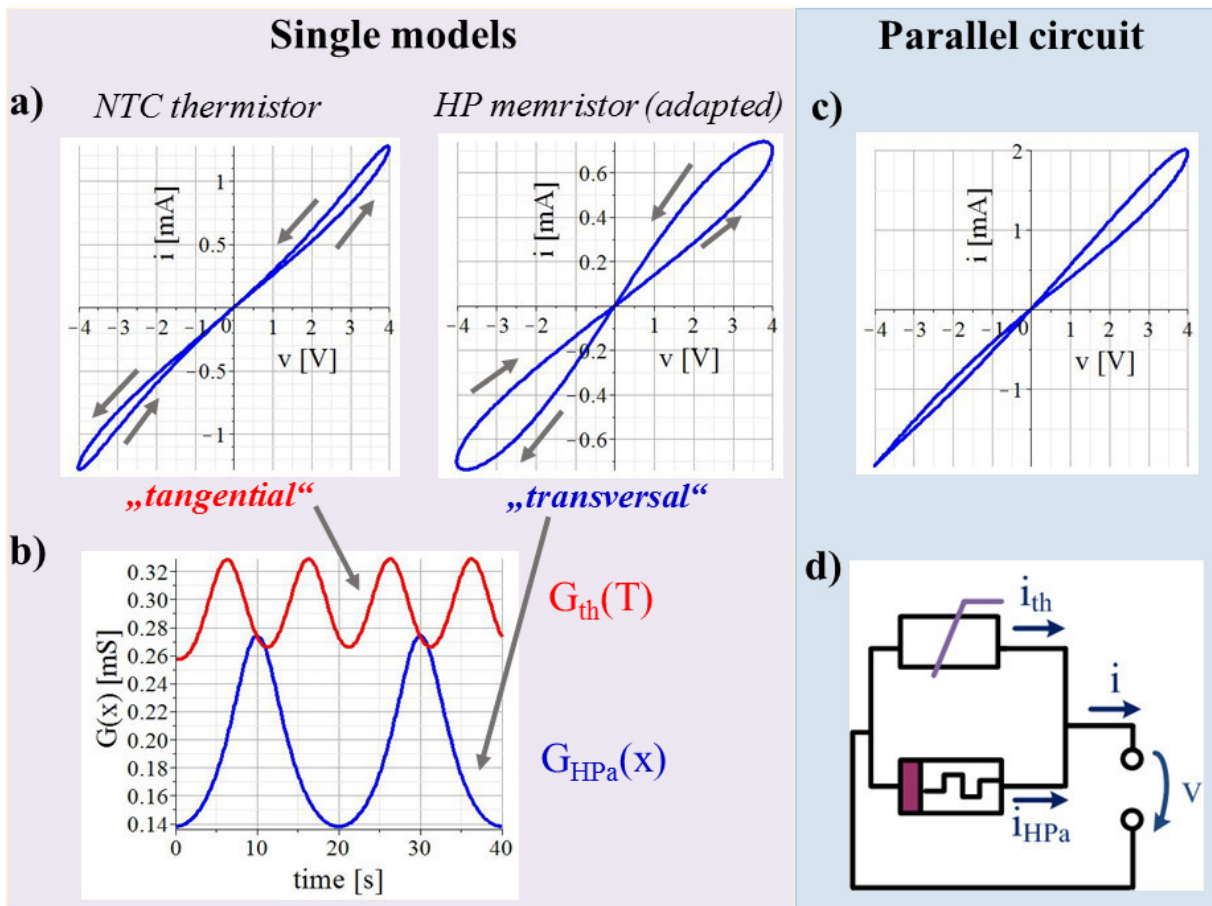


**Figure 21 | Results of simulations on two different memristor types.** The simulations are based on an adapted HP memristor model (see state equation (53)) and a NTC thermistor model. A sinusoidal voltage  $v$  with amplitude of 4 V and frequency of 0.05 Hz was used as signal source in all simulations. The initial state  $x_0$  (internal state  $x$  at simulation start) of the adapted HP memristor was 0.55. **a)** V-I plots of the chosen models. The arrows indicate the orientation of the hysteresis loops. The two branches of the hysteresis loop of the NTC memristor are touching at the pinched point while the branches of the (adapted) HP memristor are crossing the pinched point with different slopes. **b)** Corresponding memductance changes over time of both memristor types, shown over two periods. **c)** Resulting V-I plot if both memristor types are connected in parallel, as it is illustrated in **d)** Electrical equivalent circuit of the simulated parallel connection.

## 7 Conclusions and findings

The research field of non-linear electrical measurements on human skin has been initiated by this thesis. Non-linear measurements uncover the non-linear properties of the underlying tissue (like human skin) that are not noticed when applied signals with low amplitude and high frequency are chosen. As soon as the electrical properties of human skin (or any other tissue) are influenced by the applied electrical signal itself, the measurement becomes non-linear and the shape of the measured signal will be different from the applied signal. Since obtained voltage-current plots showed pinched hysteresis loops with pinched point position in (or close to) the coordinate origin<sup>22</sup> it can be confirmed that human skin is a memristor. The corresponding class of measurements has been labelled here as “(non-linear) skin memristor measurements”. It contains the recording of the AC voltage current characteristics by e.g. applying different voltage signals with appropriate amplitudes and frequencies. It further contains recordings with DC voltages pulses or constant DC voltage levels (with sufficient high level) in order to study the transient behaviour of the non-linear mechanisms behind the “skin memristor”. Small signal linear conductance (EDA) measurements can be conducted in addition in order to study the transient behaviour during recovery processes (after the non-linear recording).

It has been shown that amplitude of 0.4 V (for low frequency (e.g. 0.05 Hz) sinusoidal) voltage may be already sufficient for the transition from linear to non-linear measurements. Similar magnitude can be expected for applied DC voltages, which implies that standard EDA measurements (applied DC voltage with 0.5 V) that are supposed to be linear may become non-linear already. Within EDA recordings, any influence of the applied voltage on the skin is undesirable since it erroneously affects the measurement (effect on conductance level). It can be assured that an EDA recording is linear, if the AC method is chosen with a reasonable signal frequency (e.g. 20 Hz) and small amplitude (e.g. 0.1 V). It has been shown that EDA recordings with the DC and the AC method are comparable and the use of the AC method is recommended.

The human skin memristor is actual a combination of the sweat duct memristor (state change in the sweat ducts due to electro-osmosis (known before)) electrically in parallel with another memristor type most likely found in stratum corneum. There is evidence (here) that the stratum corneum which contains keratinized tissue behaves like a NTC thermistor which is a memristor itself. A current through the stratum corneum may change its temperature and thus its memductance. The theory of the stratum corneum thermistor (memristor) is based on the findings here and it has to be approved later. A corresponding model and a model of the sweat duct memristor based on the systematic study here may be found later. The sweat duct memristor usually

---

<sup>22</sup> Valid for different signal shapes of the applied voltage.

dominates the measurement as long as the galvanic contact through the sweat glands is given. However, in some recordings, both memristor types contributed noticeably which was indicated by a large asymmetry of the recorded pinched hysteresis loops (the lobe in the third quadrant is much narrower than the lobe in the first quadrant).

The overall skin memristors at the forehead and the earlobe are found to be a generic memristors up to a certain magnitude of applied voltage (e.g. 0.8 V at the forehead) and they become extended memristors above. Furthermore, they are found to be non-volatile memristors, implying that information can be stored within the underlying skin sites. The fingertip is also a memristor since pinched hysteresis loops were observed. However, it was not possible to classify the memristor at the fingertip since emotional sweating interfered the measurements and the capacitive properties of the stratum corneum were dominating at frequencies of 0.5 Hz and above.

Maximum current, lobe area and a non-linearity parameter<sup>23</sup> were found to be useful in order to evaluate obtained skin memristor<sup>24</sup> data over a population. Large variations among subjects were observed and it might be possible to correlate physiological properties with different geometrical properties of the pinched hysteresis loops. Diagnosis of any disease that affects the non-linear properties of human skin could be a possible application.

Instrumentation suitable for linear EDA and non-linear skin memristor measurements can be quite similar which enables the sequential use of both methods under the same electrodes. However, electrode types have to be chosen more carefully within the non-linear skin memristor measurements. The use of dry electrodes (e.g. Ag/AgCl) is recommended since electro-osmosis may affect any electrode gel (which will in turn affect the measurement). It is recommended to choose a three-electrode rather than a two-electrode system for non-linear skin memristor measurements since it enables monopolar recordings. The measurement quality of bipolar recordings is lower since the measured load will contain two sweat duct memristors (from two different skin sites) that are connected in series to each other but with opposite orientation.

The skin memristor has an internal state (e.g. determined by the amount of sweat) which has a strong effect on the measurement. The results of repeated measurements on one test subject may already differ largely just because of a variation in the initial state (internal state at measurement start). Any non-linear measurement that is conducted, may affect the initial state of an electrical measurement that is conducted short time after (at the same skin site). This has to be considered during study design and interpretation of the results. If e.g. a sinusoidal voltage was applied over several periods, the appearance of the hysteresis loop changed from period to period. The internal state itself is not only influenced by the non-linear measurement but also by

---

<sup>23</sup> Additional parameters may be found later.

<sup>24</sup> These parameters might be useful for characterization of other organic memristors, as well.

thermal and emotional sweating. It was shown that the results may differ largely before and after physical exercise.

A DC offset and a parallel capacitance (both will naturally affect electrical measurements on human skin) may explain a shift in pinched point position from the coordinate origin as it was shown by simulation (based on the HP memristor model). If the pinched hysteresis loop of a memristor is tangential, the overall V-I plot of this memristor with a capacitance in parallel may show hysteresis loops with two pinched points (shown by simulation using a generic NTC thermistor (memristor) model).

This thesis provides a first basic knowledge on the non-linear properties of human skin and these properties can be studied more in detail. Examples of open questions and potential targets of studies are given as follow:

- It is not clear how much sweat is actual moved during the electro-osmotic process in the sweat ducts. Small volumes may have already a large impact on the state-dependent conductance (memductance). However, fast changes of the memductance as soon as the voltage drops to zero may be explained by pressure driven forces of the tissue that surrounds the sweat ducts. This could be an indication that a noticeable amount of sweat is moved during electro-osmosis.
- Ionic composition of the sweat in relation to the appearance of the pinched hysteresis loops might be interesting to study.
- It is not clear of how much the temperature of the stratum corneum changes as a current is going through. It is also unknown how much the memductance of the stratum corneum changes with temperature.
- The effect of the humidity content of the stratum corneum in relation to its thermal properties might be interesting to study.
- All studies within this thesis have been conducted with applied constant voltage source. However, Yamamoto *et.al* [14] demonstrated non-linear properties on human skin also by application of constant current and further measurements by this method might be interesting, as well.

As an overall summary: Non-linear electrical measurements on human skin provide a new field of research that has been initiated by this thesis, suitable instrumentation and recording methods have been developed, and new insights into the human skin physiology have been already made here by these non-linear recording techniques. The number of potential research questions and applications within this research field is large, since only little related work has been done before.

# References

- [1] O. Pabst, C. Tronstad, S. Grimnes, D. Fowles, and Ø. G. Martinsen, "Comparison between the AC and DC measurement of electrodermal activity," *Psychophysiology*, vol. 54, no. 3, pp. 374-385, 2017.
- [2] O. Pabst, Ø. G. Martinsen, and L. Chua, "Human Skin is a generic, non-volatile memristor" *unpublished*, 2017.
- [3] O. Pabst, C. Tronstad, and Ø. G. Martinsen, "Instrumentation, electrode choice and challenges in human skin memristor measurement," in *Engineering in Medicine and Biology Society (EMBC), 2017 39th Annual International Conference of the IEEE*, 2017, pp. 1844-1848: IEEE.
- [4] O. Pabst and Ø. G. Martinsen, "Interpretation of the pinched point position in human skin memristor measurements," in *EMBEC & NBC 2017*: Springer, 2017, pp. 430-433.
- [5] L. Chua, "Memristor-the missing circuit element," *IEEE Transactions on circuit theory*, vol. 18, no. 5, pp. 507-519, 1971.
- [6] W. Boucsein, *Electrodermal activity*. Springer Science & Business Media, 2012.
- [7] P. F. Millington and R. Wilkinson, *Skin*. Cambridge University Press, 1983.
- [8] K. Sato, W. Kang, K. Saga, and K. Sato, "Biology of sweat glands and their disorders. I. Normal sweat gland function," *Journal of the American Academy of Dermatology*, vol. 20, no. 4, pp. 537-563, 1989.
- [9] S. Grimnes, "Psychogalvanic reflex and changes in electrical parameters of dry skin," *Medical and Biological Engineering and Computing*, vol. 20, no. 6, pp. 734-740, 1982.
- [10] S. Grimnes, "Pathways of ionic flow through human skin in vivo," *Acta dermatovenereologica*, vol. 64, no. 2, pp. 93-98, 1984.
- [11] S. M. Abie, J. Bergli, Y. Galperin, and Ø. G. Martinsen, "Universality of AC conductance in human hair," *Biomedical Physics & Engineering Express*, vol. 2, no. 2, p. 027002, 2016.
- [12] E. E. Benarroch, "The central autonomic network: functional organization, dysfunction, and perspective," in *Mayo Clinic Proceedings*, 1993, vol. 68, no. 10, pp. 988-1001: Elsevier.
- [13] H. Schliack and R. Schiffter, "Neurophysiologie und-pathophysiologie der Schweißsekretion," in *Normale und Pathologische Physiologie der Haut II*: Springer, 1979, pp. 349-458.
- [14] T. Yamamoto and Y. Yamamoto, "Non-linear electrical properties of skin in the low frequency range," *Medical and Biological Engineering and Computing*, vol. 19, no. 3, p. 302, 1981.
- [15] J. M. Tour and T. He, "The fourth element," *Nature*, vol. 453, no. 7191, pp. 42-43, 2008.
- [16] L. Chua, "If it's pinched it's a memristor," *Semiconductor Science and Technology*, vol. 29, no. 10, p. 104001, 2014.
- [17] L. Chua, "Resistance switching memories are memristors," in *Memristor Networks*: Springer, 2014, pp. 21-51.
- [18] M. P. Sah, C. Yang, H. Kim, B. Muthuswamy, J. Jevtic, and L. Chua, "A generic model of memristors with parasitic components," *IEEE Transactions on Circuits and Systems I: Regular Papers*, vol. 62, no. 3, pp. 891-898, 2015.
- [19] S. P. Adhikari, M. P. Sah, H. Kim, and L. O. Chua, "Three fingerprints of memristor," *IEEE Transactions on Circuits and Systems I: Regular Papers*, vol. 60, no. 11, pp. 3008-3021, 2013.
- [20] D. B. Strukov, G. S. Snider, D. R. Stewart, and R. S. Williams, "The missing memristor found," *nature*, vol. 453, no. 7191, p. 80, 2008.
- [21] L. Chua, "Everything you wish to know about memristors but are afraid to ask," *Radioengineering*, vol. 24, no. 2, p. 319, 2015.
- [22] R. S. Williams, "How we found the missing memristor," *IEEE spectrum*, vol. 45, no. 12, 2008.
- [23] A. C. Torrezan, J. P. Strachan, G. Medeiros-Ribeiro, and R. S. Williams, "Sub-nanosecond switching of a tantalum oxide memristor," *Nanotechnology*, vol. 22, no. 48, p. 485203, 2011.

- [24] J. J. Yang *et al.*, "High switching endurance in TaO<sub>x</sub> memristive devices," *Applied Physics Letters*, vol. 97, no. 23, p. 232102, 2010.
- [25] X. Zhu *et al.*, "Observation of Conductance Quantization in Oxide - Based Resistive Switching Memory," *Advanced Materials*, vol. 24, no. 29, pp. 3941-3946, 2012.
- [26] A. Wedig *et al.*, "Nanoscale cation motion in TaO<sub>x</sub>, HfO<sub>x</sub> and TiO<sub>x</sub> memristive systems," *Nature nanotechnology*, vol. 11, no. 1, pp. 67-74, 2016.
- [27] J. J. Yang *et al.*, "The mechanism of electroforming of metal oxide memristive switches," *Nanotechnology*, vol. 20, no. 21, p. 215201, 2009.
- [28] S. H. Jo, T. Chang, I. Ebong, B. B. Bhadviya, P. Mazumder, and W. Lu, "Nanoscale memristor device as synapse in neuromorphic systems," *Nano letters*, vol. 10, no. 4, pp. 1297-1301, 2010.
- [29] G. Indiveri, B. Linares-Barranco, R. Legenstein, G. Deligeorgis, and T. Prodromakis, "Integration of nanoscale memristor synapses in neuromorphic computing architectures," *Nanotechnology*, vol. 24, no. 38, p. 384010, 2013.
- [30] M. Prezioso, F. Merrikh-Bayat, B. Hoskins, G. Adam, K. K. Likharev, and D. B. Strukov, "Training and operation of an integrated neuromorphic network based on metal-oxide memristors," *Nature*, vol. 521, no. 7550, pp. 61-64, 2015.
- [31] F. Merrikh-Bayat and S. B. Shouraki, "Memristor-based circuits for performing basic arithmetic operations," *Procedia Computer Science*, vol. 3, pp. 128-132, 2011.
- [32] K. A. Bickerstaff and E. E. Swartzlander, "Memristor-based arithmetic," in *Signals, Systems and Computers (ASILOMAR), 2010 Conference Record of the Forty Fourth Asilomar Conference on*, 2010, pp. 1173-1177: IEEE.
- [33] H. Kim, M. P. Sah, C. Yang, T. Roska, and L. O. Chua, "Memristor bridge synapses," *Proceedings of the IEEE*, vol. 100, no. 6, pp. 2061-2070, 2012.
- [34] G. Z. Cohen, Y. V. Pershin, and M. Di Ventra, "Second and higher harmonics generation with memristive systems," *Applied Physics Letters*, vol. 100, no. 13, p. 133109, 2012.
- [35] O. Pabst and T. Schmidt, "Frequency dependent rectifier memristor bridge used as a programmable synaptic membrane voltage generator," *Journal of Electrical Bioimpedance*, vol. 4, no. 1, pp. 23-32, 2013.
- [36] A. G. Volkov, C. Tucket, J. Reedus, M. I. Volkova, V. S. Markin, and L. Chua, "Memristors in plants," *Plant signaling & behavior*, vol. 9, no. 3, p. e28152, 2014.
- [37] E. Gale, A. Adamatzky, and B. de Lacy Costello, "Slime mould memristors," *BioNanoScience*, vol. 5, no. 1, pp. 1-8, 2015.
- [38] Ø. G. Martinsen, S. Grimnes, and J. Karlsen, "Electrical methods for skin moisture assessment," *Skin Pharmacology and Physiology*, vol. 8, no. 5, pp. 237-245, 1995.
- [39] Ø. G. Martinsen, O. Pabst, C. Tronstad, and S. Grimnes, "Sources of error in AC measurement of skin conductance," *Journal of Electrical Bioimpedance*, vol. 6, no. 1, pp. 49-53, 2015.
- [40] L. C. Johnson and A. Lubin, "Spontaneous electrodermal activity during waking and sleeping," *Psychophysiology*, vol. 3, no. 1, pp. 8-17, 1966.
- [41] W. B. Mendes, "Assessing autonomic nervous system activity," *Methods in social neuroscience*, pp. 118-147, 2009.
- [42] T. P. Zahn, L. K. Jacobsen, C. T. Gordon, K. McKenna, J. A. Frazier, and J. L. Rapoport, "Autonomic nervous system markers of psychopathology in childhood-onset schizophrenia," *Archives of General Psychiatry*, vol. 54, no. 10, pp. 904-912, 1997.
- [43] L. Paletta, N. Pittino, M. Schwarz, V. Wagner, and K. Kallus, "Human Factors Analysis Using Wearable Sensors in the Context of Cognitive and Emotional Arousal," *Procedia Manufacturing*, vol. 3, pp. 3782-3787, 2015.
- [44] E.-H. Jang, B.-J. Park, S.-H. Kim, M.-A. Chung, M.-S. Park, and J.-H. Sohn, "Emotion classification based on bio-signals emotion recognition using machine learning algorithms," in *Information Science, Electronics and Electrical Engineering (ISEEE), 2014 International Conference on*, 2014, vol. 3, pp. 1373-1376: IEEE.

- [45] K. H. Kim, S. W. Bang, and S. R. Kim, "Emotion recognition system using short-term monitoring of physiological signals," *Medical and biological engineering and computing*, vol. 42, no. 3, pp. 419-427, 2004.
- [46] W. T. Roth, M. E. Dawson, and D. L. Filion, "Publication recommendations for electrodermal measurements," *Psychophysiology*, vol. 49, no. 8, pp. 1017-1034, 2012.
- [47] Ø. G. Martinsen and S. Grimnes, *Bioimpedance and bioelectricity basics*. Academic press, 2011.
- [48] B. J. Nordbotten, C. Tronstad, Ø. G. Martinsen, and S. Grimnes, "Estimation of skin conductance at low frequencies using measurements at higher frequencies for EDA applications," *Physiological measurement*, vol. 35, no. 6, p. 1011, 2014.
- [49] S. Grimnes, A. Jabbari, Ø. G. Martinsen, and C. Tronstad, "Electrodermal activity by DC potential and AC conductance measured simultaneously at the same skin site," *Skin Research and Technology*, vol. 17, no. 1, pp. 26-34, 2011.
- [50] C. Tronstad, G. E. Gjein, S. Grimnes, Ø. G. Martinsen, A.-L. Krogstad, and E. Fosse, "Electrical measurement of sweat activity," *Physiological measurement*, vol. 29, no. 6, p. S407, 2008.
- [51] C. Tronstad, H. Kalvøy, S. Grimnes, and Ø. G. Martinsen, "Waveform difference between skin conductance and skin potential responses in relation to electrical and evaporative properties of skin," *Psychophysiology*, vol. 50, no. 11, pp. 1070-1078, 2013.
- [52] D. Bari, H. Aldosky, C. Tronstad, H. Kalvøy, and Ø. Martinsen, "Electrodermal responses to discrete stimuli measured by skin conductance, skin potential, and skin susceptance," *Skin Research and Technology*, 2017.
- [53] J. Rutenfranz, "Zur Frage einer Tagesrhythmik des elektrischen Hautwiderstandes beim Menschen," *Internationale Zeitschrift für angewandte Physiologie einschließlich Arbeitsphysiologie*, vol. 16, no. 2, pp. 152-172, 1955.
- [54] Y. Yamamoto and T. Yamamoto, "Dispersion and correlation of the parameters for skin impedance," *Medical and Biological Engineering and Computing*, vol. 16, no. 5, pp. 592-594, 1978.
- [55] M.-Z. Poh, N. C. Swenson, and R. W. Picard, "A wearable sensor for unobtrusive, long-term assessment of electrodermal activity," *IEEE transactions on Biomedical engineering*, vol. 57, no. 5, pp. 1243-1252, 2010.
- [56] A. Martínez-Rodrigo, R. Zangróniz, J. M. Pastor, and M. V. Sokolova, "Arousal level classification of the aging adult from electro-dermal activity: From hardware development to software architecture," *Pervasive and Mobile Computing*, vol. 34, pp. 46-59, 2017.
- [57] S. Grimnes, "Skin impedance and electro-osmosis in the human epidermis," *Medical and Biological Engineering and Computing*, vol. 21, no. 6, pp. 739-749, 1983.
- [58] G. Johnsen, C. Lütken, Ø. Martinsen, and S. Grimnes, "Memristive model of electro-osmosis in skin," *Physical Review E*, vol. 83, no. 3, p. 031916, 2011.
- [59] R. Edelberg, "Electrodermal mechanisms: A critique of the two-effector hypothesis and a proposed replacement," *Progress in electrodermal research*, pp. 7-29, 1993.
- [60] J. Joshua Yang *et al.*, "Engineering nonlinearity into memristors for passive crossbar applications," *Applied Physics Letters*, vol. 100, no. 11, p. 113501, 2012.
- [61] S. Grimnes, "Impedance measurement of individual skin surface electrodes," *Medical and Biological Engineering and Computing*, vol. 21, no. 6, pp. 750-755, 1983.
- [62] S. Grimnes, Ø. G. Martinsen, and C. Tronstad, "Noise properties of the 3-electrode skin admittance measuring circuit," in *4th European Conference of the International Federation for Medical and Biological Engineering*, 2009, pp. 720-722: Springer.
- [63] C. Tronstad, G. K. Johnsen, S. Grimnes, and Ø. G. Martinsen, "A study on electrode gels for skin conductance measurements," *Physiological measurement*, vol. 31, no. 10, p. 1395, 2010.
- [64] Y. N. Joglekar and S. J. Wolf, "The elusive memristor: properties of basic electrical circuits," *European Journal of Physics*, vol. 30, no. 4, p. 661, 2009.





## Comparison between the AC and DC measurement of electrodermal activity

OLIVER PABST,<sup>a</sup> CHRISTIAN TRONSTAD,<sup>b</sup> SVERRE GRIMNES,<sup>a,b</sup>  
DON FOWLES,<sup>c</sup> AND ØRJAN G. MARTINSEN<sup>a,b</sup>

<sup>a</sup>Department of Physics, University of Oslo, Oslo, Norway

<sup>b</sup>Department of Clinical and Biomedical Engineering, Oslo University Hospital HF, Oslo, Norway

<sup>c</sup>Department of Psychological & Brain Sciences, University of Iowa, Iowa City, Iowa, USA

### Abstract

Recording electrodermal activity is a well-accepted physiological measurement for clinical approaches and research. Historically, applying a DC (direct current) signal to the skin to measure the conductance is the most common practice for exogenous recordings. However, this method can be subject to error due to electrode polarization even with “nonpolarizing” electrodes—a problem that can be eliminated with alternating current (AC) methodology. For that reason, Boucsein et al. (2012) called for research demonstrating an AC method that is validated by comparison to standard DC methodology. Additionally, the complex structure of human skin has electrical properties that include both resistance and capacitance, and AC recording enables the measurement of skin susceptance (associated with current flow through capacitors). Finally, AC recording permits the simultaneous recording of the endogenous skin potential. In this paper, the results from a direct comparison between both methods are presented, which has not been reported previously. The results demonstrated excellent agreement between a 20 Hz AC method and a standard DC method, supporting the validity of the AC recording methodology employed. The results also showed that an applied voltage of 0.2 V is sufficient for DC recordings.

**Descriptors:** Electrodermal activity (EDA), Bioimpedance, Method comparison, Exogenous, Skin conductance, Skin potential

The term electrodermal activity (EDA) was first introduced by Johnson & Lubin, (1966) and describes “all electrical phenomena in skin” (Boucsein, 2012). When measuring exogenous EDA, an external electrical signal is applied to the skin, and its passive electrical properties such as conductance or resistance are determined. These measurements can be done either by applying a DC (direct current) electrical signal or by an AC (alternating current in the form of a sine wave) electrical signal. Only conductive (resistive) properties, especially those related to the sweat gland filling (Grimnes, 1983b), are measured by using a DC signal. By using an AC signal, the measurement becomes more complex since capacitive properties are also measured. Endogenous measurements, on the other hand, pick up the innate electrical potentials at the skin without any applied current.

### The Need for AC EDA Recordings

Recording EDA by an applied AC signal has some benefits. First, applying the DC method will potentially cause polarization of the electrodes or the skin and hence a counterelectromotive force

(Martinsen, Pabst, Tronstad, & Grimnes, 2015) that undermines the accuracy of measurement. Although nonpolarizing electrodes (e.g., Ag/AgCl) are commonly used in DC recording to address this problem, in the official publication recommendations for *Psychophysiology*, Boucsein et al. (2012) expressed concern that nonpolarizing electrodes may only partially prevent polarization, creating a possible error of unknown magnitude. Electrode polarization does not occur when using the AC method since the polarity switches continuously and there is no net charge transfer. For this reason, Boucsein et al. (2012) proposed that AC measurement may be superior to DC measurement.

Secondly, AC measurement enables exogenous measuring of the skin conductance (SC) and endogenous measuring of the skin potential (SP) simultaneously at the same electrode (Grimnes, Jabbari, Martinsen, & Tronstad, 2011). This ability allows one to examine the effect of endogenous SP on the SC measured with DC, which in turn allows a determination of the minimum magnitude of applied voltage needed in DC recordings. That is, the endogenous SP is effectively added to or subtracted from the applied DC voltage, depending on whether the voltages are in the same or opposite directions. Since bipolar recordings (palm to palm) are typically employed, the endogenous potentials tend to be small. The surface negative endogenous potential is generated across the skin, observed between a palmar electrode and an electrode at an abraded site (effectively in contact with the interstitial

This work has been performed within DIATECH@UiO, a strategic research initiative of the Faculty of Mathematics and Natural Sciences, University of Oslo.

Address correspondence to: Oliver Pabst, Postboks 1048, Blindern, 0316 Oslo, Norway. E-mail: oliverpa@fys.uio.no

fluid beneath the epidermis). To the extent that these transepidermal endogenous potentials are equal at the two palmar electrodes, there will be no differential endogenous potential. Nevertheless, small potential differences can be expected.

These small endogenous potentials have little impact with the 0.5 V applied voltage often used in DC recordings. However, there is reason to employ a lower voltage. In the context of international standards on patient safety, the specifications for medical devices (according to IEC 2005, p. 171) allow values for patient auxiliary currents of 10  $\mu\text{A}$  for DC and 100  $\mu\text{A}$  for AC. Assuming a measured conductance range from 5  $\mu\text{S}$  to 60  $\mu\text{S}$  (which is in accordance with the results from this study) and an applied 0.5 V for DC recording, the DC currents through the test persons range from 2.5  $\mu\text{A}$  to 30  $\mu\text{A}$ , which means that the specification is not met for the entire range of currents. Boucsein et al. (2012) also expressed concern about the effects of the DC current on biological membranes. Since this problem can be minimized by reducing the applied DC voltage, it is important to determine how small a voltage can be applied without contamination by endogenous potentials.

Applying a DC signal for exogenous EDA measurements is easier to implement than an AC signal, which is probably the reason for its establishment as a standard. Although there are early research groups who have used the AC method (e.g., Rutenfranz, 1955; Y. Yamamoto & Yamamoto, 1978), only a few studies with AC recordings have been published to date (Boucsein, 2012) compared to the number of studies conducted with the DC method. As stated in Boucsein (2012, p. 252): “Common to most of these (AC) studies is that they could not directly compare their results with those of DC studies, because they did not use standard methodology” and “systematic comparisons between AC and DC recordings are lacking.”

Implementing the AC method is now easier with current technology, and the number of studies conducted with the AC method may increase, but the DC method is still the most commonly used. Recent examples of research groups that are developing their own EDA measurement systems are Poh, Swenson, and Picard, (2010, using the DC method), Martínez-Rodrigo, Zangróniz, Pastor, and Sokolova, (2016, using the DC method), and Tronstad et al. (2008, using the AC method). Although the AC method is becoming more accepted, in their publication recommendation report, Boucsein et al. (2012) did not yet recommend the change from DC to AC recording since more research is needed, but they strongly appealed for further research comparing AC and DC recordings.

The following clarifies the terms used in this paper: Measuring exogenous EDA by applying an AC signal (voltage or current) is referred to as the AC method and the conductance that is measured with the AC method is called AC conductance. The same applies for the DC method and DC conductance. The DC conductance contains only the frequency independent part of the skin conductance, while the AC conductance contains a frequency dependent part in addition.

### Basic Features of AC Recordings

When a DC voltage is applied to a capacitor, the current flow diminishes as the capacitor charges, reaching zero when the charge on the capacitor is equal to the applied voltage. With an applied (sine wave) AC voltage, the capacitor charge continues to increase until the AC voltage reverses polarity, at which point the current flows in the opposite direction (discharging the capacitor). In a simple circuit with only a capacitor, the voltage across the capacitor is a sine wave with a peak 90 degrees later (a quarter of a cycle) than

the peak of the applied voltage. In contrast, the voltage drop across a resistor in parallel with the capacitor is directly proportional to the applied voltage. This difference in time between the applied voltage and voltage drop across the resistor, on the one hand, and the voltage across the capacitor, on the other, is called the phase angle. When a resistor and a capacitor are combined in a circuit, the phase angle is affected by the frequency of the applied AC voltage, the resistance, and the capacitance of the capacitor.

The resistance of a capacitor to AC current flow, called reactance (X), is a function of both its capacitance and the frequency of the applied voltage, being inversely related to both. As the frequency of the applied voltage increases, there is less time for the current to flow to the capacitor before the polarity of the applied voltage is reversed, reducing the amount of charge that opposes current flow. As a result, the resistance to current flow diminishes with increased frequency. Capacitors differ in how rapidly the voltage across them increases for a given increase in charge (i.e., capacitance). With greater capacitance, a given amount of current flow results in a smaller voltage opposing the flow of current and thus less resistance to current flow.

The familiar terms resistance and conductance (G) used to describe the properties of a resistor have analogs to describe the properties of a capacitor: reactance and susceptance (B), respectively. Similarly, the corresponding descriptors for the overall properties of a circuit with a resistor and capacitor in parallel are impedance and admittance.

### Aim of the Conducted Experiments

Experiment 1 of the present study provides a direct comparison between the AC and the DC conductance measurement method, which has not yet been carried out to the authors' knowledge. To obtain a direct comparison, both recordings are done simultaneously at the same electrodes. The results recorded from several test sessions are characterized by standard EDA scores, and the obtained responses are analyzed statistically.

Thus, the aim of Experiment 1 was to examine the similarities and differences between the AC and DC methods of EDA recording under equal conditions. To the extent that our methodology of DC recording avoids polarization, we expect similar results except for the contribution of capacitance solely to AC recording. Such similar results would provide evidence of the validity of the AC methodology used here, demonstrate the methodology for estimating DC conductance from AC recording, and provide information regarding the effects of the capacitance pathway.

The aim of Experiment 2 was to examine the effects of endogenous SP on DC recordings with varying values of the applied DC voltage. The purpose was to identify the optimal levels of applied DC voltage for those who are using this method.

## Method

### Instrumentation

All recordings were done with a custom-built measuring system that applies voltage to the skin, measures the current, and calculates the conductance, specifically designed to measure with the AC and DC methods simultaneously.

**Applied voltage signal.** To perform the direct comparison between the AC and the DC method, equal conditions for both methods must be guaranteed. Superposition enables application of an

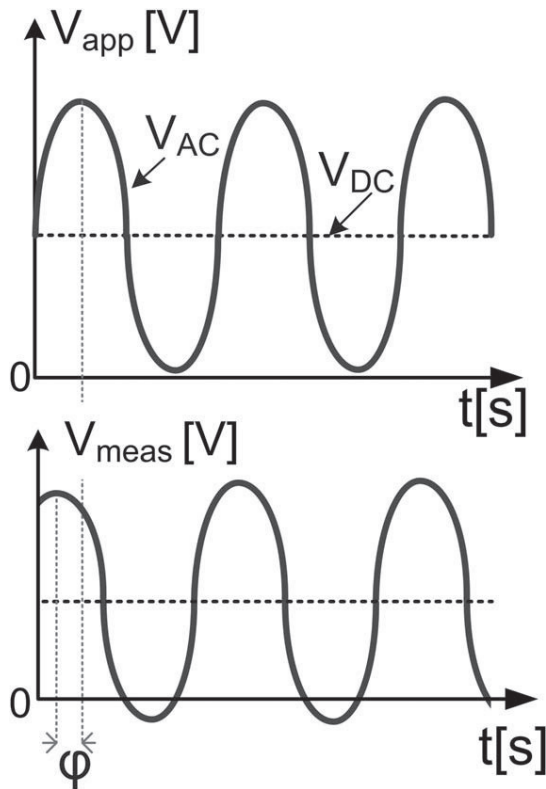


**Figure 1.** Schematic of the applied voltage and measured voltage.  $V_{DC}$  is the applied DC voltage level. The applied AC voltage  $V_{AC}$  is determined by its amplitude amp, the signal frequency  $f$ , and the phase angle  $\phi_0$ .

AC and a DC voltage at the same time and same skin site. The voltage signal applied to the skin,  $V_{app}$ , can be described by the equations:

$$V_{app} = V_{DC} + V_{AC} \quad (1)$$

$$V_{AC} = \text{amp} \cdot \sin(2\pi f \cdot t + \phi_0), \quad (2)$$

and a schematic is shown in the upper half of Figure 1.

The measured voltage signal is proportional to the AC current through the skin and is used to calculate the skin admittance. This signal is equal in shape to the applied signal, but with a DC level and AC amplitude depending on the DC conductance and AC admittance, respectively. DC conductance and AC admittance can be separated easily, since the DC conductance corresponds to the mean value of the measured voltage signal.<sup>1</sup> The two parts of the AC admittance (AC conductance and susceptance) can be separated by means of the phase-sensitive rectification (also called lock-in) technique (Grimnes & Martinsen, 2014).

For the lock-in amplification, two reference signals (one sinus and one cosine signal) with the same signal frequency as the applied voltage are used. Both reference signals are in phase with the applied voltage (the cosine signal has a phase of 90 degrees compared to the applied sinus voltage). The mean value of the measured AC signal times the sinus reference signal correlates to the AC conductance. The susceptance can be determined by using the cosine reference signal instead.

1. If a whole number of sinus signal periods is used.

By calibration (see Calibration section in Appendix A), it is assured that there is no cross-talk between the AC and the DC conductance measurement.

Choosing the signal frequency for an AC conductance measurement is a "... trade-off between the ability of the measuring system to detect quick changes (requires high frequency) and sensitivity for sweat duct activity (requires low frequency)" (Martinsen et al., 2015, p. 51).

At higher frequencies (above 1 kHz), the frequency-dependent part of the AC conductance dominates (i.e., the capacitance pathway), and the conductance changes in the sweat glands become small relative to the baseline level.

On the one hand, with respect to sensitivity to sweat gland activity, low frequencies are preferred. On the other hand, the signal frequency determines the speed of the measurement, and the quality of the rectified signal becomes better the more signal periods are used for the lock-in amplification (Grimnes & Martinsen, 2014). Given that a whole number of signal periods needs to be used for the rectification, the measurement speed (samples per time) by using a signal frequency of, for example, 20 Hz would be four times higher compared to a signal frequency of 5 Hz. For example, if five periods are used for calculating one conductance value and the signal frequency is 5 Hz (five periods per second), it would take 1 s to obtain one conductance value. If the signal frequency is 20 Hz (20 periods per second), the duration of five signal periods is only 0.25 s, which means that one conductance value can be calculated every 0.25 s.

The chosen signal frequency for this study is 20 Hz. A frequency of 20 Hz provides a good trade-off between measurement speed and sensitivity for sweat duct activity, but other signal frequencies in the range of, for example, 10 Hz to 100 Hz, could be used as well.<sup>2</sup>

The instrumentation is designed to acquire five AC and DC conductance measurement values per second, which means that the sample frequency of the instrumentation is 5 Hz. (See Appendix A for detailed information).

The chosen DC level was 0.5 V due to its common use and the recommendation in Boucsein et al. (2012). Accordingly, 0.5 V amplitude was chosen for the AC excitation voltage as well.

**Electrode type, system, and placement.** The electrodes used were Kendall 1050NPSM Neonatal Electrodes. This electrode type is found to be suitable for EDA measurements (Tronstad, Johnsen, Grimnes, & Martinsen, 2010). They are prewired Ag/AgCl electrodes that are initially covered with solid hydrogel, have an active electrode area of 5.05 cm<sup>2</sup>, and have a minimal disturbance of the measured skin conductance from the gel (Tronstad et al., 2010).

The electrodes are placed at the thenar and hypothenar site of the dominant hand as shown in Figure 2, employing a bipolar two-electrode system.

### Subjects, Recruitment, Approvals

A total of 28 test subjects (15 male/13 female, mean age 28.5 years,  $SD = 6.6$  years) were recruited and gave informed consent for

2. One exclusion: Signal frequencies that are close to the signal frequency of the mains (e.g., in the range of  $\pm 10$  Hz) should be avoided if a two-electrode system is used. By doing so, the frequency component from the mains that affects the measurement can be filtered easily (see Appendix A).

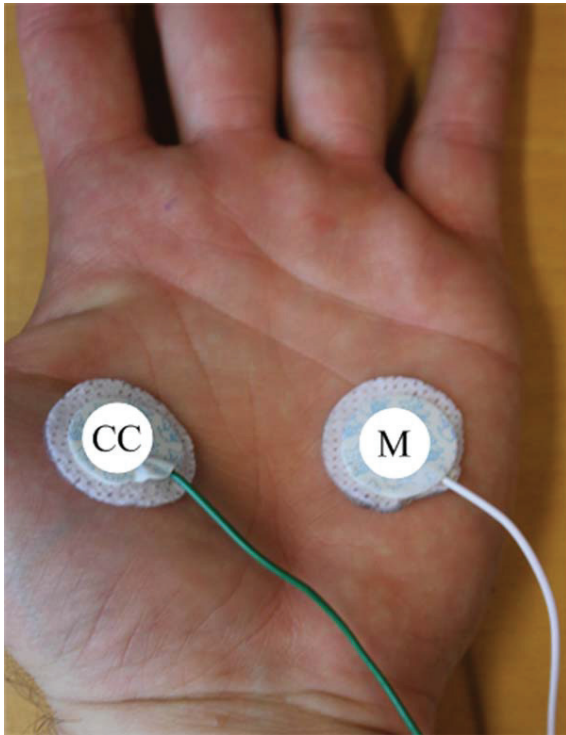


**Figure 2.** Picture showing electrode placement. The voltage provided by the instrumentation (see Figure A1) is applied to the skin through the CC electrode.

participation in the study. The measurements were conducted at the University of Oslo between June and August 2015.

### Experimental Design

Experiment 1 and 2, described below, were combined into one single session. Every test subject took part in both experiments. The measurements were done in a quiet room in the basement of the Physics Department of the University of Oslo. The participants were asked to take a seat in a comfortable chair while the gender, age, and dominant hand were noted. Electrodes were placed on the dominant hand as shown in Figure 2. The test subjects were instructed to keep the testing hand calm during the experiments. First, Experiment 1 was conducted with a schedule as shown in Figure 3. After finishing Experiment 1, an explanation of Experiment 2 was given before running the experiment according to the schedule shown in Figure 4.

During the experiments, different sounds were used to either indicate a certain point of time or as stimuli. These sounds are provided in online supporting information, Sound File 1–4. A computer program was used to control the sounds, providing exact timing of the events.

**Experiment 1.** This experiment was intended to provide data for a general comparison between the AC and DC methods. The mathematical tasks, as shown in Figure 3, are continuous subtractions of 17 from different starting numbers for each test (1,001, 1,003, and 1,007).

The participants were asked to provide the correct numbers continuously and as fast as possible, while the experimenter wrote down the answers given. During relaxation after the second

mathematical task, a sound sample of falling spoons was played for 1 s at 86 dB and used as a stimulus for the orienting response.

**Experiment 2.** In this experiment, the influence of the endogenous skin potential on the DC conductance for different excitation levels was measured. Constant amplitude of 0.5 V was used for excitation of the AC recording, which was used as a reference for valid skin conductance responses (SCRs). Recordings were done using different DC excitation levels, as shown in Figure 4. Each stimulus contains a sound, and the participant took a deep breath following each sound stimulus, in order to ensure the activation of an SCR.

The applied sound for this experiment was a disharmonic chord (recording from a guitar), lasting 1 s, and was presented with a sound pressure of 90 dB. The DC excitation level was changed 40 s before each sound stimulus. EDAs that occurred during the first 140 s of the initial phase were not used for the data analysis, as they were not elicited by any stimulus and occurred before the onset of the 10 mV DC excitation level.

### Data Analysis

The collected data were analyzed by the use of MATLAB (version 2015a, academic license).

**Criteria for response selection.** Locating the SCR onsets and peaks was done by the free software Ledalab<sup>3</sup> (Benedek & Kaernbach, 2010), employing the “trough-to-peak method” (i.e., locating the minima and maxima of the smoothed EDA signal, using the former as an SCR onset and the latter as a peak).

This onset detection is done for the DC as well as for the AC conductance measurement, and the onsets of both methods were compared. Only responses with an amplitude larger than 0.15  $\mu$ S were included in the analysis.

A small number of onsets were detected in the AC conductance measurement that were not detected in the DC conductance measurement, and vice versa. To guarantee that no response was lost, the onsets of the AC conductance measurement were stored in a list as a basis for the occurrence of a response. These are the onsets that are detected in both methods simultaneously and onsets that are detected only in the AC measurement. In a second step, the missing onsets that are only detected in the DC conductance measurement were then added. As a consequence, responses that meet the 0.15  $\mu$ S minimum in either the AC or DC measurement are included.

SCR segments were extracted from the onset of a response to the onset of the next response. Segments that consist of fewer than 10 samples are excluded. Recovery tails following each SCR were then excluded from the segments by cutting any part exceeding more than 10% below the initial level of the SCR. Responses that consist of fewer than five samples after cutting are then excluded to make sure that only true responses are used for the data analysis.

In addition, responses were not included if they did not recover to more than 90% of the initial level before the next SCR.

**EDA scores used for AC versus DC comparison.** Figure 5 gives an illustration of the scores used in this study. The conductance value at the onset is defined as the skin conductance level (SCL), and the amplitude is the difference between the response maximum and the SCL. The rise time is defined as the time

3. This software was only used for the onset and peak detection of the SCRs but not for the further analysis.

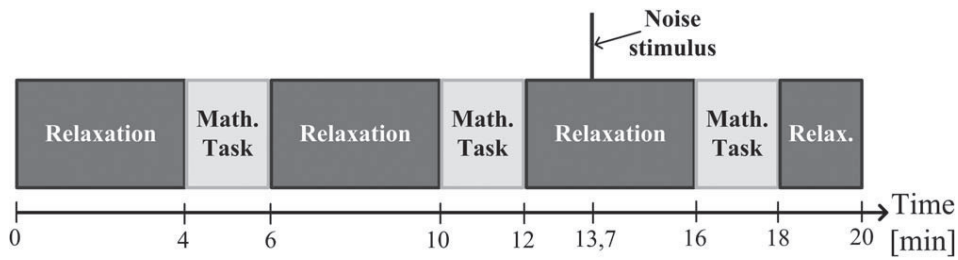


Figure 3. Time schedule of Experiment 1.

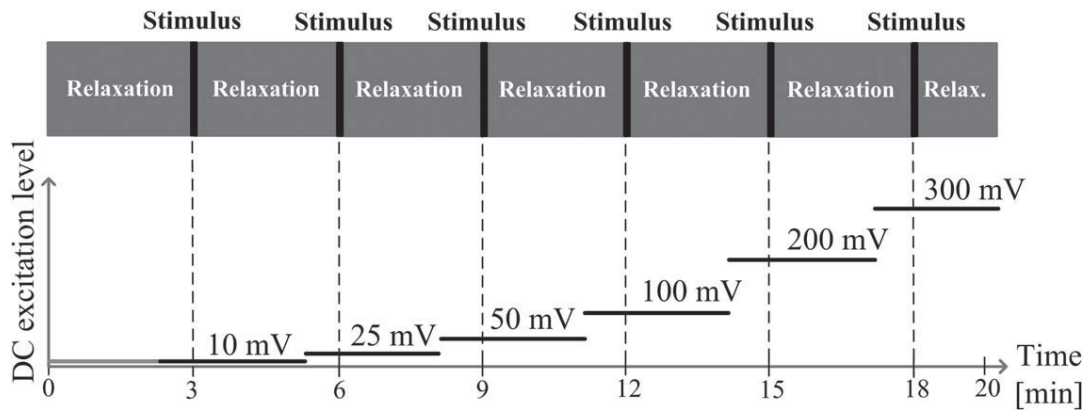


Figure 4. Time schedule of Experiment 2.

between 10% of the amplitude to 90% of the amplitude. The two recovery times are found in the same manner from 90% to 50% or 10%. A linear interpolation (`interp1(..., 'linear')` in MATLAB) was employed to determine at which point in time a certain y value is crossed. The interpolation is used for calculating rise and fall times in order to get a higher temporal resolution than 0.2 s (5 Hz sampling frequency). The last score used for the comparison is the ratio of the time when the response maximum is reached to the whole response duration,  $T_{\text{Response}}$ .

**Statistical analysis.** The differences between SCRs recorded with the AC and DC methods were evaluated statistically using all the extracted responses from all test persons. For this purpose, a linear mixed effects model was employed with subject as a random effect (random intercept), and method (AC or DC) and DC excitation level (only for Experiment 2) as fixed effects. Each score was used as the dependent variable in separate analyses. The analysis was done using MATLAB (version 2015a, academic license) with the `fitlme()` function.

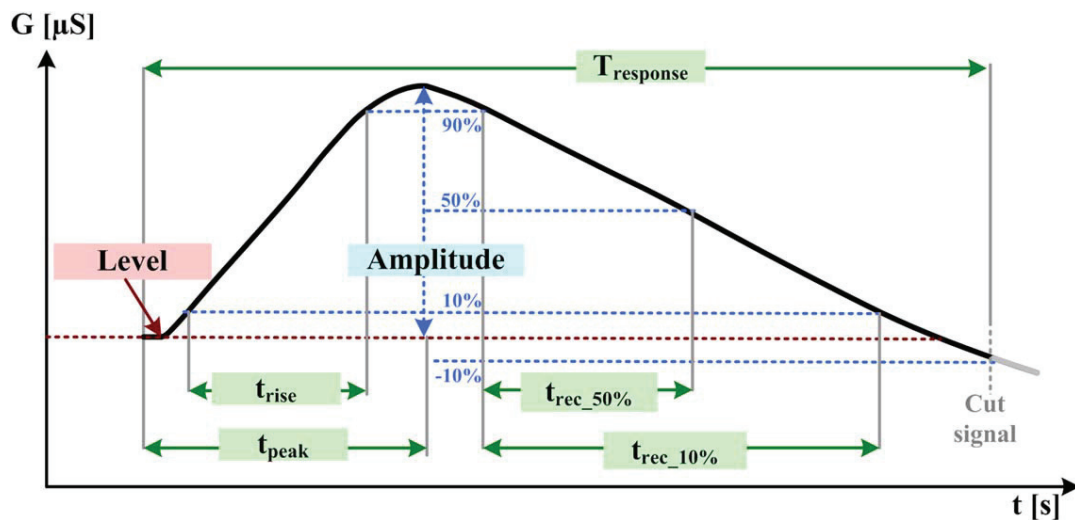
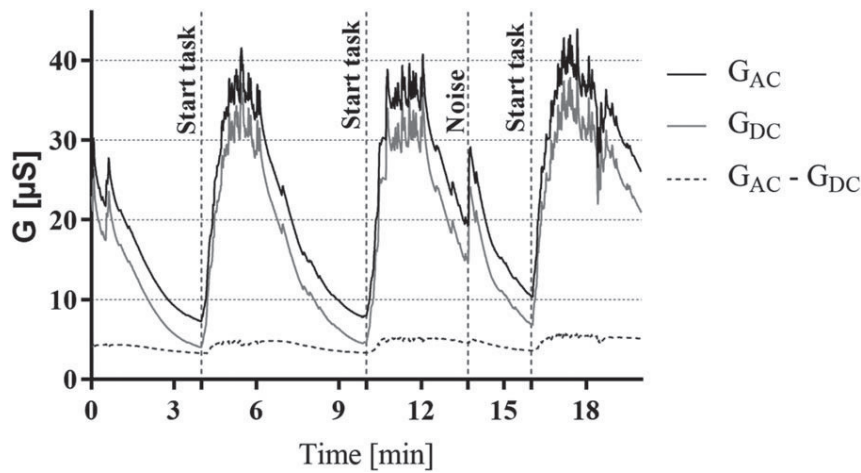


Figure 5. Sketch of a skin conductance response and illustration of the scores that are used for data analysis.



**Figure 6.** Example plot of one whole test session from Experiment 1. AC and DC conductance measurements are done simultaneously. The applied DC voltage is 500 mV and the applied AC voltage is a sinus voltage with an amplitude of 500 mV and  $f = 20$  Hz. The measurements are done on the palmar skin site.

In order to compare the shape of the SCR waveform recorded by both methods against each other, a mean response based on all SCR segments was constructed by resampling each segment to a 100-sample window before calculating the mean.

**Results**

**Experiment 1**

A total of 2,553 responses for each method (AC and DC) were extracted from all test sessions of Experiment 1. Figure 6 shows an example recording from a test session from Experiment 1. In addition to the AC and the DC conductance ( $G_{AC}$  and  $G_{DC}$ ), the difference between AC and DC conductance ( $G_{AC} - G_{DC}$ ) is shown.

A zoomed-in view of another test session is presented in Figure 7. Inspecting both figures gives a first impression that the obtained measurements of the AC and the DC method are quite similar. The DC response rises a bit less, increasing the difference between the two.

The mean response waveform for the AC- and DC-recorded SCRs are shown in Figure 8, along with the difference between

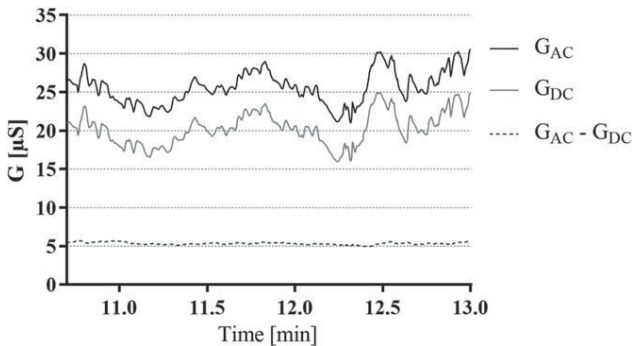


**Figure 7.** Example plot showing parts of a recording where the similarity between AC and DC SCRs are apparent. AC and DC conductance measurements are done simultaneously. The applied DC voltage is 500 mV and the applied AC voltage is a sinus voltage with an amplitude of 500 mV and  $f = 20$  Hz. The measurements are done on the palmar skin site.

these over time shown in the green curve. As can be seen from the scale at the right y axis, the variation in the mean difference plot is very small (tens of nS).

The statistical analysis on each EDA score is presented in Table 1, showing that only the EDA level score was statistically significantly different between the methods ( $p < .001$ ) with a higher level measured with the AC method than with the DC method (mean difference of 3.3  $\mu$ S). These results show excellent agreement between the two methods for SCRs, the main difference being the capacitance contribution to AC levels as discussed above. A subgroup analysis for only the responses within the arithmetic task revealed the same results on statistical significance as in Table 1, with only the EDA level score statistically significantly different between the two methods.

**Experiment 2**

A total of 1,468 responses for each method (AC and DC) were extracted from all test sessions of Experiment 2. The number of observations for each applied DC level is given in Table 2. Figure 9 shows a typical example recording from this experiment. In addition to the AC and the DC conductance ( $G_{AC}$  and  $G_{DC}$ ), the difference between AC and DC conductance ( $G_{AC} - G_{DC}$ ) is also

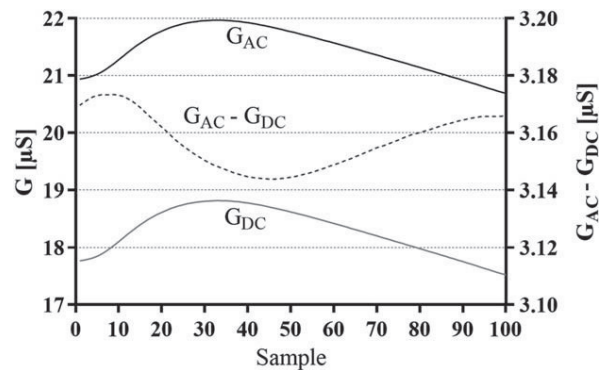


**Figure 8.** Mean of all phasic SCRs (left y axis) and the mean difference (right y axis) over all test subjects.

**Table 1.** EDA Scores from Experiment 1

EDA parameter	$\overline{DC}$	$\overline{AC}$	95% CI of $\overline{AC}-\overline{DC}$	<i>p</i> value
Level [ $\mu\text{S}$ ]	17.718	20.988	$3.270 \pm 0.297$	<.001
Amplitude [ $\mu\text{S}$ ]	1.225	1.195	$-0.030 \pm 0.108$	.585
$\frac{t_{peak}}{T_{response}}$ [%]	39.2	38.7	$-0.5 \pm 0.572$	.088
$t_{rise}$ [ms]	893.6	897.4	$3.8 \pm 21.51$	.730
$t_{rec_{50\%}}$ [ms]	983.0	986.9	$3.9 \pm 42.16$	.857
$t_{rec_{10\%}}$ [ms]	2135.0	2158.3	$23.3 \pm 99.54$	.647

Note. EDA scores calculated from all extracted responses and for both methods (AC and DC), 95% CI of the difference between both methods, and calculated *p* values are shown.

shown. The AC and DC conductance clearly differ for low DC excitation levels, but for DC levels  $\geq 100$  mV, this difference in the responses diminishes in this case.

The difference between the AC and DC methods for each EDA score in relation to the different DC excitation levels are presented in Figure 10. A statistical summary of these differences are given in Table 2.

## Discussion

### Experiment 1

Experiment 1 revealed that, with standard measuring excitation levels, there is a significant difference between the AC and DC methods in the conductance level, but not in the response scores.

Due to large interindividual differences in the skin conductance levels, which may be more related to individual skin properties than to electrodermal activity, the AC versus DC difference in the conductance level is not very relevant for clinical studies.

The main reason for the difference in conductance levels is due to the frequency-dependent part of the AC conductance. (The interested reader is referred to Martinsen et al., 2015). The frequency-dependent part of the AC conductance and the susceptance are different things, but both are correlated to each other. A discussion of the capacitive properties and a plot in which the susceptance is shown is given in Appendix B.

The results show that using the AC methodology will provide results that are identical to DC with the best methodology (nonpolarizable electrodes, bipolar system, applied DC level  $> 200$  mV) and thus could be used more broadly. On the other hand, the AC method has advantages over the DC method, which are discussed below.

**Table 2.** *P*-Values of the EDA Scores from Experiment 2

EDA parameter	<i>p</i> value					
Level	<.001	<.001	<.001	<.001	<.001	<.001
Amplitude	<.001	.001	.002	.126	.414	.641
$\frac{t_{peak}}{T_{response}}$	<.001	.058	.011	.592	.685	.491
$t_{rise}$	<.001	.821	.561	.974	.222	.720
$t_{rec_{50\%}}$	<.001	.518	.278	.463	.719	.564
$t_{rec_{10\%}}$	.002	.341	.432	.974	.528	.811
Applied DC level [mV]	10	25	50	100	200	300
Number of observations	488	488	576	524	526	334

Note. Calculated *p* values of the EDA scores in dependence of the DC excitation voltage level.

### Experiment 2

Experiment 2 revealed that, in addition to the level differences, SCR scores measured with the DC method differed from the scores from the AC method when the DC excitation level was below 100 mV. Thus, these results tell us that excitation voltage as low as 100 mV may be sufficient for DC conductance measurements, but the results may vary for a different setup. To add a margin of safety, the conclusion of Experiment 2 is that an excitation voltage as low as 200 mV may be sufficient in general if a bipolar system is used.

In addition, decreasing the DC excitation voltage (from the standard 500 mV setting) leads to advantages regarding electrode polarization, possible nonlinear effects, and power consumption (see discussion below).

### Analysis of the Data

The recordings in this study were analyzed by parameterization into selected well-known EDA scores for each SCR, and the two methods (AC and DC) were compared against each other by these scores. These scores have been used for decades as an indication of sympathetic arousal states, and vast numbers of previous studies have reported on these scores allowing for comparisons to this study.

Over the last decade, several new approaches in EDA parameterization have been proposed, including deconvolution (Alexander et al., 2005; Benedek & Kaernbach, 2010) and model-based approaches (Bach & Friston, 2013; Tronstad, Staal, Sælid, & Martinsen, 2015). These methods offer attractive features such as separation of overlapping responses and estimation of the sudomotor nerve activation signal, but these methods have not yet been fully implemented in practice and need further research for validation. Because these methods are based on the EDA waveform (as opposed to, e.g., the level), it is unlikely that there will be a difference between AC and DC recording when applying these new methods given the waveform likeness as shown in this study (Figures 6–8).

Furthermore, it seems plausible that the same model-based methods that are used for DC conductance measurements, in particular the canonical impulse response functions derived from DC

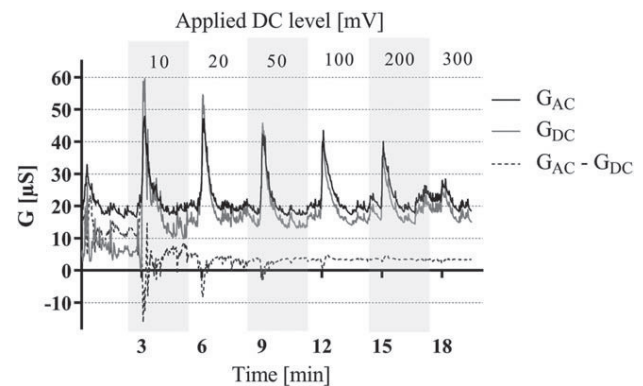


**Figure 9.** Example plot of one whole session of Experiment 2. AC and DC conductance measurements are done simultaneously. The applied DC voltage sweeps in defined steps from 10 mV to 300 mV. The applied AC voltage is the same for the whole experiment (sinus voltage with an amplitude of 500 mV and  $f = 20$  Hz). The measurements are done on the palmar skin site.

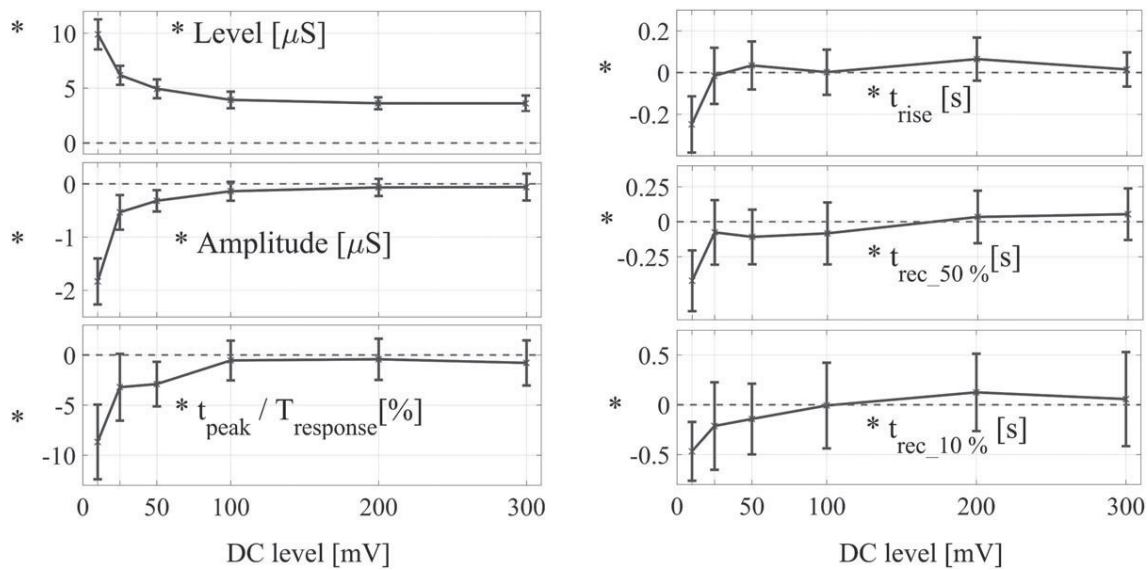


**Figure 10.** The 95% CI of the differences between both methods plotted over different DC excitation levels.

measurements (Bach, Flandin, Friston, & Dolan, 2009), could be applied on AC measurements as well.

### Measurement Speed

The lock-in amplification that is part of the AC method is usually done over several cycles of the measured signal to obtain one measurement value. The DC method, on the other hand, needs only one sample from the analog-to-digital converter per measurement. Since the speed of obtaining one AC measurement value then becomes limited by the signal frequency, the DC method allows a higher sampling rate. However, the analysis of the frequency spectrum of several skin conductance responses indicates that there are no significant frequency components above 2 Hz (Martinsen, Grimnes, & Sveen, 1997; see also Edelberg, 1967). Sampling rates well above 2 Hz are realizable with the AC method (5 Hz with the instrumentation used in this paper); hence, there is no disadvantage due to the measuring speed regarding the information content. If another signal frequency (such as 100 Hz) is used, the sampling frequency would be even higher (e.g. 20 Hz). If modern decomposition methods were used (see the section above), sampling frequencies higher than 5 Hz or even 20 Hz could increase the quality of the decomposition.

However, if the lock-in amplification is realized with a shifting window of fixed sample size (cf. moving average) for the reference signal, the sampling frequency of the AC method can be as high as the DC method.

### Advantages of the AC Method

Historically, the DC method has been established as the standard for EDA measurements, mainly due to its simplicity. The instrumentation for using the AC method has to be designed more carefully than the DC method. The signal frequency must be chosen and the AC conductance must be extracted from the admittance by phase-sensitive rectification (lock-in amplification). However, developing instrumentation for the AC method is easier now with current technology, and there are several advantages of using the AC method.

### Polarization Effects

As noted above, electrode polarization may affect the conductance level in the DC measurement due to the counterelectromotive force, and avoiding polarization of the electrodes and skin is a well-known benefit of using the AC method. Based on the results of this study, the DC electrode polarization generated when using high quality Ag/AgCl electrodes seems to be negligible for short-term recordings. This agreement provides strong support for the validity of the present AC methodology—a necessary step to move toward Boucsein et al.'s (2012) suggestion to consider adopting AC recordings as a potentially superior alternative.

The probability of polarization is greater with long-term recordings. Consequently, it would be of interest to compare the AC and the DC method in a long-term study, in which electrode polarization could alter the DC recording.

A second context for the superiority of AC methodology would be applications that may demand electrodes other than modern Ag/AgCl electrodes. For example, Tartz, Vartak, King, & Fowles (2015) suggested that using stainless steel electrodes for recording SC from a cell phone would be better and that AC methodology would make that possible.

### Eliminating Endogenous Potentials

Experiment 2 showed that effects of endogenous potentials were negligible for DC measurement with a DC level of at least 100 mV, as long as the bipolar system uses skin sites with similar or equal potential. We recommended the use of 200 mV to allow for variation across different methodologies. In any case, the choice of a minimum DC level for the excitation voltage is restricted by the endogenous potential. With the AC method, the skin potentials and the conductance are separated implicitly, completely eliminating this concern with endogenous potentials and allowing the use of lower excitation voltages, if needed.

### Safety

As noted in the introduction, the international standards on patient safety for medical devices (according to IEC 60601-1, p. 171)

allow values for auxiliary currents of 10  $\mu\text{A}$  for DC and 100  $\mu\text{A}$  for AC. Thus, the allowable AC current through the body is 10 times higher than for DC currents, providing a large margin of safety for AC measurement. Further, because the endogenous skin potential is not a possible error source for the AC measurement, the AC recording can be accomplished using much lower excitation voltages (see Grimnes, Martinsen, & Tronstad, 2009).

### Power Consumption

Transportable devices may be used for long-term recordings, placing a strain on battery power. The just-mentioned possibility of using very low excitation voltages with AC measurement is a great advantage under these circumstances. Similarly, DC measurement with 200 mV rather than 0.5 V would extend battery life.

### Simultaneous Measurement of SC, SP, and Skin Susceptance

Separation between skin conductance and potential by the AC method enables measuring both at the same time at the same electrode (Grimnes et al., 2011). The skin conductance and skin potential responses exhibit different waveforms, and recording both simultaneously may provide additional EDA information (Tronstad, Kalvøy, Grimnes, & Martinsen, 2013). These authors stated that the difference in waveform “is related to the magnitude of the SCR, the hydration of the skin, and the filling of the sweat ducts,” and that there is evidence for additional EDA factors that are not accounted for by these three variables. In addition, the susceptance (from which the capacitance can be calculated) is another source of information gained by the AC method, which is related to skin hydration (Martinsen, Grimnes, & Karlsen, 1995). The hydration-produced increase in skin susceptance can be due to wetting under the electrode as well as transport of sweat into the peritubular corneum. Wetting under the electrode can influence the measured conductance, and a change of the amount of sweat in the peritubular corneum can influence, for example, rise and fall times of the SCRs.

Measuring the skin potential and susceptance as complements to the skin conductance may provide further insights into the sweat gland physiology.

### Nonlinear Effects

Nonlinear effects in skin impedance have previously been reported (e.g., Rosendal, 1943; see also Edelberg, 1967). For example, in a plot of increasing applied voltage (or current) on the abscissa and conductance on the ordinate, there is an inflection at some point in which the conductance increases above a certain level of applied voltage (or current). Grimnes (1983a) suggested electroosmotic transport as a possible origin of these effects. T. Yamamoto & Yamamoto (1981) found that nonlinearity becomes more apparent with increasing current, decreasing frequency, and increasing impedance. Figure 14 in their paper shows nonlinearities beginning for a current density of 25  $\mu\text{A}/\text{cm}^2$  (applied sinusoidal current with  $f = 0.01$  Hz). The measured DC current density in the present study is up to 6  $\mu\text{A}/\text{cm}^2$  (with the 5  $\text{cm}^2$  electrode), which is much less than 25  $\mu\text{A}/\text{cm}^2$ . However, the nonlinearity effects need to be studied further, as they may possibly occur even at current densities less than 25  $\mu\text{A}/\text{cm}^2$  (unpublished results). Nonlinear effects would affect the conductance level in the DC measurement. The AC measurement, however, would be less affected since smaller currents and relatively high frequencies (e.g., 20 Hz) can be used.

### Conclusion

The results from this study indicate that there are no clinically significant differences between the AC and the DC method of measuring EDA and that AC recordings may replace DC recordings. The measurements of both methods are comparable given that the setup is equal, but for DC excitation voltages lower than 100 mV, the endogenous skin potentials disturb the DC-measured skin conductance response. When the excitation voltage is above 100 mV in DC measurement, the only EDA score that differs significantly is the skin conductance level. To allow variation across different methodologies, the use of 200 mV is recommended.

The AC method has attractive features that are not supported by the DC method, which include measuring skin conductance, endogenous skin potential, and skin susceptance at the same time below the same electrode, and avoiding any polarization of electrode or skin due to the measurement.

### Appendix A

#### Description of the Instrumentation

**Analogue part.** A question that arose while designing the study and the instrumentation is whether the comparison should be done using methods that have been used for many years (e.g., classical electrode types) or between modernized methods that have existed just a few years (e.g., electrode with hydrogel contact electrolytes). Due to its common use, the authors decided to develop a two-electrode bipolar system for this study.<sup>4</sup> This would increase the relevance of the comparison between the AC and the DC conductance measurement method to everyone who is familiar with EDA measurements.

The schematic of the measuring instrument is shown in Figure A1. The instrumentation is developed according to the one presented in Tronstad et al., 2010. The topology shown in Figure A1 is a two-electrode system that is adapted from a three-electrode system. If the (Ref) branch is not connected to the CC electrode but directly to the skin by another electrode, then it would be a three-electrode system. The intention of this topology was to enable simply switching between a two- and a three-electrode system to reuse this device for further studies. The operational amplifier on the “signal out” side is not necessary for the two-electrode system itself.

The operational amplifier at the signal reading side in combination with the resistance  $R_{fb}$  functions as a transimpedance amplifier that converts the current into a voltage that can be read by the data acquisition box. By connecting the capacitance  $C_{fb}$  in parallel to  $R_{fb}$ , it works additionally as a low-pass filter that reduces noise. It does not block the DC component.

Since the human body functions as an antenna, noise caused by the mains can disturb the AC measurement. In Europe, the signal of the mains has a frequency of 50 Hz. For this reason, a notch filter that particularly blocks this 50 Hz frequency component is added on the signal reading side. There would be no need for the 50 Hz band-stop filter by using a three-electrode system like the one that is presented in Grimnes et al., 2009.

4. In general, the authors would recommend the use of a monopolar three-electrode system for AC recordings instead of a two-electrode system.

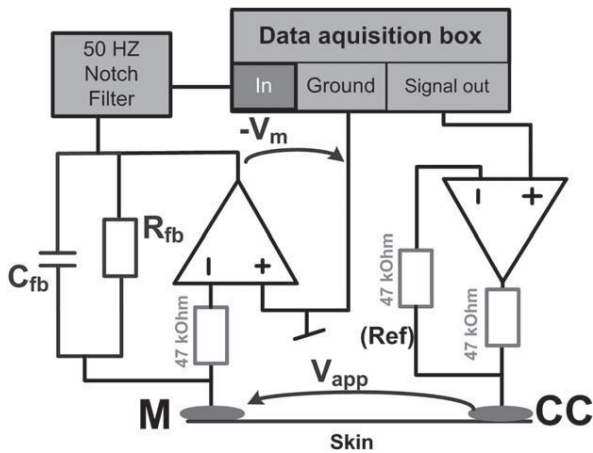


Figure A1. Schematic of the developed instrumentation.

The 47 kΩ resistors shown in Figure A1 are implemented for safety reasons in case of a breakdown of the operational amplifiers.

**Digital part.** The data acquisition box is connected to the laptop that is used to control the whole measurement system. During the test sessions, the laptop is battery powered to make sure that there is no connection between test subject and mains. The data acquisition box is the NI USB- 6211 from National Instruments. The LabVIEW software (2013 version) is used for programming the digital part of the measurement instrumentation. The digital part includes controlling of the data acquisition box (to generate and read the voltage signal) as well as the lock-in amplification. The sampling frequency used to read the analogue voltage signals is 50 kHz.

**Voltage signals.** Figure A2 illustrates the voltage signals used in the system.

Each measurement value is an average of several signal periods. The instrumentation enables signal reading and writing at the same time. In fact, three signal periods are generated to calculate one conductance value in the custom-built measuring system. The time between two signal series is designed to be 0.05 s. In total, every 0.2 s contains a conductance value.

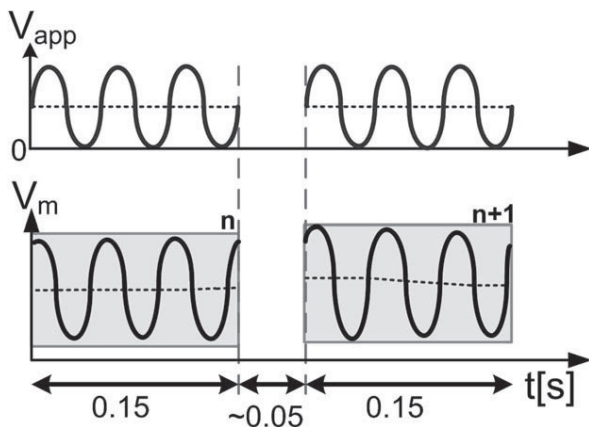


Figure A2. Schematic of the applied and measured signal.

Referring to Figure A2, the first period of each signal series of the measured signal was distorted due to the instrumentation (which is not illustrated in the figure). Therefore, the first period of each signal series is cut out digitally, and the lock-in amplification is done over two periods. The 0.05 s between two signal series is intended as a buffer for processing time that may not be needed.

In the measurement system, each conductance value is obtained by averaging the measured voltages over a specific time interval for both the AC and the DC method. One could argue that the results of the DC method in this paper would not be comparable with common DC measurements. But since there is no information above 2 Hz, averaging over several samples and obtaining a DC conductance value every 0.2 s does not mean a deformation of the result. To the contrary, it reduces the noise and creates a condition similar to the AC measurement.

**Calibration.** For the instrument calibration, different loads were tested, each consisting of a resistor in parallel with a capacitor. In total, 36 different loads were tested (combination of six resistors in the range from 14.91 kΩ [68.67 μS] to 563 kΩ [1.78 μS] and six capacitors in the range from 9.17 nF [1.15 μS for  $f=20$  Hz] to 91.29 nF [11.47 μS for  $f=20$  Hz]). The measured conductance of all test subjects except one person (who had conductance values up to 80 μS) and the measured susceptance values of all test persons were within the calibrated range. The instrumentation was designed so that the amount of the conductance error, for both AC and DC, is smaller than 0.6% in the whole range, and the amount of the susceptance error is smaller than 0.7% within the whole range. To reduce the error in the AC method, it is important to calibrate the phase angle of the lock-in reference signals. The error in the DC measurements comes from the offsets in the operational amplifiers. The DC error can be adjusted by adding a small counteracting DC offset digitally. While the amount of the AC error that is adjusted by calibration remained stable over days, the DC error changed slightly—most likely due to the operational amplifier offset temperature dependency. The DC offset correction had to be adjusted before each experiment.

However, the amounts of both AC and DC error (in percent) are not constant and differ from each other across the calibrated range. This effect can cause a slight change in the conductance difference up to, for example, 0.01 μS per 1 μS change in conductance level.

## Appendix B

### Susceptance

Figure B1 shows an EDA plot that additionally contains the susceptance (B).

The dielectric loss in the capacitive properties of the SC is the reason why the conductance difference seemingly changes together with the susceptance, but this is not the only process. The change in the conductance difference is not one to one due to the change in susceptance, raising the question of what else causes a change in the conductance difference? The changes in the conductance difference addressed by the question are in the range from 0.1 μS to 1 μS. On one hand, the errors in the measurement system (that are discussed above) can already become relevant if changes in such a small scale are investigated. On

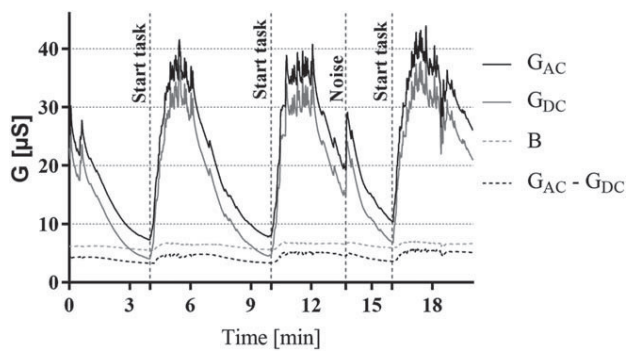


**Figure B1.** Example plot of one whole test session. AC and DC conductance measurements are done simultaneously. The applied DC voltage is 500 mV and the applied AC voltage is a sinus voltage with an amplitude of 500 mV and  $f = 20$  Hz. The measurements are done on the palmar skin site.

the other hand, it is conceivable that there are physiological processes that also contribute to the changes in the conductance difference. Further investigations on the changes in the conductance difference in combination with the susceptance potentially could give insights into the physiology of the skin. The measured susceptance is mainly attributable to the humidity in the stratum corneum, and the frequency-dependent part of the AC conductance can be seen as an additional conductive path that is in parallel to the sweat glands. One possible explanation for an increase in the susceptance itself that occurs in accordance with an increase in the conductance is the sweat that is passing

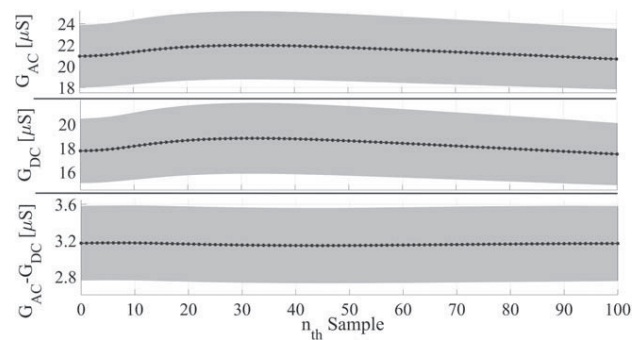


**Figure C1.** Mean phasic response and the mean difference over all test subjects and the corresponding 95% CI.

through the sweat gland duct, and sweat reaching the skin surface potentially diffuses into and hydrates the surrounding stratum corneum.

## Appendix C

### Mean Response 95% Confidence Intervals

In Figure C1, the mean phasic response and the mean difference over all test subjects is shown. It is the same data that are presented in Figure 8, but the 95% confidence intervals are shown additionally.

## References

- Alexander, D. M., Trengove, C., Johnston, P., Cooper, T., August, J. P., & Gordon, E. (2005). Separating individual skin conductance responses in a short interstimulus-interval paradigm. *Journal of Neuroscience Methods*, *146*(1), 116–123. doi: 10.1016/j.jneumeth.2005.02.001
- Bach, D. R., Flandin, G., Friston, K. J., & Dolan, R. J. (2009). Time-series analysis for rapid event-related skin conductance responses. *Journal of Neuroscience Methods*, *184*(2), 224–234. doi: 10.1016/j.jneumeth.2009.08.005
- Bach, D. R., & Friston, K. J. (2013). Model-based analysis of skin conductance responses: Towards causal models in psychophysiology. *Psychophysiology*, *50*(1), 15–22. doi: 10.1111/j.1469-8986.2012.01483.x
- Benedek, M., & Kaernbach, C. (2010). A continuous measure of phasic electrodermal activity. *Journal of Neuroscience Methods*, *190*(1), 80–91. doi: 10.1016/j.jneumeth.2010.04.028
- Boucsein, W. (2012). *Electrodermal activity* (2nd ed.). Berlin, Germany: Springer Science + Business Media. doi: 10.1007/978-1-4614-1126-0
- Boucsein, W., Fowles, D. C., Grimmes, S., Ben-Shakhar, G., Roth, W. T., Dawson, M. E., & Filion, D. L. (2012). Publication recommendations for electrodermal measurements. *Psychophysiology*, *49*, 1017–1034. doi: 10.1111/j.1469-8986.2012.01384.x
- Edelberg, R. (1967). Electrical properties of the skin. In C. C. Brown (Ed.), *Methods in psychophysiology* (pp. 1–53). Baltimore, MD: Williams & Wilkins.
- Grimmes, S. (1983a). Skin impedance and electro-osmosis in the human epidermis. *Medical and Biological Engineering and Computing*, *21*(6), 739–749. doi: 10.1007/BF02464037
- Grimmes, S. (1983b). Pathways of ionic flow through human skin in vivo. *Acta Dermato-venereologica*, *64*(2), 93–98.
- Grimmes, S., Jabbari, A., Martinsen, Ø. G., & Tronstad, C. (2011). Electrodermal activity by DC potential and AC conductance measured simultaneously at the same skin site. *Skin Research and Technology*, *17*(1), 26–34. doi: 10.1111/j.1600-0846.2010.00459.x
- Grimmes, S., & Martinsen, Ø. G. (2014). *Bioimpedance and bioelectricity basics*. (3rd ed., pp. 295–299). Cambridge, MA: Academic Press.
- Grimmes, S., Martinsen, Ø. G., & Tronstad, C. (2009). *Noise properties of the 3-electrode skin admittance measuring circuit*. Presented at the 4th European Conference of the International Federation for Medical and Biological Engineering (pp. 720–722). doi: 10.1007/978-3-540-89208-3\_172
- IEC 60601-1. (2005). *Medical electrical equipment—Part 1: General requirements for basic safety and essential performance*. Geneva, Switzerland: International Electrotechnical Commission.
- Johnson, L. C., & Lubin, A. (1966). Spontaneous electrodermal activity during waking and sleeping. *Psychophysiology*, *3*(1), 8–17. doi: 10.1111/j.1469-8986.1966.tb02673.x
- Martínez-Rodrigo, A., Zangróniz, R., Pastor, J. M., & Sokolova, M. V. (2016). Arousal level classification of the aging adult from electrodermal activity: From hardware development to software architecture. *Pervasive and Mobile Computing*. doi: 10.1016/j.pmcj.2016.04.006
- Martinsen, Ø. G., Grimmes, S., & Karlsen, J. (1995). Electrical methods for skin moisture assessment. *Skin Pharmacology and Physiology*, *8*(5), 237–245. doi: 10.1159/000211353
- Martinsen, Ø. G., Grimmes, S., & Sveen, O. (1997). Dielectric properties of some keratinised tissues. Part 1: Stratum corneum and nail in situ. *Medical and Biological Engineering and Computing* *35*(3), 172–176. doi: 10.1007/BF02530033
- Martinsen, Ø. G., Pabst, O., Tronstad, C., & Grimmes, S. (2015). Sources of error in AC measurement of skin conductance. *Journal of Electrical Bioimpedance*, *6*(1), 49–53. doi: 10.5617/jeb.2640
- Poh, M.-Z., Swenson, N. C., & Picard, R. W. (2010). A wearable sensor for unobtrusive, long-term assessment of electrodermal activity. *IEEE Transactions on Biomedical Engineering*, *57*(5), 1243–1252. doi: 10.1109/TBME.2009.2038487
- Rosendal, T. (1943). Studies on the conducting properties of the human skin to direct current. *Acta Physiologica Scandinavica*, *5*(2–3), 130–151. doi: 10.1111/j.1748-1716.1943.tb02040.x
- Rutenfranz, J. (1955). Zur Frage einer Tagesrhythmik des elektrischen Hautwiderstandes beim Menschen [Question of a daily rhythm of the electrical skin resistance in humans]. *European Journal of Applied Physiology and Occupational Physiology*, *16*(2), 152–172. doi: 10.1007/BF00693743

- Tartz, R., Vartak, A., King, J., & Fowles, D. (2015). Effects of grip force on skin conductance measured from a handheld device. *Psychophysiology*, *52*(1), 8–19. doi: 10.1111/psyp.12237
- Tronstad, C., Gjein, G. E., Grimnes, S., Martinsen, Ø. G., Krogstad, A. L., & Fosse, E. (2008). Electrical measurement of sweat activity. *Physiological Measurement*, *29*(6), S407–S415. doi: 10.1088/0967-3334/29/6/S34
- Tronstad, C., Johnsen, G. K., Grimnes, S., & Martinsen, Ø. G. (2010). A study on electrode gels for skin conductance measurements. *Physiological Measurement*, *31*(10), 1395–1410. doi: 10.1088/0967-3334/31/10/008
- Tronstad, C., Kalvøy, H., Grimnes, S., & Martinsen, Ø. G. (2013). Waveform difference between skin conductance and skin potential responses in relation to electrical and evaporative properties of skin. *Psychophysiology*, *50*(11), 1070–1078. doi: 10.1111/psyp.12092
- Tronstad, C., Staal, O. M., Sælid, S., & Martinsen, Ø. G. (2015). *Model-based filtering for artifact and noise suppression with state estimation for electrodermal activity measurements in real time*. Presented at the 37th Annual International Conference of the IEEE Engineering in Medicine and Biology Society (EMBC), pp. 2750–2753. doi: 10.1109/EMBC.2015.7318961
- Yamamoto, T., & Yamamoto, Y. (1981). Non-linear electrical properties of skin in the low frequency range. *Medical and Biological Engineering and Computing*, *19*(3), 302–310. doi: 10.1007/BF02442549
- Yamamoto, Y., & Yamamoto, T. (1978). Dispersion and correlation of the parameters for skin impedance. *Medical and Biological Engineering and Computing*, *16*(5), 592–594. doi: 10.1007/BF02457817

(RECEIVED August 26, 2016; ACCEPTED November 2, 2016)

### Supporting Information

Additional Supporting Information may be found in the online version of this article.

**Sound File 1:** Noise stimulus in Experiment 1.

**Sound File 2:** Noise stimulus in Experiment 2.

**Sound File 3:** Sound that indicates the end of a subtraction task in Experiment 1.

**Sound File 4:** Sound that indicates the end of a subtraction task in Experiment 2.





# Human Skin is a generic, non-volatile memristor

Oliver Pabst<sup>1</sup>, Ørjan G. Martinsen<sup>1,2</sup> and Leon Chua<sup>3</sup>

Examples of non-linear electrical behavior of human skin were reported almost 40 years ago, but the underlying mechanisms and its appearance have never been studied in any detail. In 2011, we reanalyzed data published in 1983 and found them to be consistent with memristive behavior of the human skin. By the systematic study presented in this paper, we confirm that the skin is a memristor and demonstrate that this behavior occurs at much lower signal amplitudes than expected. Beside the sweat duct memristor in which the inner state will change by electro osmotic forces, our results also indicate that a second type of memristor may found in the stratum corneum. The pinched-hysteresis-loop, which is the fingerprint of memristors, varies largely in shape among subjects and skin sites and it might be possible to correlate the recordings with physiological properties of potential use in medical diagnostics. Shifting the focus from linear to non-linear properties provides in general a new class of measurements that may apply to other tissues than the human skin, as well. Furthermore, we discover that skin is a non-volatile memristor, meaning that it can store information over time spans of minutes and probably hours. This finding may have significant implications in medical, health, and sport applications, where non-volatile, analogue memory in the skin may be used in wearable sensors and wireless body area networks. An example circuit made of skin memristors that acts under certain conditions as a frequency doubler or half-wave rectifier is also presented in this paper.

---

<sup>1</sup> Department of Physics, University of Oslo, Oslo, Norway

<sup>2</sup> Department of Clinical and Biomedical Engineering Oslo University hospital, Oslo, Norway

<sup>3</sup> Department of EECS, University of California, Berkeley, Berkeley, CA USA

When a constant low frequency sinusoidal voltage of high amplitude (e.g. 13 V) was applied to human skin [1], the shape of the measured current was different from sinusoidal. The observation implies that the measurement was non-linear and electro-osmosis, the directed motion of liquid caused by an electric field, within the sweat ducts was suggested as the underlying mechanism. Human sweat contains ions and is therefore highly conductive. The level of sweating determines the conductance of the skin in the low frequency range. It may be affected by an applied voltage itself which has impact on the resulting current or vice versa [2]. Resulting voltage-current (V-I) plots (Lissajous figures) showed hysteresis loops with pinched point in the coordinate origin, which is the “fingerprint” of a memristor (**memory resistor**) [3], the fourth passive electrical circuit element [4]. The interpretation of human skin as a memristor was first time given in [5]. A memristor relates voltage and current by state-dependent Ohm’s law. If the memristor is e.g. a generic one [6] it can be described by

$$v = M(\mathbf{x}) \cdot i \quad (1)$$

$$\frac{dx}{dt} = f(\mathbf{x}, i) \quad (2)$$

with memristance  $M(\mathbf{x})$  (in analogy to resistance), where  $\mathbf{x}$  is a vector of state variables. The memductance  $G(\mathbf{x})$  is the state-dependent analog of the conductance  $G$ .

An electrical circuit model of human skin (based on our findings) is shown in Figure 1. The skin memristor as it was described in [5] has to be labelled more precisely as “sweat duct memristor” since our measurements indicate that there is a second, non-linear mechanism that most likely originates from the stratum corneum. The latter may be modelled as a negative-temperature-coefficient (NTC) thermistor, which is a memristor itself. The overall skin memristor is a combination of both, the sweat duct memristor and the stratum corneum thermistor. However, it seems that the sweat duct memristor  $G_D(\mathbf{x})$  more or less dominates as long as there is a galvanic contact through the sweat ducts. Capacitive properties of the stratum corneum ( $C_S$ ) that are related to its humidity [7], will also affect the measurements (especially at higher frequencies). Electrical potentials occur naturally among skin sites (endogenous skin potentials) and potential differences between the skin sites under the recording electrodes will contribute a DC offset to the measurement [8]. The small-signal behavior about an equilibrium state ( $x_Q, T_Q$ ) of the parallel circuit in Figure 1 can be described by state-dependent mem-admittance (analog to admittance), defined by

$$Y(x_Q, T_Q) = G(x_Q, T_Q) + jB \quad (3)$$

$$= G_D(x_Q) + G_S(T_Q) + j\omega C_S, \quad (4)$$

with susceptance  $B$ , imaginary unit  $j$  and  $\omega=2\pi f$ . If the frequency  $f$  is zero (DC signal), the memristance at a certain state will be one divided by the corresponding memductance. Memductance is the “state-dependent conductance” in

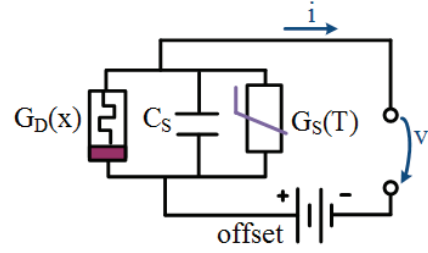


**Figure 1 | Simple electrical circuit model of skin in non-linear measurements.** The sweat duct memristor (represented by its memductance  $G_D(\mathbf{x})$ ) consists of several sweat ducts and its ability to conduct current is dependent on the sweat duct filling. The state dependent conductance of the stratum corneum  $G_S(T)$  increases with increasing temperature. Capacitive properties ( $C_S$ ) of the stratum corneum and a DC offset will affect the measurements.

the non-linear range. The term “conductance” is used for linear measurements or for small signal memductances at specific equilibrium states ( $x_Q, T_Q$ ).

The interest for the memristor as a subject of research increased when Hewlett Packard presented the first realization based on titanium dioxide in 2008 [9]. Until 2017, most of the research is related to technical memristors (realization based on different materials e.g. tantalum oxide [10, 11], zinc oxide [12]) and their applications e.g. in neuromorphic computing [13-15], or in circuits emulating arithmetic operations [16, 17]. On the other hand, first biological/organic memristors like the Venus flytrap [18] and the slime mould memristors [19] have been demonstrated. A recording system, including electrode choice, that is suitable for skin memristor measurements was presented by us in [20].

This study consists of three experiments and provides data that is recorded from 28 subjects on the forehead. Additional recordings from the earlobe and the fingertip of the same subjects are shown in the Extended Data Figure 1 to 6. The first experiment was all about the voltage-current characteristics (V-I plots) of the human skin. Sinusoidal (with amplitudes of 0.4 V, 0.8 V, and 1.2 V), triangular and non-periodic voltage signals were applied with six different frequencies (0.05 Hz to 2.5 Hz) each, in order to verify whether human skin is a memristor and under which signal conditions a measurement becomes non-linear. Classification of the underlying memristor type was done, as well. Odd-symmetric pinched hysteresis loops are indication of ideal memristors. Asymmetric loops that tend to become a straight line with increasing frequency will identify generic memristors while the tendency towards single valued curves indicate extended memristors [6]. The electro-osmotic effect itself is studied in experiment 2. Three series (duration of three minutes each) of DC voltage pulses were applied. The memductance changes between and within pulses, as well as from pulse to pulse give information about the impact of applied voltages on the level of sweating. Small signal conductance was measured for three minutes after each series, in order to study the natural recovery process. By experiment 2, the skin memristor can be classified as either vola-

tile or non-volatile. If the current responses to periodic DC voltage pulses are not periodic, the skin memristor is non-volatile. A possible application of the skin memristor in an electrical circuit is demonstrated by experiment 3, here the circuit functions as frequency doubler, or half-wave rectifier, under certain conditions.

### AC voltage-current characteristics of human skin.

Pinched hysteresis loops in the V-I plot could be observed from different subjects, voltage signals (see Figure 2) and skin sites (see results of the earlobe and fingertip in the Extended Data Figure 1 and 4). The results confirm that human skin is a memristor. This is not just a unique phenomenon of single subjects; it is a general property of human skin across different ages and gender. In the positive half of the period, the sweat is moved by the electric field (electro-osmotic effect) towards the skin surface, resulting in further filling of the sweat ducts and better conducting pathways. The memristance decreases, or equivalently the memductance increases. During the negative half period, the opposite occurs. Consequently, the orientation of all measured pinched hysteresis loops was counter-clockwise.

The measured hysteresis loops are in general not odd-symmetric, implying that the skin memristor is not an ideal memristor, and their appearances differ largely among subjects (see Figure 2 c)). Pinched hysteresis loops were also observed in cases where the measured currents were very small (e.g. maximum current of 2  $\mu\text{A}$ ). On the other hand, if the amplitude of the voltage was low (0.4 V), fewer subjects showed pinched hysteresis loop compared to the recordings with 1.2 V. This might be an indication that the skin memristor is flux-controlled.

The decrease in lobe area with increasing signal frequency (see Figure 2 b)) is another fingerprint of memristors [21] that applies also over the recorded population (see Figure 3 a)). As the frequency increases, less time remains for the ions to move which affects the lobe area, as well as the non-linearity parameter (adapted from [22]). In Figure 3 c) it can be seen that the measurements tend to become linear with increase in frequency (compare with Figure 2 b)) and decrease in amplitude. The V-I relation at 1 Hz and 2.5 Hz of most subjects is a straight line up to a certain magnitude followed by a small curve. Even though the curve at 2.5 Hz in Figure 2 b) is very close to a straight line it bends slightly above 0.6 V. The interpretation is that the skin memristor at the forehead is a generic memristor up to a certain voltage magnitude and tends to be an extended memristor above. The non-linearity values in Figure 3 c) might confirm that human skin at the forehead is a generic memristor up to a certain magnitude (0.8 V) (mean and median non-linearity (NL) values at 2.5 Hz are very close to 2, indicating a straight line)<sup>4</sup>. The shape different from a straight line for amplitude of 1.2 V and frequency of 2.5 Hz

<sup>4</sup> Those NL values have to be evaluated carefully since a phase shift from the capacitance of the stratum corneum will erroneously affect the NL value (causing a decrease, see methods part).

(NL values are larger than 2) implies that the skin memristor has entered the domain of an extended memristor<sup>5</sup> [6] defined by  $i = G(x,v) \cdot v$ . A straight line within the full magnitude of the applied voltage at high frequencies as it is observed for some subjects, indicates generic memristors, described by  $i = G(x) \cdot v$ , where the memductance  $G(x)$  is not a function of the voltage  $v$ . The maximum measured currents seem to be more or less constant among the frequencies (see Figure 3 b). The results show that memristive properties can be measured with applied voltage magnitudes of 1.2 V and smaller. The resulting currents through all subjects (except of one outlier at the forehead) were below 100  $\mu\text{A}$ , which is much lower than the threshold of perception. This is an important issue for test subject safety in potential clinical and commercial use of this new kind of measurement.

Shifts in the pinched point position from the coordinate origin can be explained by the endogenous skin potential differences that result in a DC offset to the measurement and the capacitive properties of the stratum corneum [8]. Half-cell potentials will add as DC offset, as well. The fact that the pinched point position is usually very close to the origin for applied voltages with frequency of 0.05 Hz and shifts away with increasing frequency (see Figure 2 b)), is a confirmation that the measurements are affected by a capacitance. Recordings from organic memristors in general contain parasitic elements that cause a shift in the pinched point position [3, 21].

The appearance of the hysteresis loops may change slightly from period to period as it can be seen in Figure 2 a). The changes are even smaller in the recordings of other subjects or at higher frequencies. Furthermore, the appearance of the hysteresis loops seem to stabilize with increasing period number and the use of the third period for further presentation and analysis was found to be a good trade-off between final appearance and recording time. Possible reasons for the small changes from period to period are the DC offset that interferes with the measurements [8] and different duration between filling and emptying processes in the sweat ducts.

V-I plots similar to the one of subject F (hysteresis loops with two pinched points, see Figure 2 c) are indication that there is little or no galvanic contact through the sweat ducts and hence that the recorded current went mainly through the stratum corneum (measured currents are small). The two pinched points are first indications that there is another non-linear mechanism (NTC thermistor) beside the sweat duct memristor. A current of about 2  $\mu\text{A}$  to 10  $\mu\text{A}$  through the stratum corneum under the measuring electrode might increase the temperature only little and the temperature will decrease again as soon as the current flow stops. The memductance will increase with increasing temperature, which is independent of the polarity of the applied voltage.

<sup>5</sup> Some subjects still showed pinched hysteresis loops under these signal conditions which will also result in NL values larger than 2.

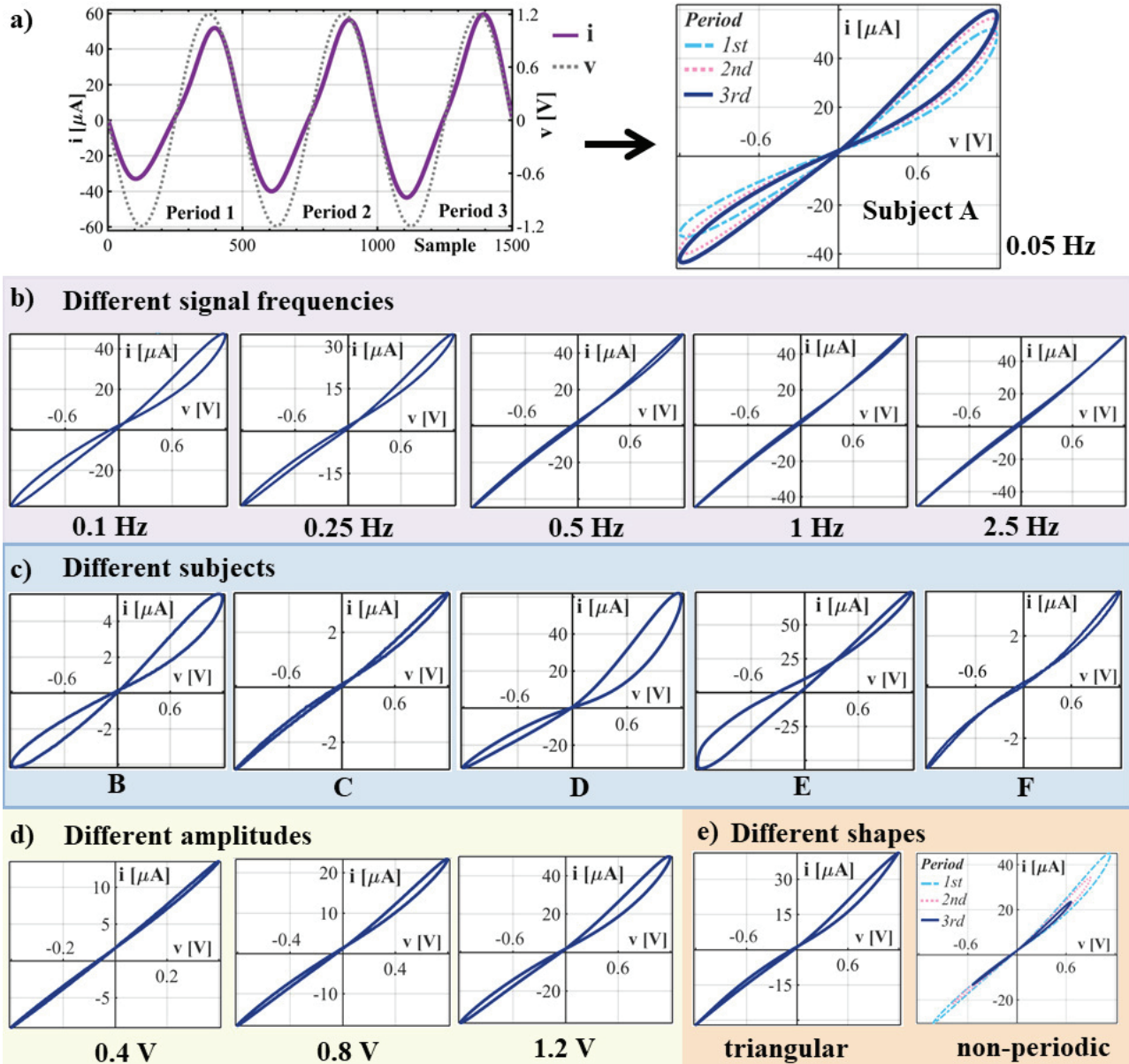


**Figure 2 | Voltage-current (V-I) plots recorded from the forehead (experiment 1), always shown for the third period of each applied signal.** Each signal was continuously applied for three periods as it is shown in **a)** Applied sinusoidal voltage (amplitude of 1.2 V and  $f=0.05$  Hz) and measured current over time (left) and corresponding V-I plot (right) shown for subject A. **b)** Same applied signal and subject (A) like in **a)** but different frequencies. The lobe area of the pinched hysteresis loop becomes smaller with increasing frequency (applies for all subjects). The presented V-I plot at 1 Hz still shows a pinched hysteresis loop with very small lobes and large shift of the pinched point position. **c)** Same signal conditions like in **a)** but different subjects. Loops that were quite symmetric and had a relative large lobe were observed from 6 subjects for different current levels (compare subject A with subject B) if this high amplitude and very low frequency voltage signal was applied. Loops that had a relatively small area in each lobe instead (see subject C) were observed for 10 subjects. Asymmetric loops with relative large lobe in the first quadrant but small lobe in the third (see subject D) were observed for 8 subjects. The asymmetric shape with very large shift in pinched point position (see subject E) was unique. Twenty-five subjects in total (out of 28) showed hysteresis loops with one pinched point (but different shapes) like subjects A to E and might reflect the sweat duct memristor. The remaining three subjects showed quite symmetric hysteresis loops with small lobes and 2 pinched points (see subject F) which is indication that the galvanic contact through the sweat ducts was not given and the current went mainly through the stratum corneum. **d)** Sinusoidal voltage signal with  $f=0.05$  Hz but different amplitudes are shown for subject G. The relative lobe area increases with increasing amplitude (applies for all subjects). Pinched hysteresis loops for amplitude of 0.4 V were only observed for 21 subjects (most of them with very small lobe area). Remaining seven subjects showed linear relation. **e)** Other applied voltage shapes than sinusoidal shown for  $f=0.05$  Hz and subject G. As soon as a pinched hysteresis loop was obtained from the recording with sinusoidal voltage, it was obtained with triangular and non-periodic (sinusoidal signal with decreasing amplitude) waveform. The recording of the latter is shown over three periods and was only recorded from fifteen test subjects due to instrumentation error.

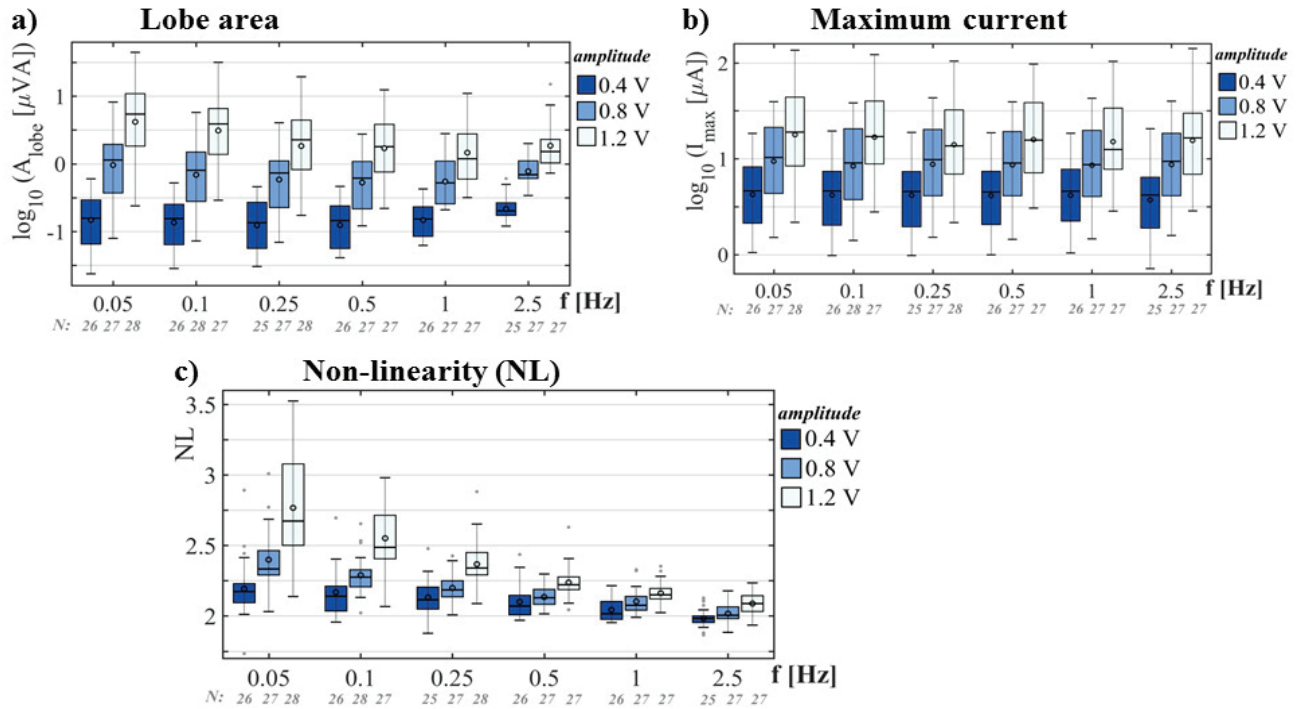


**Figure 3 | Box plots over all test subjects** shown for 3<sup>rd</sup> period of all applied sinusoidal voltages (3 amplitudes, 6 frequencies), recorded from the forehead. The plots give information of how the V-I characteristics change with amplitude and frequency. The horizontal line in the middle of each boxplot denotes the median, the circle the mean value, the whiskers the 5% and 95% percentiles. The number N of subjects, included in the evaluations, is written under each boxplot. Sinusoidal signal with amplitude of 0.4 V was not recorded from 2 subjects at 2.5 Hz and 1 subject at 0.25 Hz due to instrumentation error. Two subjects had very low memductance and the measured currents were quite noisy. Signals were excluded from the evaluation if  $I_{\text{max}}$  was smaller than  $\text{amplitude}/0.4\text{V} \cdot 0.7 \mu\text{A}$ . **a)** Lobe area (logarithm to base 10). Mean and median of the lobe area continuously decrease up to a certain frequency (e.g. up to 1 Hz for 1.2 V amplitude) and increase above, when the capacitive properties of the stratum corneum start to interfere noticeably. **b)** Maximum current (logarithm to base 10), **c)** A Non-linearity (NL) value equal 2 implies a linear measurement (straight line in the V-I plot) and the higher the value of NL the higher the non-linearity of the measurement. The pinched hysteresis loop of the third period in Figure 2 a) e.g. results in a NL value of around 3.1, the one of subject F in Figure 2 c) (example with two pinched points) results in a NL value of 2.52. A single valued-curve that is not a straight line will also have a value larger than 2. Results from the linear mixed effects model analysis (see methods part, number of observations at the forehead was 481) show that, frequency (as logarithm to base 2 in the used model) and absolute value of the amplitude (p-value < 0.001 for both) have significant effects on the non-linearity parameter. The value of the NL parameter increased by  $0.328 \pm 0.039$  (95%-CI) with an increase in amplitude by 1 V and each bisection of the frequency increased the value by  $0.075 \pm 0.007$  in the obtained model.

The memductance of the stratum corneum will consequently obtain two maximum states within one period of applied sinusoidal voltage (at  $\frac{1}{4} T$  and  $\frac{3}{4} T$ ) and the pinched hysteresis loop will be a tangential one. In opposite, all observed hysteresis loops of the sweat duct memristor were “transversal” ones since the 2 branches of the loop crossed the pinched point with different slopes. Within a signal period, the memductance will obtain one maximum state at around  $\frac{1}{2} T$  (if sinusoidal signal with positive amplitude is applied) and one minimum state after the negative half of the signal (at  $T$ ). It is possible to obtain a hysteresis loop with two pinched points if a “tangential” memristor (like a NTC thermistor) is connected in parallel with a capacitance (see simulations in Extended Data Figure 8). The same will not be possible with the “transversal” sweat duct memristor. The thermal properties of the stratum corneum will have to be studied further but it is already known that conductance of human hair increases with increasing temperature [23].

Human hair (studied in [15]) and stratum corneum consist both of keratinized tissue.

### Response to series of applied DC pulses (experiment 2)

Since the current responses to periodic constant voltage steps are not periodic (see Figure 4 a)), the conclusion is that the skin memristor (at the forehead) is a *non-volatile memory* which might be the most significant characteristic. For a volatile memory, the current response would have been periodic. However, the peak of the current response changes after each additional voltage step, which implies a cumulative memductance change. The chosen DC levels within the pulse-series in experiment 2 were strong enough to cause a change in memductance by electro-osmotic forces. It can be seen that the amount of measured current changed within pulses but also from pulse to pulse (net change) (see Figure 4 a) and c)). As soon as the applied DC voltage level changed to 0 V, the memductance of the skin memristor did not keep at the same level.

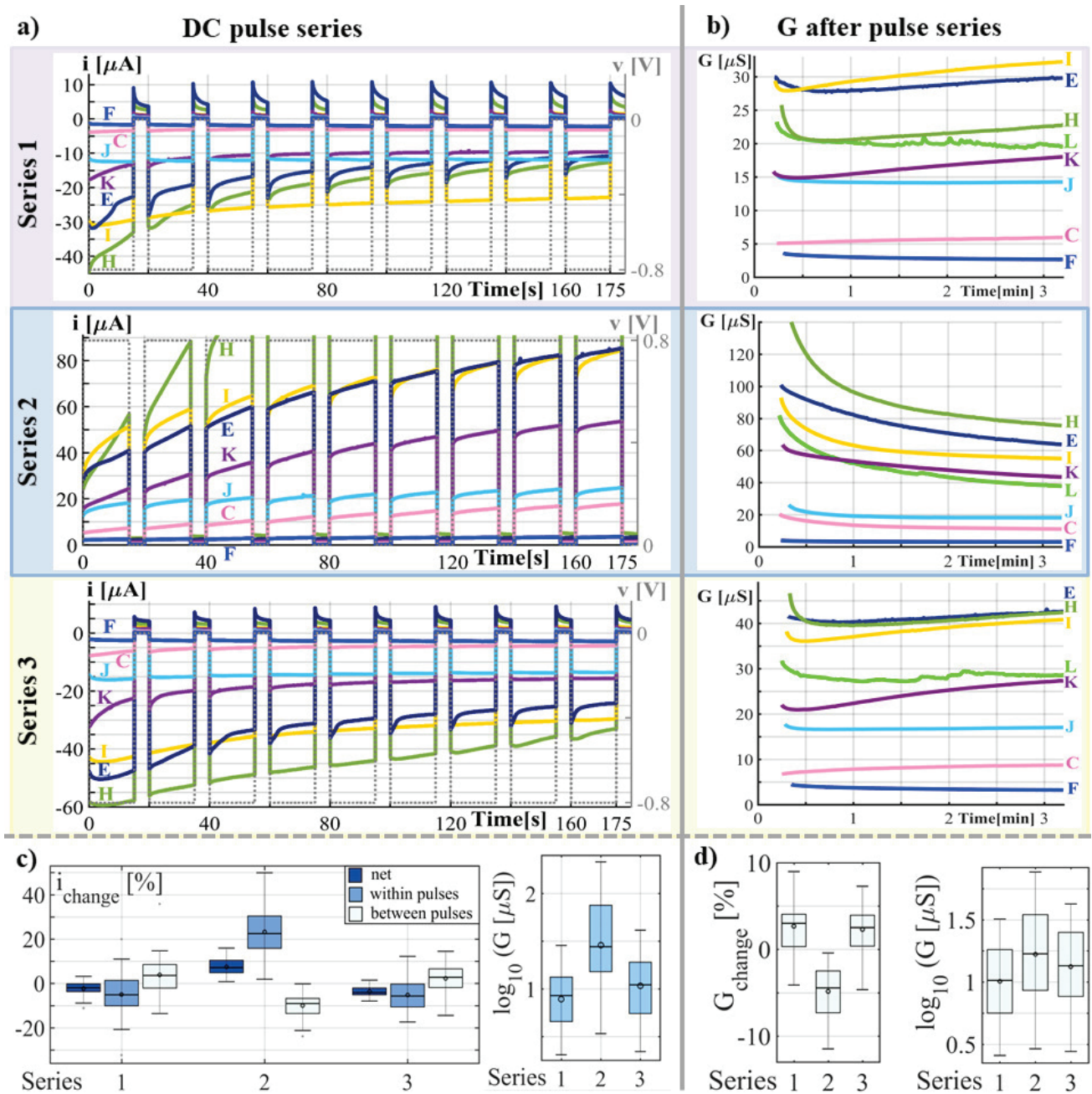


**Figure 4 | Results from experiment 2 (forehead).** Three series of DC pulses were applied and the small signal conductance measurements were done after each series. **a)** Measured current  $i$  and applied voltage  $v$  plotted over time shown for seven test subjects (C, E, F, H, I, J, K). The limit of the y-axis in series 2 is set to  $91 \mu\text{A}$  in order to see the development of the other plots better. The current of subject H that is an outlier goes up to  $171.5 \mu\text{A}$  in the end of the last pulse (the corresponding memductance is  $214 \mu\text{S}$ ). **b)** Small signal conductance measurements after each DC pulse series (shown for the same subjects) give information of how the state of the skin memristor develops naturally (unaffected by the applied voltage). The time is related to the end of the last pulse of the DC pulse series. The limit of the y-axis in series 2 is set to  $140 \mu\text{S}$  in order to see the development of the other plots better. The initial conductance at 0 minutes of subject H is  $177.3 \mu\text{S}$ . The results of an additional subject L show that the skin at the forehead might be emotional active for some subjects. **c)-d)** Boxplots over all subjects. The horizontal line in the middle of each boxplot denotes the median, the circle the mean value, the whiskers the 5% and 95% percentiles. **c)** Boxplots related to the DC pulse series. Average change of current  $i$  within pulses (within 15 seconds), between pulses (within 5 seconds) and net change from pulse to pulse presented as ratios shown for all three series (left). Memductance  $G$  (logarithm to base 10) at the end of the last pulse (at 175 s) of each series (right). **d)** Boxplots related to the small signal conductance measurements after each pulse series. Small signal conductance change from minute 2 to minute 3 after the last DC pulse (left). Small signal conductance  $G$  (Logarithm to base 10) 3 minutes after the last pulse (right). Result from Friedman test show that there are significant differences in the conductance values (logarithm to base 10) among the three groups ( $p$ -value  $< 0.001$ ). Pairwise comparison (Tukey Test with  $p$ -Value  $< 0.05$ ) shows that all groups differ from each other.

This behavior was observed during the 5 seconds between pulses<sup>6</sup> but also during the three minutes of small signal conductance measurements<sup>7</sup> after each series (see Figure 4 b) and d)).

When negative pulses were applied (in series 1 and 3), the sweat was pushed towards deeper skin layers and the memductance decreased consequently (if the galvanic contact through the sweat ducts was provided). The accumulation of sweat in the deeper parts of the duct/gland may cause a counter force, driven by pressure from the surrounding tissue that drives the sweat back as soon as the voltage is released. Another explanation might be that the applied voltage creates differences in ion concentration and the gradient driven diffusion processes will cause a change, as well. The resulting memductance (conductance) increase can be seen between the DC pulses of series 1 and 3 (see Figure 4 c)) and within the three minutes of small signal measurements after series 1 and 3 (see Figure 4 d)). For some subjects the small signal conductance increased after a small drop within the first 5 to 10 seconds while other subjects showed an immediate increase.

The subjects that showed hysteresis loops with two pinched points in experiment 1 (recordings dominated by the stratum corneum), had opposite trends during series 1 and 3. The memductance increased when negative pulses were applied and as soon as the voltage was released, it decreased (see subjects F and J in Figure 4 a) and b)). Those observations support the stratum corneum NTC thermistor theory. The memductance of a NTC thermistor will increase for both positive and negative applied voltages.

When positive pulses were applied (series 2), the sweat was pulled towards the skin surface, resulting in a memductance increase within the pulses but also from pulse to pulse (see Figure 4 c)), which applied for all subjects. If the voltage was released, the memductance decreased immediately for all subjects, which might be explained by counter-driven forces of the surrounding tissue, as well as reabsorption processes.

The recording of subject L (see Figure 4 b)) implies that emotional sweating (compare recordings from the fingertip in Extended Data Figure 6) can also occur at the forehead and might interfere slightly the memristor measurements.

The variations in the rate of memductance (conductance) change among subjects may relate to physiological properties like the number and the diameter of the sweat ducts and the amount of the sweat available. The memductance of many subjects changed noticeably between pulses (as an example) but not for all<sup>8</sup>. The measured current (and consequently memductance) in e.g. series 1 increased in average by 3.6 % (median) between pulses (within 5 sec-

onds) and decreased in average by 5.1 % within each pulse (within 15 seconds) (see Figure 4 c)). An average memductance decrease of 2 % was observed with each pulse (net change). The memductance changes in series 2 occurred faster. An average decrease between pulses of 9 % (median), an average increase within pulse of 22.5% and an average net increase of 7.2 % with each pulse were observed.

Both the memductance change within the pulse series and the natural conductance change after the series slow down with time (see Figure 4 a) and b)) and become little after the three minutes of each recording. The states at the end of each DC pulses series (see Figure 4 c)) give a first approximation of the minimum (see series 1) and maximum (see series 2) memductance of the skin memristor<sup>9</sup>. The skin memristor at the forehead will range from about 8.5  $\mu\text{S}$  to about 27.5  $\mu\text{S}$  (median values); extreme outliers with memductances up to 214  $\mu\text{S}$  (subject H) were recorded. The memductance states directly at the end of pulse series 2 are obviously very different from those at the end of series 1 or 3 (see Figure 4 c)) but do those states still differ after a period of recovery? There are still significant differences in the small signal conductance values among the series after three minutes of recovery (see Figure 4 d)). This means that skin has an analog memory that lasts at least for three minutes. The conductance plots of some subjects suggest that this memory could even last for hours or longer (see e.g. subject E in Figure 4 b)<sup>10</sup>.

The small signal AC conductance (sinusoidal with  $f=20$  Hz) cannot be directly compared to the DC conductance (memductance) at the end of each pulse series since additional pathways will contribute to the AC conductance and the expected level is a little bit higher [24]. If the sweat reaches the skin surface, it will add moisture to the stratum corneum around the sweat duct. Its susceptance [7] and conductance will consequently increase, which contributes to the measurement. On the other hand, the higher the moisture content in the stratum corneum, the less sweat can diffuse into it from the duct and the more sweat may remain in the sweat duct/gland itself, which will affect the equilibrium state of the skin memristor. A confirmation of this is that the measured currents at the end of the DC pulse series 1 and 3 are different, as well (compare results in series 1 and 3 of e.g. subject K or I in Figure 4 a)). Even if the sweat is forced by an electric field, different states seem to emerge, i.e., more sweat is in the ducts/glands themselves that cannot be pushed further. These results show that human skin memristor has several equilibrium states, which is a confirmation of the non-volatile memory property.

<sup>6</sup> The current changes from the end of one pulse to the beginning of the following for most subjects (see Figure 4 a) and c)).

<sup>7</sup> Based on the results from experiment 1 it is clear that the applied sinusoidal voltage with amplitude of 0.1 V and frequency of 20 Hz does not affect the state of the skin memristor.

<sup>8</sup> Compare e.g. subjects E and I in Figure 4 a).

<sup>9</sup> If applied voltage levels are  $\pm 0.8$  V.

<sup>10</sup> The small signal conductance values at minute three after all three series are very different from each other and it seems that those would not become equal even after a longer periods.

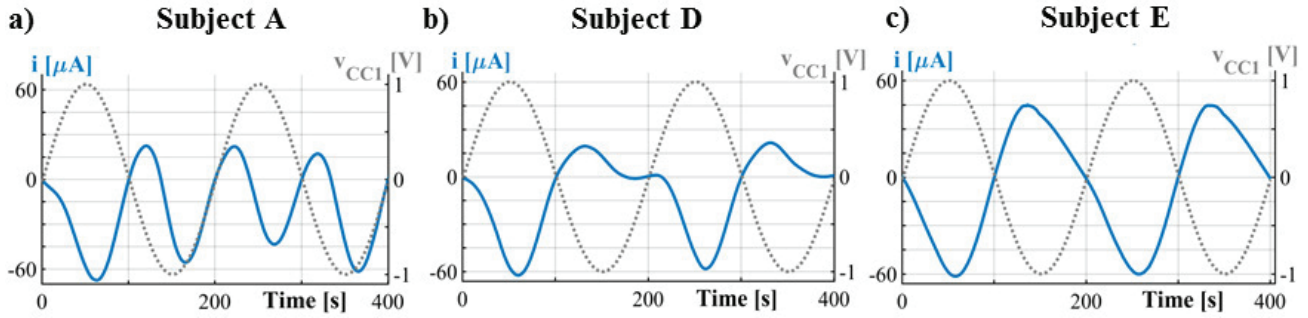


**Figure 5 | Example recording of three subjects in experiment 3 shown for  $f=0.005$  Hz.** Applied voltage (on CC1) and measured current ( $i$ ) over time. Applied sinusoidal voltage:  $f=0.005$  Hz, amplitude=1 V (at CC1) and amplitude = -1 (at CC2). **a)** Subject A. The frequency of the measured is double the frequency of the applied voltage (that had a frequency of 0.005 Hz). The measured currents of five (2 out of 12 with CC1 electrode at earlobe, 3 out of 16 with CC1 electrode at the forehead) subjects in total were comparable for frequency of 0.005 Hz. Two out of those subjects showed similar results at 0.05 Hz and one out of those two even at 0.5 Hz. **b)** Subject D. The measured current has a large magnitude in one period half and more or less a cut off during the other period half. Five subjects in total (3 out of 12 with CC1 electrode at earlobe, 2 out of 16 with CC1 electrode at the forehead) showed a behavior like this. **c)** Subject E. The measured current is non-linear but neither half-wave rectification nor frequency doubling was observed. Eighteen subjects in total showed behaviour like this.

### Rectifying skin memristor circuit (experiment 3)

An electrical circuit based on two skin memristors was built in experiment 3 (see Figure 7 b)). This circuit is the two-memristor version (see [25]) of the 4-memristor bridge that is used as full-wave rectifier in [25], for synaptic weight programming in [26] and for the generation of  $n$ -th order harmonics and frequency-doubling in [27].

If the contributing memristors are similar (e.g. similar initial state, similar maximum and minimum conductance) and the state changes are relatively fast, the measured currents with double frequency like those shown in Figure 5 a) can be observed. When  $v_{cc1}$  is positive, the voltage  $v_{cc2}$  is negative (opposite sign of both voltages). The memductance of the skin under CC1 decreases<sup>11</sup> while the one under CC2 increases. Consequently, the current through the skin under CC2 will become dominant. In the other half of the period, the opposite occurs and after a while, the measured current will be mainly the current through the skin under CC1. The results show that the human skin can be used as a frequency doubler<sup>12</sup> (see Figure 5 a)). If the skin memristor under CC1 had initially a much lower memductance than the one under CC2 instead, the resulting current will be half-wave rectified (see Figure 5 b)). The memductance under CC2 decreases in the second half period, while the one under CC1 increase but both end up at similar states. The resulting current is almost zero, since it is the sum of a negative and a positive current of almost the same magnitude. The current in Figure 5 c) implies that the memductance under CC1 is initially much lower than the one under CC2 and does not change significantly. The measured current is more or less the current through the skin under CC2.

<sup>11</sup> A decrease of memductance during positive half of applied voltage is opposite to the observations in experiments 1 and 2. The difference occurs in the opposite direction of the skin memristor regarding the applied voltage in the chosen two-electrode setup.

<sup>12</sup> If the current development towards positive half would have been reduced (by using slower frequency than 0.005 Hz), the overall skin memristor circuit would act more or less as a full-wave rectifier.

### Different skin sites

It was quite easy to obtain galvanic contact through the sweat ducts and to show pinched hysteresis loops at the forehead. The memristive properties at the earlobe were comparable but the galvanic contact through the sweat ducts was obtained for fewer subjects (9 out of 28) with our methods. The recordings of the remaining subjects consequently reflected the non-linear properties of the stratum corneum (hysteresis loop with two pinched points and small currents). If the electrode was pressed against the earlobe (only for testing), a sudden increase in conductance and hysteresis loop with one pinched point was observed. However, the initial sweat level is crucial for the appearance of the pinched hysteresis loop and it was found that the voltage-current relation at the forearm of one subject changed completely after physical exercise [20]. It is likely that the galvanic contact becomes better in a warm and humid environment. The average relative humidity and room temperature in this study were 30.6 % (SD of 5.1%) and 21.6 °C (SD of 0.8 °C), respectively.

The skin of the fingertip (see Extended Data Figure 4 to 6) behaved differently from the forehead and the earlobe and voltage-current relations were usually less non-linear.

The fingertip is an emotionally active site (sweating caused by stimulation through the sympathetic and parasympathetic nerve system), that is less sensitive to thermo-regulation [28]. Further, the thickness of the epidermis is much higher at the palmar and plantar skin sites (including the fingertip, thickness of about 1mm) [28] than at other skin sites (thickness of 50 to 200  $\mu$ m).

Pinched hysteresis loops (if existent) had small lobe areas and only one pinched point (in or close to the origin), which is indication that the sweat duct memristor is existent at the fingertip, as well. It was even possible to observe pinched hysteresis loops at the fingertip for amplitude of 0.4 V (some subjects) which is an indication that non-linear effects may occur in standard electro dermal activity measurements with an applied DC voltage level of 0.5 V [29].

This is a further argument for using the AC method (see [24]).

No hysteresis loops with two pinched points were recorded from the fingertip, indicating that any contribution of a stratum corneum NTC thermistor (if existent) was negligible. Reasons are the good galvanic contact through the sweat ducts that was usually given at the fingertip and the thickness of the epidermis of about 1mm (overall memristance of the epidermis including the stratum corneum is much higher than at the other skin sites).

The measured current during the pulse series did not follow a clear tendency and those measurements were obviously influenced by emotional sweating. Therefore, it is not certain from these results whether the memristor at the fingertip is volatile or non-volatile.

### Significance of the results and further research

In general, the non-linear properties and especially the shape of the pinched hysteresis loops differed largely among subjects and recordings. Part of our further research will be the search for quantitative measures that are related to physiological properties and to compare them between groups. Beside the non-linearity and the lobe area, a measure of asymmetry between positive and negative part of the loop could be useful. Physiological properties that may affect the shape of the measured current and the hysteresis loop are the number and diameter of sweat ducts, initial sweat duct filling, skin thickness, ion concentration, composition of the sweat, pH value of the skin, moisture content of the stratum corneum, endogenous skin potential differences and possibly more. Diseases that will affect at least one of those properties (like ion channel diseases) may then possibly be diagnosed by means of human skin memristor measurements. The NTC thermistor property of the stratum corneum itself might also contain useful information and will be studied further.

The results of experiment 2 indicate the possibility of information storage (analog memory) in human skin. It is possible to apply e.g. a constant DC voltage, or DC pulses, to the skin and change its memductance. Stored information can be read by small signal conductance measurements. A further study with longer relaxation periods needs to be done but the results in this study already suggest that information can be stored for at least several minutes, if not even hours. It is known that emotional sweating occurs at palmar and plantar skin sites [28]. If the initial sweat level is high enough, other skin sites might show emotional sweating, as well and the use of electro-osmosis may enable the recording of those.

Under certain conditions, the skin memristor circuit can act similarly to a frequency doubler and a half- or full-wave rectifier. The result depends on initial states of the memristors and its specific properties. This application could e.g. be used in authentication systems.

### References

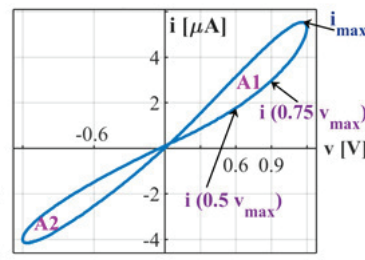
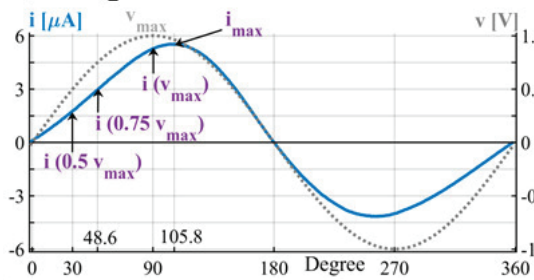
- [1] S. Grimnes, "Skin impedance and electro-osmosis in the human epidermis," *Medical and Biological Engineering and Computing*, vol. 21, no. 6, pp. 739-749, 1983.
- [2] T. Yamamoto and Y. Yamamoto, "Non-linear electrical properties of skin in the low frequency range," *Medical and Biological Engineering and Computing*, vol. 19, no. 3, p. 302, 1981.
- [3] L. Chua, "If it's pinched it's a memristor," *Semiconductor Science and Technology*, vol. 29, no. 10, p. 104001, 2014.
- [4] L. Chua, "Memristor-the missing circuit element," *IEEE Transactions on circuit theory*, vol. 18, no. 5, pp. 507-519, 1971.
- [5] G. Johnsen, C. Lütken, Ø. Martinsen, and S. Grimnes, "Memristive model of electro-osmosis in skin," *Physical Review E*, vol. 83, no. 3, p. 031916, 2011.
- [6] L. Chua, "Everything you wish to know about memristors but are afraid to ask," *Radioengineering*, vol. 24, no. 2, p. 319, 2015.
- [7] Ø. G. Martinsen, S. Grimnes, and J. Karlsen, "Electrical methods for skin moisture assessment," *Skin Pharmacology and Physiology*, vol. 8, no. 5, pp. 237-245, 1995.
- [8] O. Pabst and Ø. G. Martinsen, "Interpretation of the pinched point position in human skin memristor measurements," in *EMBE & NBC 2017*: Springer, 2017, pp. 430-433.
- [9] D. B. Strukov, G. S. Snider, D. R. Stewart, and R. S. Williams, "The missing memristor found," *nature*, vol. 453, no. 7191, p. 80, 2008.
- [10] A. C. Torrezan, J. P. Strachan, G. Medeiros-Ribeiro, and R. S. Williams, "Sub-nanosecond switching of a tantalum oxide memristor," *Nanotechnology*, vol. 22, no. 48, p. 485203, 2011.
- [11] J. J. Yang *et al.*, "High switching endurance in TaO<sub>x</sub> memristive devices," *Applied Physics Letters*, vol. 97, no. 23, p. 232102, 2010.
- [12] X. Zhu *et al.*, "Observation of Conductance Quantization in Oxide-Based Resistive Switching Memory," *Advanced Materials*, vol. 24, no. 29, pp. 3941-3946, 2012.
- [13] S. H. Jo, T. Chang, I. Ebong, B. B. Bhadviya, P. Mazumder, and W. Lu, "Nanoscale memristor device as synapse in neuromorphic systems," *Nano letters*, vol. 10, no. 4, pp. 1297-1301, 2010.
- [14] G. Indiveri, B. Linares-Barranco, R. Legenstein, G. Deligeorgis, and T. Prodromakis, "Integration of nanoscale memristor synapses in neuromorphic computing architectures," *Nanotechnology*, vol. 24, no. 38, p. 384010, 2013.
- [15] M. Prezioso, F. Merrih-Bayat, B. Hoskins, G. Adam, K. K. Likharev, and D. B. Strukov, "Training and operation of an integrated neuromorphic network based on metal-oxide memristors," *Nature*, vol. 521, no. 7550, pp. 61-64, 2015.
- [16] F. Merrih-Bayat and S. B. Shouraki, "Memristor-based circuits for performing basic arithmetic operations," *Procedia Computer Science*, vol. 3, pp. 128-132, 2011.
- [17] K. A. Bickerstaff and E. E. Swartzlander, "Memristor-based arithmetic," in *Signals, Systems and Computers (ASILOMAR), 2010 Conference Record of the Forty*

- Fourth Asilomar Conference on*, 2010, pp. 1173-1177: IEEE.
- [18] A. G. Volkov, C. Tucket, J. Reedus, M. I. Volkova, V. S. Markin, and L. Chua, "Memristors in plants," *Plant signaling & behavior*, vol. 9, no. 3, p. e28152, 2014.
- [19] E. Gale, A. Adamatzky, and B. de Lacy Costello, "Slime mould memristors," *BioNanoScience*, vol. 5, no. 1, pp. 1-8, 2015.
- [20] O. Pabst, C. Tronstad, and Ø. G. Martinsen, "Instrumentation, electrode choice and challenges in human skin memristor measurement," in *Engineering in Medicine and Biology Society (EMBC), 2017 39th Annual International Conference of the IEEE*, 2017, pp. 1844-1848: IEEE.
- [21] M. P. Sah, C. Yang, H. Kim, B. Muthuswamy, J. Jevtic, and L. Chua, "A generic model of memristors with parasitic components," *IEEE Transactions on Circuits and Systems I: Regular Papers*, vol. 62, no. 3, pp. 891-898, 2015.
- [22] J. Joshua Yang *et al.*, "Engineering nonlinearity into memristors for passive crossbar applications," *Applied Physics Letters*, vol. 100, no. 11, p. 113501, 2012.
- [23] S. M. Abie, J. Bergli, Y. Galperin, and Ø. G. Martinsen, "Universality of AC conductance in human hair," *Biomedical Physics & Engineering Express*, vol. 2, no. 2, p. 027002, 2016.
- [24] O. Pabst, C. Tronstad, S. Grimnes, D. Fowles, and Ø. G. Martinsen, "Comparison between the AC and DC measurement of electrodermal activity," *Psychophysiology*, vol. 54, no. 3, pp. 374-385, 2017.
- [25] O. Pabst and T. Schmidt, "Frequency dependent rectifier memristor bridge used as a programmable synaptic membrane voltage generator," *Journal of Electrical Bioimpedance*, vol. 4, no. 1, pp. 23-32, 2013.
- [26] H. Kim, M. P. Sah, C. Yang, T. Roska, and L. O. Chua, "Memristor bridge synapses," *Proceedings of the IEEE*, vol. 100, no. 6, pp. 2061-2070, 2012.
- [27] G. Z. Cohen, Y. V. Pershin, and M. Di Ventra, "Second and higher harmonics generation with memristive systems," *Applied Physics Letters*, vol. 100, no. 13, p. 133109, 2012.
- [28] W. Boucsein, *Electrodermal activity*. Springer Science & Business Media, 2012.
- [29] W. T. Roth, M. E. Dawson, and D. L. Fillion, "Publication recommendations for electrodermal measurements," *Psychophysiology*, vol. 49, no. 8, pp. 1017-1034, 2012.
- [30] S. Grimnes, "Impedance measurement of individual skin surface electrodes," *Medical and Biological Engineering and Computing*, vol. 21, no. 6, pp. 750-755, 1983.
- [31] Ø. G. Martinsen and S. Grimnes, *Bioimpedance and bioelectricity basics*. Academic press, 2011.

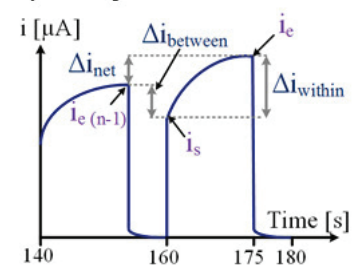
#### Acknowledgments

We thank the strategic research environment DIATECH@UiO at University of Oslo for funding. O.P. is also thankful to his co-supervisor Christian Tronstad for his comments especially regarding the statistical analysis.

### a) Experiment 1



### b) Experiment 2



**c)**

Shape	Amplitude [V]	f [Hz]
sinusoidal	0.4, 0.8, 1.2	0.05, 0.1, 0.25, 0.5, 1, 2.5
triangular	1.2	
non-periodic with $v(t) = (1.2 - 0.24 \cdot t \cdot f) \cdot \sin(\omega t)$ [V]		

**d)**

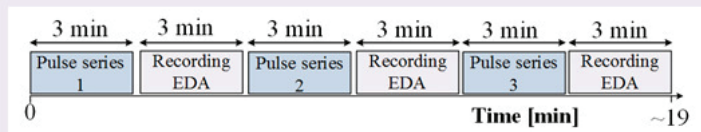


**Figure 6** | a) One period of measured current  $i$  and applied voltage  $v$  ( $f=0.05$  Hz) of an example measurement and corresponding V-I plot. Current values that are used for the calculation of non-linearity are illustrated, as well as, the lobe area, which is the sum of A1 and A2. b) Schematic of the measured current in the last 2 DC pulses of a series. c) Signal shapes used in experiment 1 with corresponding amplitudes and signal frequencies. d) Time schedule of experiment 2.

## METHODS

### Subjects Recruitment, Approval

A total of 28<sup>13</sup> test subjects (16 male/12 female, mean age 31 years,  $SD = 9.5$  years) were recruited and gave informed consent for participation in the study. The study was done in accordance with regulations from the Norwegian Ethics committee. The measurements were conducted at the University of Oslo in December 2016.

### Experimental design

Each test session contained three experiments and the total duration was one hour. It was randomly chosen whether the measurements were done on the side of the preferred or non-preferred hand. Electrodes were placed before the experiment series started and a test measurement was done. If there was only noise measured in one channel, the corresponding electrode was re-attached. Room humidity and temperature were measured before and after the test session.

In experiment 1, the V-I characteristics were investigated for different signal shapes, amplitudes and frequencies (see Figure 6 c)). In total, 30 different signals (6 different frequencies for each of the 5 different combinations of signal shape and amplitude) were applied for three periods each.

The sign of each applied voltage signal was randomized. Further, shape and amplitude appeared in a random sequence. For each of these five combinations a frequency sweep over all six frequencies in a randomized order was applied. The waiting time before a signal with a new fre-

quency was applied was 1 second. The waiting time before a run with new signal shape or amplitude was 2 seconds. Electrodermal activity (including conductance, susceptance and skin potential) (see “Recording modes” below) was measured before (for 30 seconds) and after (duration of 60 seconds) experiment 1.

Experiment 2 consists of three series of applied voltage DC pulses. The voltage steps are always from 0 V to -0.8 V (first and third series) and from 0 to +0.8 V (second series). Each single pulse has a duration of 15 seconds in high state followed by 5 seconds in low state (0 Volts). A continuation of 9 pulses was applied, the total duration per pulse series was three minutes. Electrodermal activity (including small signal conductance) was measured for three minutes after each DC pulse series. The time schedule of experiment 2 is shown in Figure 6 d). The change between recording modes was done manually. The recordings of EDA started around 10 seconds (median time, 5%-quartile was 7 seconds, 95%-quartile was 16 seconds) after the pulse series were finished.

Before experiment 3 started, all electrodes were disconnected from the instrumentation and the test subjects were asked to do an one-minute workout on a stationary bike. The instrumentation was switched into two-electrode mode and after the test subjects were finished with the work-out the electrodes were connected to the instrumentation in a different way (see Figure 7 b)) and experiment three was started. Two sinusoidal voltages of opposite sign (randomized order), same frequency and amplitude of 1V were applied for two periods. This was done three times for frequencies of 0.005 Hz, 0.05 Hz and 0.5 Hz in randomized order. The time of no applied signal between runs was 4 seconds.

<sup>13</sup> A 29<sup>th</sup> test subject was recruited, as well, but its skin was initially covered by body lotion and the collected data were excluded from further analysis.

### Parameterization in experiment 1

A measure of “non-linearity” (NL) is introduced in [22] and used in order to characterize technical memristors (based on TiO<sub>2-x</sub>/TaO<sub>x</sub> oxide). It is defined as the current at  $V$  to the current at  $V/2$ . A quantitative evaluation of non-linearity in biological memristors might be useful, as well. DC offsets will add naturally to skin memristor measurements [8] and would affect the non-linearity value as it is defined in [22]. In order to correct for DC offsets a slightly different definition of non-linearity is presented in this paper, which is

$$NL = \frac{i_{max} - i(0.5 \cdot v_{max})}{i(0.75 \cdot v_{max}) - i(0.5 \cdot v_{max})} \quad (5)$$

with  $v_{max}$  equal to the amplitude of the applied sinusoidal voltage. The current values are illustrated in Figure 6 a) in which one period of an actual measurement is presented. The current  $i$  has a small DC offset and may have a very small phase shift compared to the applied voltage but the maximum current value  $i_{max}$  (see Figure 6 a) (left)) is shifted noticeable among the x-axis (at around 105.8 Degree).

This shift can be explained by the state change of the skin memristor. At 90 degrees the applied sinusoidal voltage starts to decrease slowly but the state of the memristor changes further resulting in a continuing increase of the current. In order to take this aspect of non-linearity into account,  $i_{max}$  is preferred over  $i(v_{max})$  in equation (5).

If the measured current is linear<sup>14</sup> (and without any phase shift), NL becomes 2 in analogy to the parameter in [22]. As the value of NL becomes greater, the measured current becomes non-linear. The rise of the loop of the human skin memristor becomes larger with increasing voltage as it can be seen in Figure 6 a) (right).

The increase in current from  $0.5 v_{max}$  to  $0.75 v_{max}$  will be smaller than the increase of the current from  $0.75 v_{max}$  to its maximum  $i_{max}$  and NL becomes greater than 2, as a consequence. A phase shift between voltage and current on the other hand will misleadingly reduce the NL value<sup>15</sup>, since the current is ahead. At very low frequencies like 0.05 Hz the effect is negligible (see estimated phase shifts in the supplemental material) but with increasing frequency, NL values significantly smaller than 2 become possible. Assuming a linear current at 2.5 Hz and two example phase shifts of 2.1 and 13.26 degrees, NL would be 1.93 in the former and 1.60 in the latter case. Signal noise will affect the NL value in addition.

The total lobe area  $A_{lobe}$  ( $A1+A2$ ) in the V-I plot (see Figure 6 a) (right)) is another quantitative measure used in this paper. A rough approximation for e.g. A1 is to calculate the areas under the upper and lower branch of the loop in the first quadrant and obtain the difference between both. The difference would have different signs before and after the pinched point and lead to an error. To correct for this,

the absolute values of the differences were calculated stepwise (from sample to sample) and summed afterwards. The area under the current was calculated by trapezoidal numerical integration using the “trapz” function in MATLAB (version 2016b, academic license). Log transformation (to the base 10) of the total area  $A_{lobe}$  was used to decrease the skewness among test subjects.

### Parameterization in experiment 2: DC pulse series

The memductance state at the end of each series and average current changes between pulses are used as quantitative measures. Those are based on the current measures that are illustrated in Figure 6 b).

Each period of the pulse series is recorded with 500 samples and consists of 15 seconds in which the pulse is applied followed by 5 seconds relaxation. The measures  $i_s$  and  $i_e$  are the current values at the beginning<sup>16</sup> and end<sup>17</sup> of each pulse. The relative change between pulses is calculated by the difference  $-\Delta i_{between}$  divided by  $i_e(n-1)$ , the one within pulses is  $\Delta i_{within}$  divided by  $i_s$  and the relative net change is calculated by  $\Delta i_{net}$  divided by  $i_e(n-1)$ . Averages of those measures were taken over all pulses of one series.

The conductance  $G$  at the end of the last pulse of each series is calculated from the corresponding current value  $i_e$  divided by the voltage level of the DC pulse. It is log transformed (to the base 10) in order to decrease the skewness.

### Statistical analysis

Each statistical analysis was done separately for the three different skin sites.

The linear mixed effects model that was obtained for the non-linearity parameter in experiment 1 was done by the use of the fitlme() function in MATLAB (version 2016b, academic license) with subject as random effect (random intercept). Signal amplitude (absolute value) and frequency (logarithm to base 2) were fixed effects and non-linearity was the independent variable in the model. The evaluation is done over the third period of each applied sinusoidal voltage signal.

The repeated measures ANOVA on ranks (Friedman test for non-normal or heteroskedastic data) and the pairwise comparison (Tukey test) that were performed to compare the conductance states in experiment 2 were done in SigmaPlot (version 11).

### Instrumentation

A custom-build measurement system (see Figure 7 and [20] for further information) is used for the recording. A Data acquisition card (DAQ) (type USB-6356 from National instruments in this study) enables the application of a constant voltage and simultaneous reading. The generated signal is provided at the “Signal out” port. It is directly connected to the input channel “In1” in order to measure the

<sup>14</sup> Sinusoidal shape without any deformations

<sup>15</sup> It would also affect the non-linearity as it is defined in [22].

<sup>16</sup> The current at sample 3 of each new period.

<sup>17</sup> The current at sample 375.

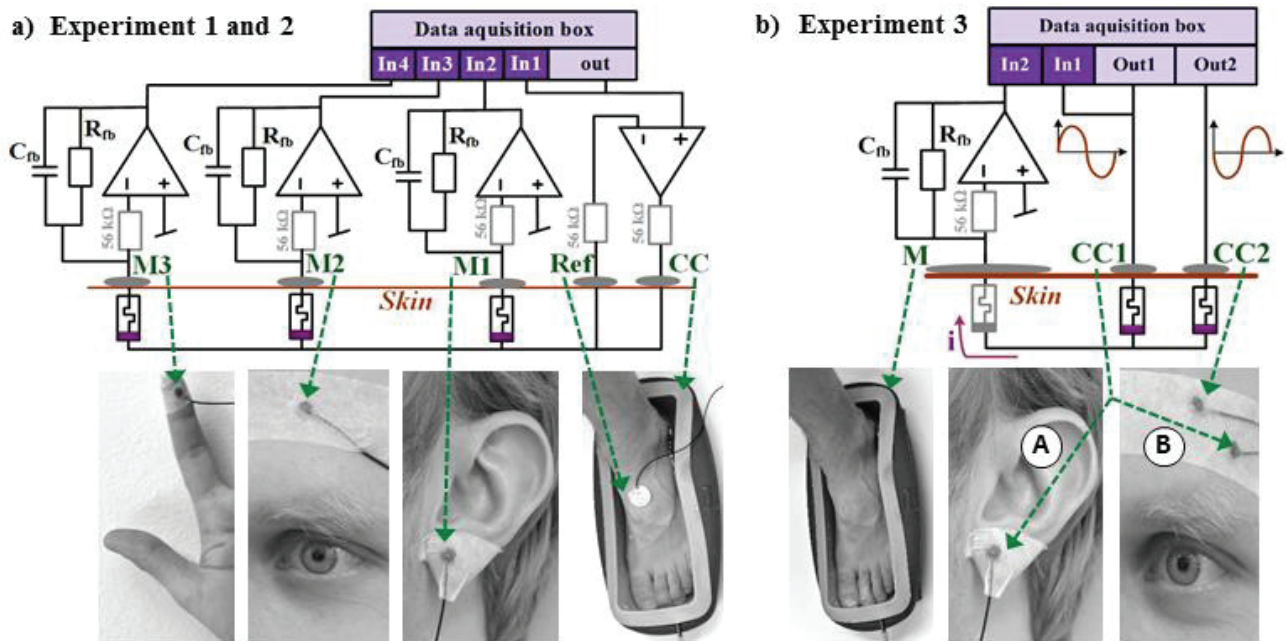


**Figure 7** | Schematic of the chosen measurement system and corresponding electrode placement (shown for left hand side). The electrode setup on the right hand side was equivalent. **a)** Instrumentation setup in experiments 1 and 2. A three-electrode configuration [30] with “CC” as the current carrying electrode and “Ref” as the reference electrode is chosen. **b)** Instrumentation setup in experiment 3. The instrument was switched into two-electrode configuration for this experiment. Only one reading channel but two different output channels are used. CC1 electrode was attached to the earlobe (variant A, chosen for 16 out of 28 subjects) or to the forehead (variant B, chosen for 12 out of 28 subjects).

delay from signal generating inside the DAQ to the actual provision by the Analog to Digital converter at the “Signal out” port.

The data acquisition box was connected to a personal computer. In order to ensure separation between mains and the test subjects, the personal computer, the monitor and the data acquisition box were powered through an international medical isolation device (IMEDe 1000 from Noratel AG, Germany), which enables physical separation from the mains. The software of the measurement system that i.e. controls the Data acquisition card, enables randomization of applied signal order and stores the results in an excel file is written in NI LabVIEW (version 2014).

#### Recording modes

The developed instrumentation enables two different recording modes. The first one is used to study the non-linear properties of skin. Different voltages (sinusoidal, triangular, non-periodic, DC pulse series) can be applied with different amplitudes and frequencies. Signal generating and reading is done with 500 samples per period (independent of the signal frequency). All recorded samples of the measured current are stored in an MS Excel file for further processing. Signal frequencies from 0.05 Hz to 2.5 Hz and amplitudes from 0.4 V to 1.2 V were used in this mode during the experiment series.

A second mode of the instrumentation enables recording of electrodermal activity (EDA) (within linear range). A sinusoidal voltage with amplitude of 100 mV and frequency

of 20 Hz is applied in order to measure the skin admittance without affecting it. The admittance can be separated into real part (conductance) and imaginary part (susceptance) by lockin technique [31]. EDA was measured before and after experiment 1, as well as after each pulse series in experiment 2. The instrumentation is capable of recording approximately two conductance and susceptance values per second.

#### Instrumentation setup in experiments 1 and 2

The instrument (see Figure 7 a)) is capable of recording at three different skin sites (under the measuring electrodes M1, M2 and M3) at the same time. In each recording channel, a transimpedance amplifier is used in order to convert the current through the skin into a voltage that can be read by the DAQ (inputs “In2”, “In3” and “In4”).

The feedback resistor  $R_{fb}$  of each transimpedance amplifier has a value of 56 k $\Omega$  and in combination with a small capacitance  $C_{fb}$  (here 4.7 nF) in parallel it functions additionally as a low pass filter in order to reduce noise. In this three-electrode configuration, the voltage is basically applied from deeper layers of the skin (under the M electrodes) to the skin surface (since the tissue under the CC electrode does not contribute to the measurement).

The used measurement electrodes (M1, M2 and M3) were prewired, dry Ag/AgCl<sup>18</sup> ones with an active area of 0.283cm<sup>2</sup>. These were taped to the skin. Dry electrodes

<sup>18</sup> From the company Wuhan Greentek PTY LTD

were used to exclude any possible influence of ionic gel to the measurements (see [20]). The electrodes were cleaned with ethanol for reuse.

Compared to the M-electrode, the choice of the reference electrode is less critical. A prewired Ag/AgCl electrode that is initially covered with solid hydrogel<sup>19</sup> and has an active area of 5.05 cm<sup>2</sup> was used as reference electrode to ensure good electrical contact. A saline solution was used as current carrying electrode (CC) in order to implement a very large electrode that will in turn reduce the voltage that has to be supplied by the operational amplifier in the three-electrode setup.

All electrodes were placed at the same side of the body to avoid current paths through the heart. It was randomly chosen whether the preferred or non-preferred hand side was used for the recording. The measurement electrodes were placed at three different skin sites (see Figure 7 a)). One was placed at the earlobe and another one at the fingertip of the pointing finger. The third measurement electrode was placed at the forehead above the iris of the eye of the chosen side, about the width of two fingers above the eyebrow.

The foot of the same side was placed in the saline solution (CC electrode) and the reference electrode was placed on top of the foot, which was not covered by the saline solution. The foot was chosen to be placed in the saline solution since it is a comfortable setup. In order to reduce the endogenous skin potential difference it would be useful to place the reference electrode on a skin site of similar potential as the measurement electrode.

### *Instrumentation setup in experiment 3*

Two sinus signals with same amplitude but opposing sign are applied to the skin like illustrated in Figure 7 b).

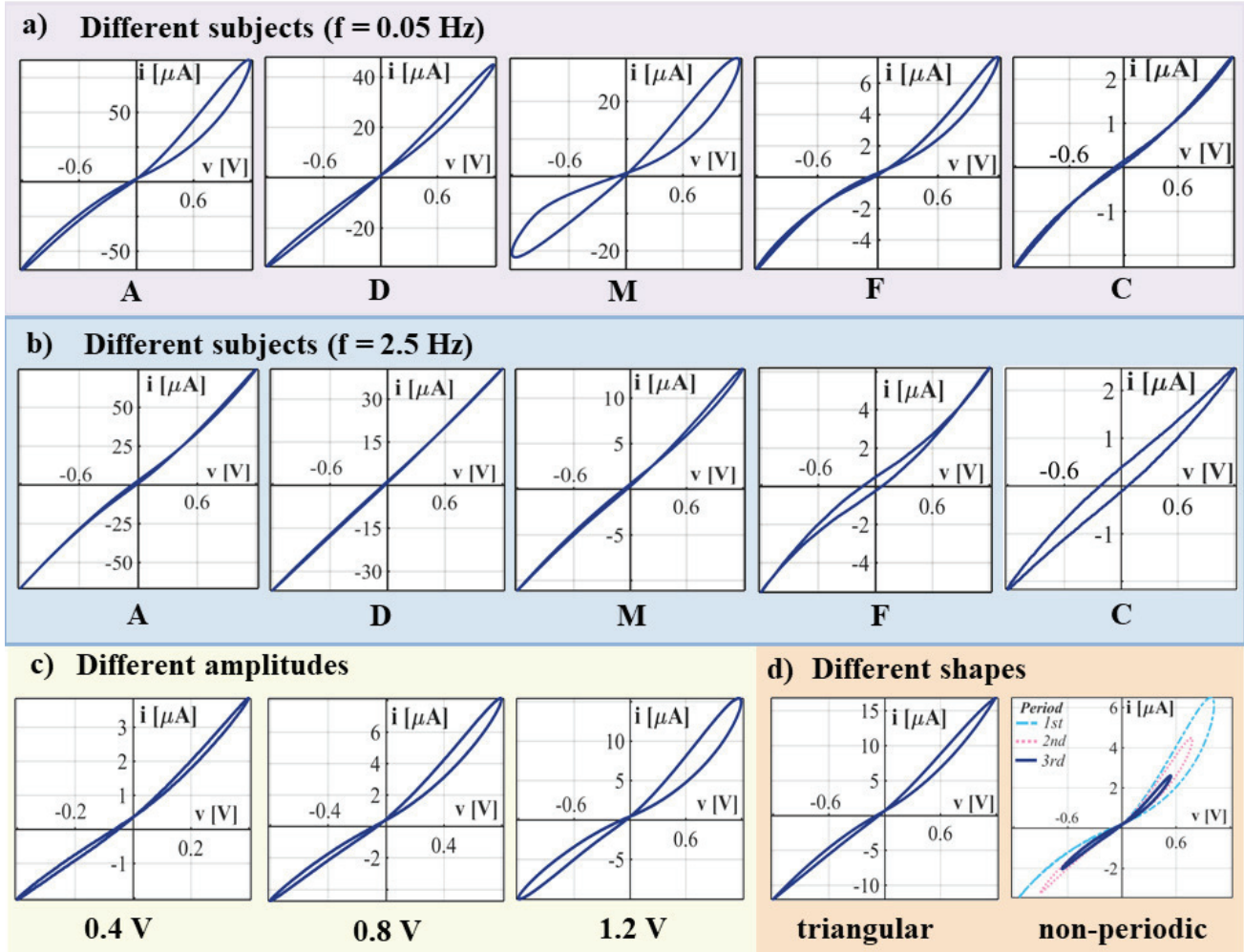
After experiment 2, the electrode M3 on the fingertip and the reference electrode were removed. The electrode at the earlobe (M<sub>1</sub> in see Figure 7 a)) was now used as CC1 (variant A) (see Figure 7 b)) and the electrode at the forehead was used as CC2. For 12 out of 28 test subjects the CC1 electrode was attached to the forehead as well (variant B) instead of the earlobe. In this setup a fourth dry Ag/AgCl electrode of the same type was placed about two centimeters away from the electrode that was used as M<sub>2</sub> in experiment 1 and 2 and as CC2 in experiment 3 (see Figure 7 b)) towards the outer part of the head and about 0.5 centimeters downwards. This fourth electrode was only used in experiment three but it was placed at the same time like the other electrodes before experiment one. The saline solution was used as big M-electrode in order to minimize the contribution of the corresponding skin memristor to the measurement (see [20]). In this two-electrode configuration, the voltages are applied from skin surface (under CC1 and CC2) to deeper layers of the skin.

---

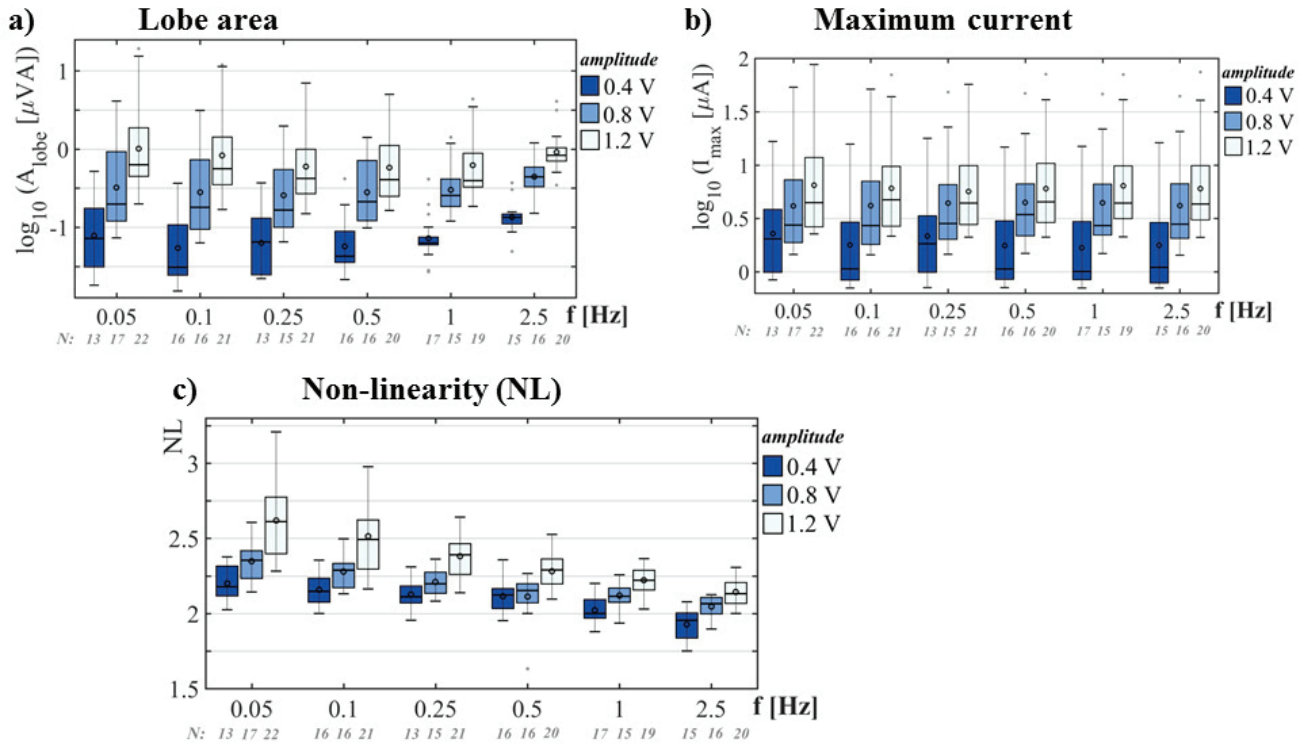
<sup>19</sup> Type: Kendall 1050NPSM

# Supplemental Material

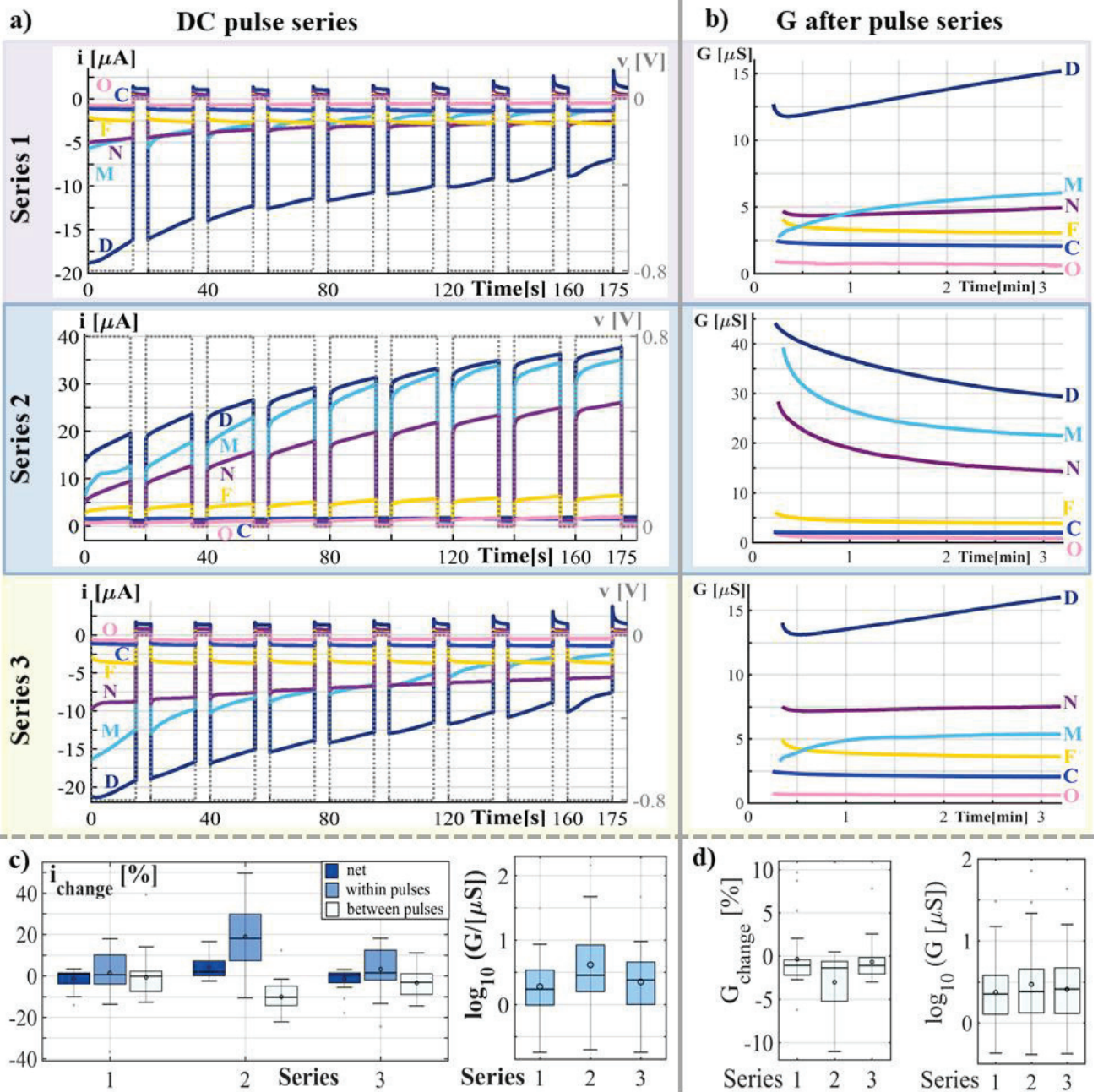
## EARLOBE



**Extended Data Figure 1 | Voltage-current (V-I) plots recorded from the earlobe (experiment 1), always shown for the third period of each applied signal.** **a):** Recordings of 5 different subjects (A,D,M,F,C) with applied sinusoidal voltage with amplitude of 1.2 V and frequency of  $f=0.05$  Hz. The galvanic contact through the sweat ducts was only achieved for 9 subjects. Five out of those showed hysteresis loops with one pinched point and asymmetric shape with very small lobe in the third quadrant (see subject A). Quite symmetric hysteresis loops with relative large lobe (total of 2 subjects) (see subject M) and relative small lobe (total of 2 subjects, see subject D) were observed, as well. The galvanic contact through the sweat ducts was not obtained for 18 subjects since those subjects showed hysteresis loops with two pinched points and a small maximum current similar to the ones of subjects C and F. The electrode at the earlobe of one subject was not well attached and the electrical contact was not given at all. **b)** Same applied signal and subjects like in a) but a different signal frequency (2.5 Hz). The lobe area of the pinched hysteresis loop becomes smaller with increasing frequency (applies for all subjects). Some subjects showed pinched hysteresis loop even at 2.5 Hz (see subject M). An example of a hysteresis loop that develops towards a clear straight line is shown (see subject D). **c)** Sinusoidal voltage signal with  $f=0.05$  Hz but different amplitudes are shown for subject N. The relative lobe area increases with increasing amplitude (applies for all subjects). Hysteresis loops with one pinched point (and with very small lobe area) were observed for 8 subjects when amplitude of 0.4 V was applied. Subjects those showed pinched hysteresis loops with two pinched points when amplitude was 1.2 V had linear voltage current relation, when the amplitude was 0.4 V. An indication that 0.4 V amplitude is too low in order to change the state of the stratum corneum thermistor of the earlobe. **d)** Other applied voltage shapes than sinusoidal shown for  $f= 0.05$  Hz and subject N. As soon as a pinched hysteresis loop was obtained from the recording with sinusoidal voltage, it was obtained with triangular and non-periodic (sinusoidal signal with decreasing amplitude) waveform. The recording of the latter is shown over three periods and was only recorded from fifteen test subjects due to instrumentation error.

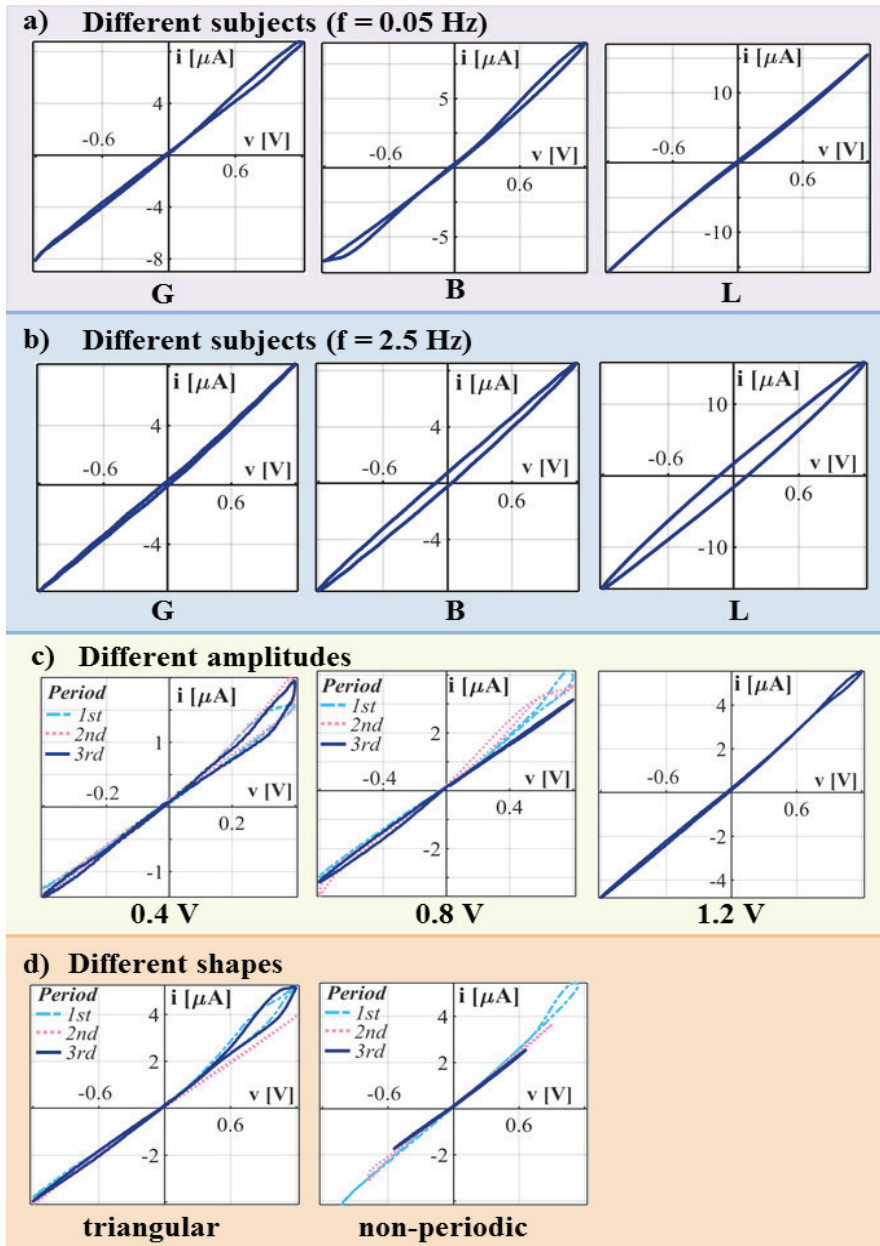


**Extended Data Figure 2 | Box plots over all test subjects** shown for 3<sup>rd</sup> period of all applied sinusoidal voltages (3 amplitudes, 6 frequencies), recorded from the earlobe. The plots give information of how the V-I characteristics change with amplitude and frequency. The horizontal line in the middle of each boxplot denotes the median, the circle the mean value, the whiskers the 5% and 95% percentiles. The number N of subjects, included in the evaluations, is written under each boxplot. Sinusoidal signal with amplitude of 0.4 V was not recorded from 2 subjects at 2.5 Hz and 1 subject at 0.25 Hz due to instrumentation error. The recording of one subject at 0.8 V and frequency of 0.5 Hz (3<sup>rd</sup> period) was excluded since the electrode was touched by accident. Several subjects had very low membrane conductance and the measured currents were quite noisy. Signals were excluded from the evaluation if  $i_{\text{max}}$  was smaller than  $\text{amplitude}/0.4\text{V} \cdot 0.7 \mu\text{A}$ . **a)** Lobe area (logarithm to base 10). Mean and median of the lobe area continuously decrease up to a certain frequency (e.g. median up to 1 Hz, mean up to 0.5 Hz for 1.2 V amplitude) and increase above, when the capacitive properties of the stratum corneum start to interfere noticeably. **b)** Maximum current (logarithm to base 10), **c)** A Non-linearity (NL) value equal 2 implies a linear measurement (straight line in the V-I plot) and the higher the value of NL the higher the non-linearity of the measurement. A single value-curve that is not a straight line will also have a value larger than 2. Results from the linear mixed effects model analysis (see methods part, number of observations at the earlobe was 307) show that, frequency (as logarithm to base 2 in the used model) and absolute value of the amplitude (p-value < 0.001 for both) have significant effects on the non-linearity parameter. The value of the NL parameter increased by  $0.360 \pm 0.036$  (95%-CI) with an increase in amplitude by 1 V and each bisection of the frequency increased the value by  $0.062 \pm 0.006$  in the obtained model.

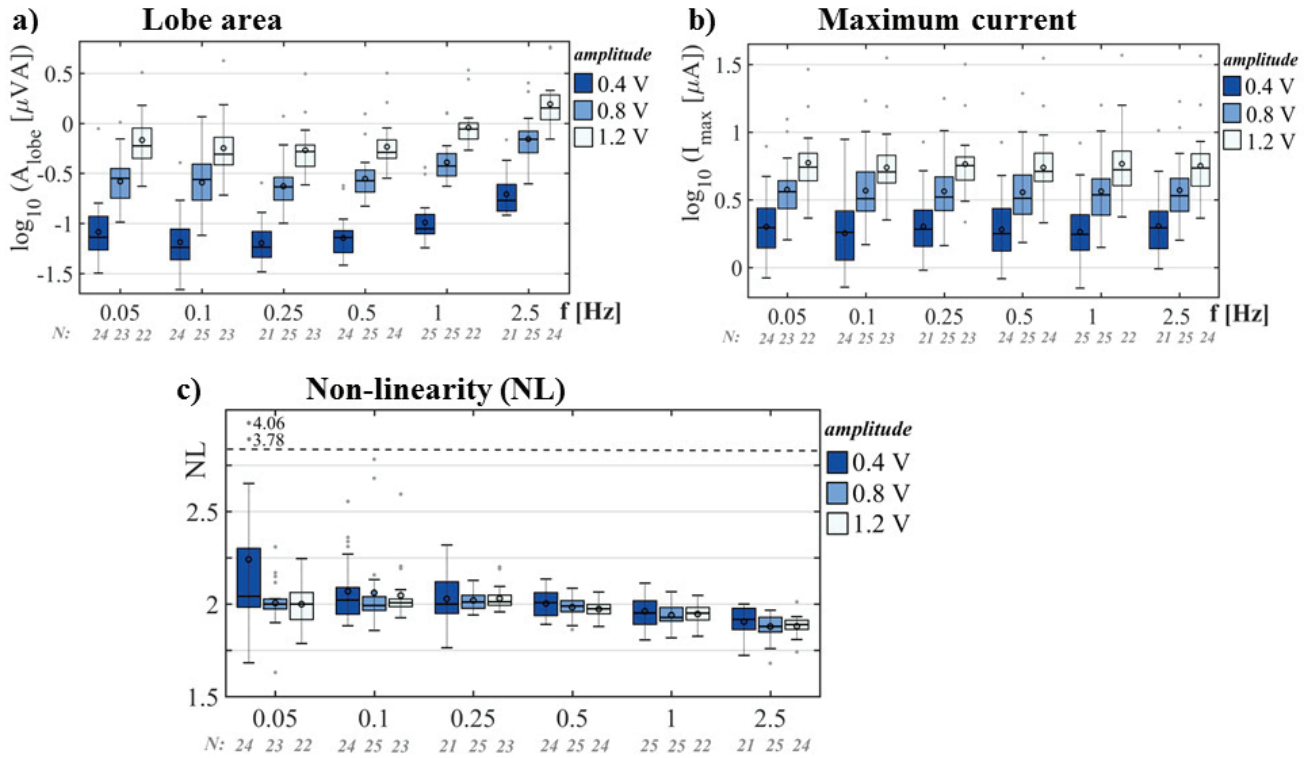


**Extended Data Figure 3 | Results from experiment 2 (earlobe).** Three series of DC pulses were applied and the small signal conductance measurements were done after each series. **a)** Measured current  $i$  and applied voltage  $v$  plotted over time shown for 6 test subjects (C, D, F, M, N, O). The results from the recordings at the earlobe are similar to the ones from the forehead with the exception that the amount of measured currents and current changes were much smaller in general (e.g. the measured currents of all subject except of two were within  $-0.1 \mu\text{A}$  to  $-6 \mu\text{A}$  in series 1). **b)** Small signal conductance measurements after each DC pulse series (shown for the same subjects) give information of how the state of the skin memristor develops naturally (unaffected by the applied voltage). The time is related to the end of the last pulse of the series. The conductance after series 1 and 3 usually increases after a small drop in the beginning. Some other subjects show an immediate increase and the conductance of further subjects decrease continuously within the 3 minutes of recording. The conductance values of all subjects after series 2 are continuously decreasing. The conductance drop slows down with time. **c-d)** Boxplots over all subjects. The horizontal line in the middle of each boxplot denotes the median, the circle the mean value, the whiskers the 5% and 95% percentiles. **c)** Boxplots related to the DC pulse series. Average change of current  $i$  within pulses (within 15 seconds), between pulses (within 5 seconds) and net change from pulse to pulse presented as ratios shown for all three series (left). Memductance  $G$  (logarithm to base 10) at the end of the last pulse (at 175 s) of each series (right). **d)** Boxplots related to the small signal conductance measurements after each pulse series. Small signal conductance  $G$  (Logarithm to base 10) 3 minutes after the last pulse (left). Small signal conductance  $G$  (Logarithm to base 10) 3 minutes after the last pulse (right). Results from Friedman test and pairwise comparison (Tukey Test with  $p\text{-Value} < 0.05$ ) show that the conductance value (logarithm to base 10) from series 1 differs significantly from the other two but there is no significant difference between the conductance values in series 2 and 3. This result is different from the forehead and may origin in the little galvanic contact through the sweat ducts of several subjects.

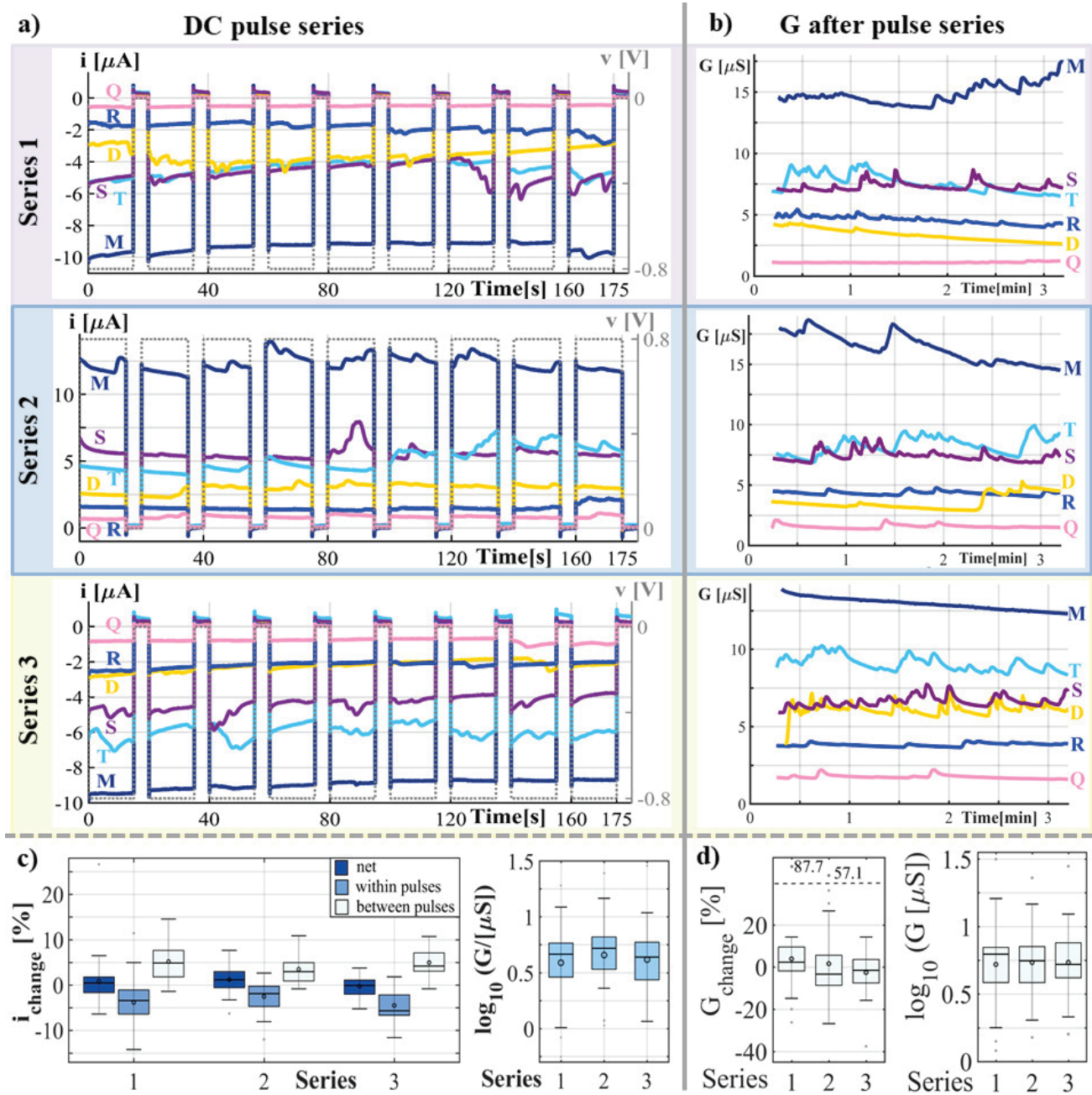
## FINGERTIP



**Extended Data Figure 4 | Voltage-current (V-I) plots recorded from the fingertip (experiment 1), always shown for the third period of each applied signal. a)** Recordings of 3 different subjects (G,B,L) with applied sinusoidal voltage with amplitude of 1.2 V and frequency of=0.05 Hz. The recordings from the fingertip looked quite different compared to the earlobe and the forehead. The recordings of 15 test subjects showed pinched hysteresis loops with very small lobe like subjects G and B or even smaller. No hysteresis loop and a (almost) linear measurement (see subject L) was obtained for the other 13 subjects. No hysteresis loop with two pinched points was observed. **b)** Same applied signal and subjects like in a) but a different signal frequency (2.5 Hz). The capacitive properties dominate in most recordings from the fingertip at 1 Hz, 2.5 Hz (and even 0.5 Hz) and an elliptic shape (see subjects B and L) can be observed. **c)** Sinusoidal voltage signal with  $f=0.05$  Hz but different amplitudes are shown for subject O. The lobe area is not necessarily increasing with increasing amplitude like demonstrated in this example. The recording with 0.4 V shows also largest NL value and seems to be stable over the three shown periods, which is an indication that electro-osmosis really applied. This is in accordance with the boxplot in **Error! Reference source not found**. **c)** On the other hand, pinched hysteresis loops for amplitude of 0.4 V were only observed for 8 subjects (most of them with very small lobe area). The recording of subject O with 0.8 V differed largely among the periods which might be an indication that emotional sweating interfered. The plots of the three periods of the recording with 1.2 V amplitude (only third period shown) were very close together, but only the third period showed pinched hysteresis loop. **d)** Other applied voltage shapes than sinusoidal shown for  $f= 0.05$  Hz and subject O. Only second and third period of the recording with triangular waveform showed pinched hysteresis loop. Pinched hysteresis loop was only obtained in first period of the recording from subject O with non-periodic waveform. The recording with non-periodic waveform was only done on fifteen test subjects due to instrumentation error.

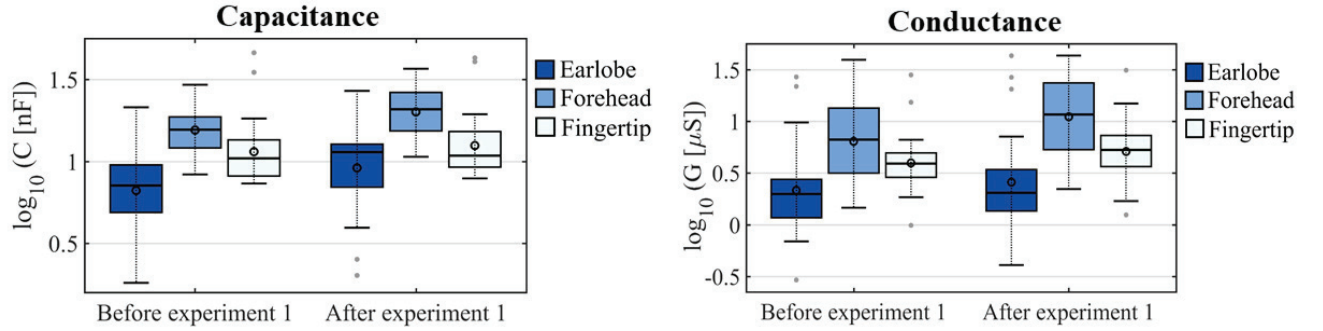


**Extended Data Figure 5 | Box plots over all test subjects** shown for 3<sup>rd</sup> period of all applied sinusoidal voltages (3 amplitudes, 6 frequencies), recorded from the fingertip. The plots give information of how the V-I characteristics change with amplitude and frequency. The horizontal line in the middle of each boxplot denotes the median, the circle the mean value, the whiskers the 5% and 95% percentiles. The number N of subjects, included in the evaluations, is written under each boxplot. Sinusoidal signal with amplitude of 0.4 V was not recorded from 2 subjects at 2.5 Hz and 1 subject at 0.25 Hz due to instrumentation error. Several subjects had very low memductance and the measured currents were quite noisy. Signals were excluded from the evaluation if  $i_{\text{max}}$  was smaller than  $\text{amplitude}/0.4\text{V} \cdot 0.7 \mu\text{A}$ . **a)** Lobe area (logarithm to base 10). The increase in area within loop from 0.25 Hz to 2.5 Hz can be explained by the capacitive properties that start to have a significant effect at those frequencies. **b)** Maximum current (logarithm to base 10), **c)** A Non-linearity (NL) value equal 2 implies a linear measurement (straight line in the V-I plot) and the higher the value of NL the higher the non-linearity of the measurement. The NL values of the fingertip are much smaller compared to the forehead and earlobe, reflecting the observation that many recordings were (almost) linear. Highest NL values are obtained with signal amplitude of 0.4 V, which is in accordance to the example shown in **Error! Reference source not found.** **c)** This observation is different to the results from the forehead and earlobe. The outliers with values 3.78 (corresponding value of subject O, see **Error! Reference source not found.** **c)**) and 4.06 at 0.05 Hz of amplitude 0.4 V are actual reflecting measured pinched hysteresis loops. Other outliers may origin in signal noise or emotional sweating. Results from the linear mixed effects model analysis (see methods part, number of observations at the earlobe was 425) show that, frequency (as logarithm to base 2 in the used model,  $p$ -value < 0.001) and absolute value of the amplitude ( $p$ -value = 0.006) have significant effects on the non-linearity parameter. The value of the NL parameter decreased by  $0.070 \pm 0.050$  (95%-CI) with an increase in amplitude by 1 V. The decrease in the non-linearity value with increase in amplitude is opposite from the earlobe and forehead. Each bisection of the frequency increased the value by  $0.035 \pm 0.008$  in the obtained model.



**Extended Data Figure 6 | Results from experiment 2 (fingertip).** Three series of DC pulses were applied and the small signal conductance measurements were done after each series. **a)** Measured current  $i$  and applied voltage  $v$  plotted over time shown for 6 test subjects (D, M, Q, R, S, T). The behavior at the fingertip was different from the earlobe and forehead since it is not possible to observe a clear trend in current change and emotional sweating interferes the measurement. **b)** Small signal conductance measurements after each DC pulse series (shown for the same subjects) give information of how the state of the skin memristor develops naturally (unaffected by the applied voltage). The time is related to the end of the last pulse of the series. No clear trend in small signal conductance change can be seen which is different from the earlobe and forehead and the recordings look like usual conductance measurements at an emotional active skin site. **c)-d)** Boxplots over all subjects. The horizontal line in the middle of each boxplot denotes the median, the circle the mean value, the whiskers the 5% and 95% percentiles. **c)** Boxplots related to the DC pulse series. Average change of current  $i$  within pulses (within 15 seconds), between pulses (within 5 seconds) and net change by pulse to pulse presented as ratios shown for all three series (left). Memductance  $G$  (logarithm to base 10) at the end of the last pulse (at 175 s) of each series (right). **d)** Boxplots related to the small signal conductance measurements after each pulse series. Small signal conductance change from minute 2 to minute 3 after the last DC pulse (left). Small signal conductance  $G$  (Logarithm to base 10) 3 minutes after the last pulse (right). Results from repeated measures ANOVA on ranks show that there are no significant differences in the small signal conductance values (logarithm to base 10) at minute three among the three series.

## Phase shift estimation



**Extended Data Figure 7 |** Boxplots over all subjects of small signal skin capacitance and conductance (both presented as logarithm to base 10) direct before and about 1 min after experiment 1.

A possible phase shift between voltage and current in human skin (memristor) measurements originates in the capacitive properties of the stratum corneum, that is in parallel to the sweat ducts. A phase shift will affect the pinched point position [8] and the non-linearity parameter (see below). The phase shift  $\alpha$  of simple resistor – capacitor circuit (linear range) can be calculated by

$$\alpha = \tan^{-1} \frac{2\pi f C}{G} \quad (6)$$

To get an estimation in which range  $\alpha$  takes place during experiment 1, the susceptance and conductance were measured before and after (see Extended Data Figure 7). If  $G$  is  $6.7 \mu\text{S}$  and  $C$  is  $15.6 \text{ nF}$ <sup>20</sup> as an example,  $\alpha$  becomes 0.04 degree for frequency equal 0.05 Hz and 2.1 degree for frequency equal 2.5 Hz. If the capacitance is e.g. 30 nF and the conductance is about  $2 \mu\text{S}$  (just as an extreme example within the range), the phase shift would be 0.27 degree at  $f=0.05$  Hz and 13.26 degree at  $f=2.5$  Hz.

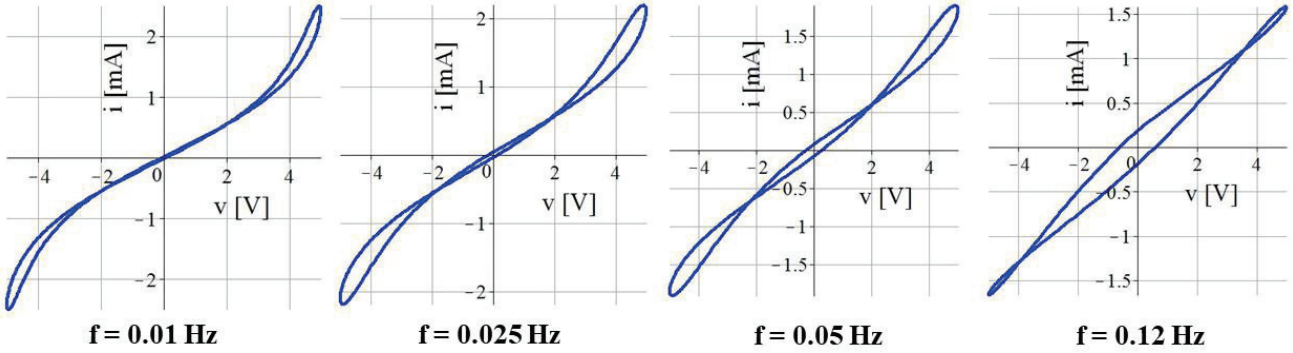
The calculated values are rough estimations based on the values from a linear measurement (at 20 Hz) applied to a frequency range in which non-linear effects occur. It is difficult to estimate an exact phase shift regarding the measurement in the non-linear range. The level of the measured conductance at 20 Hz is slightly greater than the one measured with a DC voltage [24] or very low AC voltage like 0.05 Hz. Furthermore, if the state of the skin memristor changes during one period in the non-linear measurement range, the phase angle also changes consequently. A modification of equation (6) would be

$$\alpha(x) = \tan^{-1} \frac{2\pi f C}{G(x,T)}, \quad (7)$$

with  $G(x,T)$  as the state dependent conductance with  $x$  and  $T$  as the inner states that are affected by the applied signal.

<sup>20</sup> Both are the median values of the forehead at the measurement before experiment 1.

## Thermistor simulation



**Extended Data Figure 8 | Simulation of a thermistor model with a capacitance (50  $\mu\text{F}$ ) in parallel.** The simulation is done for different signal frequencies of applied sinusoidal voltage  $v$  with amplitude of 5 V. Simulations were done over one signal period by the use of Maple (Version 2016.2). The differential equations were solved numerically (using command “dsolve” with the option “type=numeric”) by the use of the Fehlberg fourth-fifth order Runge-Kutta method.

The simulations (see Extended Data Figure 8) are based on the NTC thermistor model that is presented in [21]. This thermistor is described by

$$G(T_N) = \left( R_{0N} \cdot e^{\beta_N \left( \frac{1}{T_N} - \frac{1}{T_{0N}} \right)} \right)^{-1} \quad (8)$$

$$\frac{dT_N}{dt} = \frac{\delta_N}{H_{CN}} (T_{0N} - T_N) + \frac{G(T_N)}{H_{CN}} \cdot v^2, \quad (9)$$

with  $G(T_N)$  as the temperature dependent conductance,  $R_{0N} = 3.89 \text{ k}\Omega$  as resistance at ambient temperature  $T_{0N} = 300 \text{ K}$ ,  $\beta_N = 5 \cdot 10^5 \text{ K}$  as material specific constant,  $\delta_N = 0.1 \text{ W/K}$  as dissipation constant and  $H_{CN} = 0.14 \text{ J/K}$  as heat capacitance.

The thermistor model and a large capacitance in parallel (50  $\mu\text{F}$ ) were simulated with applied sinusoidal voltage  $v$  as signal source. The corresponding current was calculated by

$$i = i_{Th} + i_C = v \cdot G(T_N) + C \cdot \frac{dv}{dt}. \quad (10)$$

A skin thermistor model might be similar to the used model but with different constant values and the simulation results (see Extended Data Figure 8) cannot be directly related. However, the simulations illustrate how the V-I plots of a NTC thermistor will look like for different frequencies if a capacitor is connected in parallel. Hysteresis loops with two pinched points were achieved and the shapes of the simulated hysteresis loops are comparable to the corresponding recordings at the forehead (see subject F in Figure 2 c)) and earlobe (see subjects C and F in Extended Data Figure 1 a) and b)).